UNIVERSITY OF SOUTHAMPTON

FACULTY OF ENGINEERING AND THE ENVIRONMENT

Civil, Maritime and Environmental Engineering and Science

Hygrothermal ageing and its effects on the flexural properties and failure modes of plant oil based composites for maritime applications

by

Mari Valgma

Thesis for the degree of Doctor of Philosophy

May 2014

UNIVERSITY OF SOUTHAMPTON

ABSTRACT

FACULTY OF ENGINEERING AND THE ENVIRONMENT
Civil, Maritime and Environmental Engineering and Science

Doctor of Philosophy

HYGROTHERMAL AGEING AND ITS EFFECTS ON THE FLEXURAL PROPERTIES AND FAILURE MODES OF PLANT OIL BASED COMPOSITES FOR MARITIME APPLICATIONS

by Mari Valgma

This research looks at moisture uptake and its effects on the flexural properties of glass reinforced epoxy, linseed oil and castor oil composites. Water uptake damages the material through chemical, physical and mechanical ageing. At the same time there is a need to reduce the environmental effects of the maritime industry and using composites from renewable resources could be a viable solution. While the conventional composites like glass/epoxy are trusted as a structural material in harsh humid conditions, there is very little known about more sustainable composite materials. As resins have a greater environmental impact when manufactured, and no information on their long term performance is available, this research looks at the flexural performance of glass reinforced castor and linseed oil resins over 2 years of ageing in comparison with glass/epoxy.

As a result of accelerated ageing it has been shown that the degradation of all three composites is significant, ranging between 18–87% over the 2 year testing period. The moisture equilibrium content in glass/epoxy was 2.11%, glass/castor oil 3.62% and glass/linseed oil 2.87%. While the moisture uptake of glass/epoxy follows an expected trend, the moisture uptake of plant oil based resin composites does not and differs from conventional models. After 2 years of ageing the properties of glass/castor oil are comparable with glass/epoxy. The degradation of properties in glass/linseed oil is the greatest.

MicroCT and AE techniques were used to look at the failure modes in glass/epoxy and glass/linseed oil specimens showing changes in the failure mode of glass/linseed oil only after 3 days of ageing. The failure modes of glass/epoxy were found to be mainly fibre dominated and most of the damage occurred on the tensile side of the specimens while the failure in glass/linseed oil was largely dominated by compressive damage. For the first time the failure mechanisms of glass/linseed oil have been proposed.

Contents

List of Figures

List of Tables

Declaration of Authorship

I, Mari Valgma, declare that the thesis entitled *Hygrothermal ageing and its effects on the flexural properties and failure modes of plant oil based composites for maritime applications* and the work presented in the thesis are both my own, and have been generated by me as the result of my own original research. I confirm that:

- this work was done wholly or mainly while in candidature for a research degree at this University;
- where any part of this thesis has previously been submitted for a degree or any other qualification at this University or any other institution, this has been clearly stated;
- where I have consulted the published work of others, this is always clearly attributed;
- where I have quoted from the work of others, the source is always given. With the exception of such quotations, this thesis is entirely my own work;
- I have acknowledged all main sources of help;
- where the thesis is based on work done by myself jointly with others, I have made clear exactly what was done by others and what I have contributed myself;
- parts of this work have been published as:

  M. Malmstein, A. R. Chambers, and J. I. R.Blake. Hygrothermal ageing of plant oil based marine composites. *Composite Structures*, 101: 138–143, 2013.

  M. Malmstein, A. R. Chambers, and J. I. R.Blake. The effects of hygrothermal ageing on the mechanical properties of sustainable composites. In, *18th International Conference on Composite Materials*, Jeju Island, KR, 21 - 26 Aug 2011.

  M. Malmstein, A. R. Chambers, and J. I. R.Blake. Hygrothermal ageing of sustainable composite materials for marine applications. In, *4th International Conference of Sustainable Materials, Polymers and Composites*, Ecocomp, Birmingham, GB, 06 - 07 Jul 2011.

  M. Malmstein, A. R. Chambers, and J. I. R.Blake. Hygrothermal ageing and the implications on adopting sustainable composite materials for structural marine applications. In, *18th International Conference on Composite Structures*, Porto, PT, 28 - 30 Jun 2011.

Signed:.....

Date:.....

Acknowledgements

I would like to thank my supervisors James and Alan for their understanding, continuous help and guidance.

This work would not have been possible without the materials provided kindly by Sustainable Composites Ltd., Bioresin and the additional funding from IMarEST.

I am grateful for my mum encouraging me to study abroad, Memme for her endless optimism and support, Mooru and Maarja-Liisa for always listening to me and helping out when needed, Juhan for making it possible for me to stay away from home.

George, Rachael, Pramod, Lauren and Kaija, thank you for always supporting me, no matter what. The giggles, boardgames and fun times we have together are very much appreciated.

Liivi, Inks and Kata, your help with introducing Estonian culture (and food) in the UK was absolutely essential. Go Tipsuklubi!

Inga, thank you for trusting me with this amazing ball of fluff called Kino. She is the sunshine and generator of fun in our home.

Marit, Mihkel, Maarja, thank you for not forgetting about me despite me being away for many years. I like our movie evenings Maarja!

Last but not the least I would like to thank my employer for providing me with all the extra time needed for finishing this thesis, Agnieszka for the advice from the chemistry side of things, and Richard for fun sailing times and help with the AE.

Chapter 1

Introduction

1.1 Background

Pressures on the limited material resources and increasing societal awareness require new, more sustainable and 'greener' materials for structural applications [1]. One of the goals in the modern world of structural composite materials is to produce a high performance composite material that is fully 'green'. This composite should be made by combining bio-based fibres with resins from sustainable resources and be fully recyclable or biodegradable under certain conditions [1]. The suspicion of variability in natural constituents leads to an opinion among manufacturers that the material performance is not acceptable for structural applications. Therefore, the suitability of new bio-based constituent materials for structural composites still needs to be investigated and proven in order to meet the high expectations of consumers and ensure the safety and reliability of the structures.

In maritime structures the materials are expected to demonstrate adequate strength, stiffness, ease of fabrication, fire resistance, impact resistance and damage tolerance, long-term performance of material, and cost [2]. In this work the focus is on flexural strength, stiffness and the long-term performance of the material. Flexural properties are often used for assessing the quality of marine composites, especially for assessing the effects of ageing on the mechanical performance [3]. Different performance is required of materials for different structural components, for example yacht decks needs to be stiff while the hull needs to show good impact resistance [2]. Regardless of the role of a composite in a maritime structure, the material needs to demonstrate sufficient water resistance among other properties in order to be approved by classification bodies [4].

Considering the current options, 'green' composites are here defined as non-biodegradable (not capable of being decomposed by biological means) composites that are fully or partially made from renewable resources. Resin has been found to have a bigger environmental impact than fibres to manufacture (greater CO_2 emissions [5] and greater

energy consumption [6]). While there is a lot of information available on plant fibres [1, 7, 8, 9, 10, 11], the data available on the performance of plant oil based resins is very poor and they cannot be used in high performance applications before more information becomes available. In order to reduce the environmental impact of manufacturing maritime composites, which is one of the biggest consumers of structural composites [12], and providing more information on plant oil based resins, this research seeks to determine the opportunities of using new environmentally considerate castor and linseed oil resins in maritime applications. This is done by investigating the moisture uptake and its effects on the flexural properties of two novel and more sustainable plant oil based composites. The changes in the properties are related to the failure mechanisms that have not been investigated before with these materials.

In this work, a test programme has been developed to determine the effects of moisture uptake on the flexural properties through accelerated and non-accelerated hygrothermal ageing. Tests will be carried out with glass reinforced linseed oil and castor oil in comparison with industry standard glass reinforced epoxy. It has been hypothesised that hygrothermal ageing causes changes in the failure modes, thus affecting the strength of composites [13]. In this research these changes in the failure modes have been detected with X-ray computed microtomography (microCT) and monitored further with acoustic emission (AE) testing giving real time data on the changes of damage mechanisms inside the material during flexural tests. The long-term performance and failure modes of plant oil based resin composites have not been investigated before.

1.2 Aims and Objectives

The aim of this project is to determine the moisture absorption behaviour and its effects on the flexural properties and failure modes of glass/epoxy, glass/linseed oil and glass/-castor oil composites as a function of time in different environments and temperatures. At the end of the project there will be a better understanding about the damaging processes taking place in both conventional and new sustainable composites during the hygrothermal ageing. In addition, there will be data available on the mechanical properties of glass/castor oil and glass/linseed oil composites to be used in the design stage of maritime structures. To achieve the set aims, the following objectives were to:

- Choose a proper conditioning method (both accelerated and non-accelerated) for the glass/epoxy, glass/castor oil and glass/linseed oil specimens considering the time limit and desired results;
- Investigate the water uptake behaviour and its effects on the flexural properties of plant oil based composites in comparison with glass/epoxy composites using accelerated and non-accelerated conditions;

- Determine the changes in the flexural failure modes in glass/epoxy and glass/linseed oil specimens with the aid of microCT and AE techniques, propose the order of the failure events in both dry and aged samples;
- Discuss and explain the processes and mechanisms behind the reduction of flexural properties as a result of moisture uptake in studied composites.

1.3 Novelty and Implications

This work will provide the reader with information about the long term performance of glass/linseed oil and glass/castor oil composites, currently there is no such information available. The focus of the work is on moisture uptake and its effects on the flexural properties of these composites in addition to conventional glass/epoxy. The information presented can be used in structural engineering and the design stage of structures when new plant oil based composites are being implemented or when optimising the performance of structures operating in wet environments.

For the first time, the changes in the failure mechanisms in glass/linseed oil have been investigated and the order of failure events in both glass/linseed oil and glass/epoxy presented. These findings can help to improve structural health monitoring (SHM), especially as AE, as one of the SHM methods, was used in this work.

There will also be presented other points of interest like the effects of UV-curing on the long-term performance of composites and relating accelerated ageing test results to non-accelerated ones.

1.4 Outline of the Thesis

In Chapter 2 the literature review and current state of art is presented including 'green' composites, moisture uptake in composites, hygrothermal ageing and description of the damage detection techniques.

The literature review is followed by Chapter 3 which provides a detailed description of the testing methodology and experimental procedures used. A detailed overview of moisture uptake, flexural and imaging techniques is given.

The results of this work are divided into two chapters. Firstly, Chapter 4 discusses the moisture uptake and changes in flexural properties of all three materials. Finally, Chapter 5 looks at the failure mode analysis in glass/epoxy and glass/linseed oil composites.

Chapter 6 summarises the findings regarding failure modes, Chapter 7 concentrates on the conclusions drawn from this work, and Chapter 8 gives ideas for future work directions.

Chapter 2

Literature Review

The literature review first introduces the plant oil based thermosetting and UV-curing resin systems. Then the mechanisms of moisture uptake and its effects on the performance of composites will be discussed. Finally an overview of the flexural failure modes will be given together with the damage detection techniques.

2.1 Composites From Renewable Resources

Polymers from renewable resources must compete on price and performance with petrochemical resins including polyesters, epoxies and polyurethanes among others. Currently, a renewed interest in renewable sources for these resins is being witnessed. The recurrence of bio-based plastics is dictated by several factors including political, technological and environmental developments. Plant fibres are hydrophilic and that is somewhat limiting their use in sustainable composites for maritime applications. However, the water sensitivity of the resins can be avoided by using oil based constituents like vegetable/plant oils. Therefore, plant/vegetable oils may be a suitable replacement in resins for maritime composites.

2.1.1 'Green' E-glass Fibres

E-glass fibres are the most common reinforcement used in small craft composites due to their relatively good mechanical properties at an affordable cost. Compared with plant fibres, glass fibres have a superior performance with less varying properties (Table 2.1), making uniform performance easier to achieve.

As E-glass fibres are derived from natural materials like sand, clay and dolomite, the origin of the fibres is not an environmental issue like it is with petroleum based resins. However, conventional E-glass is considered to be harmful to the environment due to

lack of recycling and reusing options for glass reinforced composites and toxic emissions when manufacturing the fibres.

In addition to other constituents, conventional E-glass fibres contain 0.3–0.9% fluorine and 6–8% boron oxide that cause particulate and toxic emissions from production furnaces. Removing these emissions would result in 'greener' glass fibres. Currently, conventional E-glass fibres are being replaced by fluorine and boron free 'environmentally friendly' E-glass fibres [14]. However, boron gives glass fibres their chemical resistance and reduces the environmental degradation of the fibres [15]. Removing boron from E-glass fibres, whilst giving more environmentally friendly fibres, may increase their vulnerability to the environment and reduce their performance in maritime structures.

2.1.2 Plant Oil Based Resins

Resins from vegetable oils with potential industrial significance are polyurethanes, epoxies, and unsaturated polyesters. In this work two plant oil based resins are used: castor oil based polyurethane and epoxidized UV-curing linseed oil; which is why only polyurethanes and epoxidized resins will be discussed here.

Vegetable oils are triglycerides, i.e. esters of different fatty acids and glycerin. Double bonds in fatty acids are not very reactive. In order to make oils reactive for polymerisation, it is necessary to introduce functional groups, such as hydroxyl, carboxyl, amine, and epoxy groups, usually at the positions of double bonds of fatty acids [16].

2.1.2.1 Plant Oil Based Polyurethanes

Polyurethanes are the products of two components — polyols and isocyanates where the isocyanate is the curing agent. Only the polyol components are available as bio-based materials [16]. The mechanical, thermal and chemical properties of polyurethanes can be

Table 2.1: Mechanical properties of glass fibres and natural fibres [1, 7]

	Fibres					
Properties	E-glass	Hemp	Jute	Flax	Bamboo	**Unit**
Density	2.55	1.48	1.46	1.4	0.8	g/cm^3
Tensile stress at failure	2400	550–900	400–800	800–1500	391 –1000	MPa
Young's modulus	73	70	10–30	60–80	48–89	GPa
Specific strength	941	371–609	274–548	571–1071	489–1250	$MPa/(g/cm^3)$
Specific modulus	29	47	7–21	26–46	60–111	$GPa/(g/cm^3)$
Strain at failure	3	1.6	1.8	1.2–1.6	–	%
Moisture uptake	N/A	8	12	7	–	%

tailored by reactions with various polyols and isocyanates [17]. In polyurethanes the isocyanates react with the hydrogen in polyols thus crating an urethane link. Polyurethanes often use moisture for curing [18].

Vegetable oils impart high hydrophobicity and good thermal properties to polyurethanes. These resins also have good processability — good flow properties, suitability for machine applications, adjustable gel and curing time. Although vegetable oils are biodegradable materials, the crosslinked polymers are not. The claims of biodegradability are often made with the assumption that the biological origin of oils would necessarily translate into biodegradability [16].

Polyurethane resins represent a viable alternative to epoxy and polyester resins in their performance [14]. Polyurethane systems compare particularly well with epoxy resins of petrochemical origin because of easier processing and lower price [16]. Polyurethanes offer several advantages: no volatile components, fast reaction rates which could be adjusted with catalysts and temperature, high oil content and high crosslink density if necessary [16].

Crosslink density will directly affect the properties of the polyurethanes. A study showed that increasing crosslink density increases glass transition temperature T_g, modulus and strength of a polymer and decreases elongation at break [16]. There are different unsaturated fatty acids within plant oils. The placement of the double bonds in these acids is uneven, which leads to an uneven distribution of the hydroxyl groups in the polyol and thus an uneven distribution of crosslink sites in the network chains. By increasing the OH number (a description of the hydroxyl content of a polyol), one increases functionality of the polyol and its molecular weight, hence the increase in crosslink density. Canola, corn, soybean and sunflower oils give polyurethane matrix resins of very similar crosslink density and thus similar T_g values [16]. Crosslink density can be regulated with the addition of a low molecular weight crosslinker and the selection of the isocyanate component [16].

Castor oil is one of the few natural polyols that has been directly used as a raw polyol [17]. One of the characteristics of the oil-based polyols is that the reacting groups are not at the ends of fatty acid chains but somewhere in the middle. This gives a higher crosslink density than would occur if they were at chain ends, but also leaves a part of the chain pending (dangling chains). Dangling chains do not support stress when the sample is under load, and they could in fact act as plasticisers [16].

2.1.2.2 Epoxidized Plant Oils

Epoxy resins are formed by a long chain molecular structure that has reactive epoxy groups at either end. An epoxy group consists of two carbon atoms and an oxygen atom bonded to them. During curing with an hardener (typically amine) both of the materials

participate in the chemical reaction and both of the epoxy groups bind to each amine site forming a three-dimensional molecular structure [19].

Traditionally, epoxidized plant oils (especially soybean and linseed oils) are used as plasticisers for PVC [16, 17, 20]. The abundance of soybean and linseed oil has naturally stimulated research in polymerization of epoxidized oils and study of their applicability in coatings and as matrix resins for composites [16]. Fatty epoxides can be used directly as plasticisers to improve the flexibility, elasticity and stability of polymers [21]. The transition from glassy to rubbery behaviour is extremely broad for these polymers as a result of the triglyceride molecules acting both as cross-linkers and as plasticisers in the system. Saturated fatty acid chains are unable to attach to the polymer network, causing relaxations to occur in the network [22]. Epoxidized seed oils are also widely used for the synthesis of cationic UV-curable coatings [20].

Just like with polyurethanes, the OH number of plant oils needs to be increased to make the triglycerides more reactive in order to carry epoxidation out successfully [20, 21]. Epoxidized vegetable oils have internal epoxy groups, which are much less reactive and cannot be cured the same way as those with primary epoxy groups resulting in relatively low molecular weight and insufficient strength. Epoxidized vegetable oils often require hybriding with bisphenol-A type resins to improve the properties [16].

2.1.2.3 Castor Oil

Castor oil is a natural polyol with about 2.7 hydroxy groups per molecule. It gives rubbery polyurethane networks with insufficient crosslink density for application in composites as it stands, without processing [16]. The basic fatty acid constituent of castor oil is ricinoleic acid, which is a hydroxy monounsaturated fatty acid.

Castor oil is obtained by extracting or pressing the seed of a plant *Ricinus communis* that is native of tropical Asia and Africa [23]. The castor oil plant is a fast growing shrub or tree, reaching 12 m in height [23]. The oil is a naturally occurring resource, inexpensive and environmentally considerate. Castor oil has high viscosity, it is a pale yellow non-volatile and non-drying oil. It has a slight odour and slightly acid taste. In comparison with other vegetable oils, it has a good shelf life and it does not turn rancid unless subjected to excessive heat [24].

Before extraction, the castor beans have to undergo different steps of processing: clearing, drying, winnowing and grinding the beans into a paste. The extraction of oil from a castor seed is generally done by a combination of mechanical pressing and solvent extraction. In mechanical pressing, the seeds are crushed, steamed and then pressed by mechanical means. This procedure removes only around 45% of the oil in the seeds and the remaining can only be removed by solvent extraction. Solvents used for extraction

include heptane, hexane and petroleum ethers [24]. These solvents increase the environmental impact of the castor oil resin and further research is needed to investigate their environmental effect.

The extracted oil needs then to be refined to remove moisture, dirt, and other contaminants. After oil extraction and refining there is residue left that cannot be used as livestock feed due to the presence of toxic compounds and an allergen. The cake can be detoxified to reduce the risks to humans and animals [23]. Castor oil is used in applications including lubricants, process oils, feedstock for fuels, paints, coatings, polymers and foams [23].

Akaranta and Anusiem [25] showed that it is possible to use bioresource solvent for castor oil extraction. Cangemi et al. [26, 27] have investigated biodegradability of castor oil based polyurethane and showed that this material does biodegrade in the presence of specific microorganisms.

It has been found that increasing styrene concentrations (up to 30 wt%) during epoxidation of castor oil based polymers lead to an increase in flexural strength and modulus. Cross-link densities of castor oil polymers were compared to soybean oil based polymers. With the same amount of styrene, castor oil polymers showed better performance. The cross-link density increases with increasing styrene concentration thus leading to a higher strength. The resulting mechanical properties of 30 wt% styrene polymers are: flexural strength 104.23 MPa, flexural modulus 1.95 GPa, T_g 144 °C. Additionally, castor oil was directly malinated and castor oil maleates (control specimens without styrene) were also prepared. Control specimens showed flexural strength of 32.83 MPa and flexural modulus of 0.78 GPa, T_g 72 °C [22].

Castor oil resin Rescon 502 with unknown chemistry by Bioresin is used in this research. The mechanical properties of the pure resin system have been investigated by Derobert [28] showing Young's modulus of 0.8 GPa and tensile failure stress of 18 MPa. The properties of different resin systems are given in Table 2.2.

2.1.2.4 Linseed Oil

Linseed oil and flax fibres are manufactured from two different types of linen plants, one has been grown for seeds and the other for fibres specifically [29]. The oil extraction from linseed seeds is carried out with mechanical pressing and the oil is usually used as a drying oil for surface-coating applications. Andjelkovic et al. [30] present tensile properties for linseed oil based copolymer: Young's modulus was found to be 99.9 MPa and tensile failure stress 5.6 MPa. Wallenberger and Weston [16] report on tensile properties of linseed oil based polyurethane showing tensile strength of 57 MPa, elongation at break 6%, Young's modulus of 1.3 GPa and glass transition temperature 76 °C. These very different values show how much the properties vary with different chemistry.

The linseed oil resin used in this research is UV-cured. According to the resin manufacturer Sustainable Composites Ltd., the resin is made of 95% vegetable oils and 5% photoinitiator. Unfortunately there is no information on the mechanical properties of this specific linseed oil resin. However, Zong et al. [31] looked at the mechanical properties of UV-cured epoxidized linseed oil based films. The authors used different combinations of the resin system, one of them containing 96% epoxidized linseed oil and 4% photo initiator. This combination is similar to the linseed oil resin manufactured by Sustainable Composites Ltd. The authors found tensile strength to be around 18 MPa, tensile modulus 1 GPa, and elongation at break 2.5%. Glass transition temperature was found to be 89 °C. The comparison of mechanical properties of different resin systems is brought out in Table 2.2. There are also other properties, like dimensional stability, heat resistance, impact resistance, processing and chemical resistance, that need to be considered when choosing materials for maritime structures. However, investigating these properties is beyond the scope of this thesis and the focus will be on moisture uptake and its effects on the flexural properties.

Table 2.2: Mechanical properties of epoxy and plant oil based resins [16, 22, 28, 30, 31, 32]

Properties	**Resins**			
	Epoxy	Castor Oil	Linseed Oil	Linseed Oil (UV-cure)
Tensile strength, MPa	75	18	6–57	18
Tensile modulus, GPa	3.2	0.8	0.1–1.3	1
Flexural strength, MPa	–	33–104	–	–
Flexural modulus, GPa	–	0.8–2	–	–
Strain at failure, %	4.1	7.2	6.0	2.5
T_g, °C	83	72–144	76	89

2.1.3 UV-Curing

Ultraviolet (UV) curing is known to be a hardening process of liquid material when it is exposed to UV radiation. Depending on an application, UV-curing resin systems are composed of base polymer, non-solvent, diluent and photoinitiator. UV-curing can be based on either free radical systems or cationic systems. Cationic systems, like the linseed oil resin used in this research, are based on epoxidized components. With a free radical system, polymerization stops as soon as the light is eliminated. In cationic systems some cure does continue after the light source is removed [31].

The linseed oil resin used in the current research is cured by exposure to UV-light. UV-curing differs from thermosetting curing process in the sense that by exposing photoinitiator to the UV-light the photoinitiator generates a species that acts as a catalyst.

Once the catalyst has been formed the curing process can start [33]. However, the need for exposure to UV-light still introduces some new aspects to consider when analysing the performance of the UV cured resin systems.

2.1.3.1 Advantages and Limitations of UV-Curing

The advantages of UV-curing are very fast room temperature cure (matter of minutes rather than hours), reduced volatile organic compound emissions, absence of gel time leading to improved laminate quality [34], one part resin systems negating the need to mix or pot life concerns, cure on command that allows precise fibre alignment before curing, complete fibre wetting and the removal of entrapped air [34], and low energy consumption [35].

On the downside, UV-curing needs UV-light to penetrate the whole material, restricting the thickness of the material. Also, UV-light cannot reach complex corners and shady areas. Park et al. [35] found that the degree of cure in UV-curing systems is lower than in thermal curing settings because of the penetrating limitation of UV-radiation. That leads to lower interfacial strength in UV-curing composites. In the work carried out by Park et al. [35] the interfacial strength of UV-cured composites was only half of the interfacial strength in thermally cured composites. In addition, the tensile stress-strain curve showed lower failure stresses and higher elongation for UV-cured composites.

2.1.3.2 UV-Curing of Linseed Oil

Wallenberger and Weston [16] report on the manufacturing process of UV-cured modified epoxidized linseed oil (ELO). The curing process involved cationic polymerization with onium salt initiators in the presence of UV-light. The initiator and ELO were mixed and applied by brush to the glass cloth. Since cationic polymerization is affected by bases, it was found that sizing agents on the glass fabric and solvents affected gel time which varied from 7 minutes for the control sample to 32 min for the sample with 3% extract of the sizing agent. The composite was irradiated with UV-light and the depth of curing was up to 1–1.6 mm.

Tensile strength of the glass fabric reinforced composites with ELO was relatively low, of the order of 20–30 MPa, and moduli were about 3 GPa. T_g was 68 °C. Combining of ELO with bisphenol-A epoxy resins was necessary to improve mechanical properties. The authors of the research have envisaged the potential use of linseed oil based composites in low-performance applications. In general, UV-curing is difficult to apply to materials that are not transparent and are in thick layers, and requires fairly complex and expensive initiators [16].

2.1.3.3 UV-Curing of Other Composites

Compston et al. [34] looked at the mechanical properties of glass/vinylester composites after UV-curing in comparison with room temperature curing and post curing. The authors found that UV-cured material resulted in higher tensile and flexural strength. Interlaminar shear strength was similar for both UV-cured and post-cured specimens. However, micrographs of the specimens showed clean fibres for all three types of specimens indicating that fibre-matrix bonding was not good in any of the specimens. Therefore, the comparison did not really identify the differences between UV-cured and thermally cured specimens.

In addition to the mechanical testing Compston et al. [34] looked at secondary bonding with UV-curing. They first cured 10 layers of resin infused reinforcement. After it had fully cured they added additional 10 layers and cured the material. The curing time for both cases was 10 minutes. As a result, the interlaminar shear strength of UV-cured and secondary bond UV-cured specimen was similar. This means that UV-curing allows the manufacture of products in steps without affecting the mechanical properties of a laminate. This feature may be useful when repairing structures.

Ramli et al. [36, 37] looked at the effects of UV-curing time and photoinitiator addition to the tensile properties of woven glass reinforced epoxy and vinylester resins. The authors found that for both materials the optimum curing time was between 6 and 9 minutes, beyond that time the tensile properties started reducing. The tensile strength after 6–9 minutes of curing was between 150 and 200 MPa for both materials. At the same time, the density of the materials was highest with longer curing time, 12 minutes. The authors also mentioned that actually vinylester resin did not fully cure before 2 days after UV exposure. In their second paper [37] the authors find that a small amount of photoinitiator increases the tensile properties of epoxy and vinylester composites. However, when this amount was increased by 10 times, the tensile strength dropped around 20% for both materials.

As a conclusion, the performance of UV-cured specimens depends on the transparency of the resin system, sizing on the fibres, UV-light exposure time, thickness of the laminate, and the amount of photoinitiator used. If not properly understood, varying these parameters can result in a poor composite performance.

2.2 Moisture Uptake in Composites

Durability is one of the key requirements for composites in maritime structures. As the materials are exposed to extreme humidity, UV-light and temperature, it is important to understand how materials behave in the varying environmental conditions. Moisture

absorption and its effects on the mechanical performance of composites is one of the key problems in maritime applications and is the main concern of this research.

Ingression of water in a laminate occurs through diffusion in matrix (transport of water molecules into the matrix [38]) and capillary flow in voids, cracks and also the imperfect fibre-matrix interface. Some of the known effects of water absorption include plasticisation, debonding stresses across the resin-fibre interface induced by resin swelling and chemical attack by the water on the fibre-resin bond leading to a reduction of the mechanical properties [3].

2.2.1 Diffusion

In a wet environment, a composite material absorbs water via its surfaces and the water is often assumed to penetrate into the material obeying the existing diffusion laws. In 1979, Loos and Springer [39] published research looking at moisture absorption of glass/polyester composites in different fluids. The extensive research included moisture absorption in distilled and salt water at 23 and 50 °C. As a result, it was found that at room temperature the moisture uptake followed Fick's diffusion in both distilled and salt water. However, contrary to Fick's diffusion model, immersion in distilled water at 50 °C eventually led to a loss in weight whilst conversely in salt water the moisture uptake continued after the initial equilibrium content was achieved. From the research carried out it was obvious that a more complex model is needed to describe moisture absorption beyond the limits of Fick's model. Nowadays there are two laws generally used to describe diffusion in composite materials: Fick's and Langmuir's law. Fick's has been found to apply for temperatures up to 40 °C, Langmuir's law generally applies at temperatures higher than that [40].

2.2.1.1 Fick's Law

Fick's law (also known as Fickian) assumes that water enters freely into the material without reacting with the components ('single-phase' model) [41]. However, it has been generally accepted that the matrix does react with water (see section 2.3.1) contradicting strongly with the key assumption used in Fick's diffusion.

Fick's law predicts that the mass of water absorbed increases linearly (at least 60% of the maximum moisture uptake) with the square root of time, and then gradually slows down until an equilibrium condition is reached [42, 43] (Figure 2.1).

Fick's diffusion model was originally meant to be used with homogeneous materials and assumes the diffusion to be constant throughout the material [43]. This, unfortunately, is not the case with composites due to their heterogeneous nature. However, the Fick's

model (see equation 2.1 [41]) has been found to give fairly good results with composites [3].

$$D_x \frac{\partial^2 c}{\partial x^2} = \frac{\partial c}{\partial t} \tag{2.1}$$

Where c is the concentration of the diffusing substance, x the space coordinate measured normal to the section, D the diffusion coefficient, and t is time.

There are two different coefficients of diffusion: one parallel to the fibres and the other perpendicular to them. When the edges of specimens are sealed, the diffusion can be considered to occur only in one direction. The through-thickness diffusivity is determined from the slope of the initial linear region of the moisture uptake curve.

2.2.1.2 Langmuir's Law

Langmuir's model, contrary to the Fick's law, assumes that a number of water molecules become chemically bonded to the resin and can no longer diffuse. The number of bonded and free molecules varies over time until equilibrium is reached. Langmuir's model describes 'two-phase' diffusion, since bonded and free water phases are present (see equations 2.2, 2.3 and 2.4). Initially, the weight increase in the specimen is directly proportional to the square root of time, but then continues to increase slowly (unlike Fick's model) until saturation is reached (Figure 2.1). If the quantity of bonded water can be neglected, the model becomes equivalent to Fick's law. This is can be seen in the following Langmuir's equations where C drops out and equation 2.2 becomes equivalent to Fick's law [40].

$$D_x \frac{\partial^2 C}{\partial x^2} = \frac{\partial C}{\partial t} + \frac{\partial c}{\partial t} \tag{2.2}$$

$$\frac{\partial c}{\partial t} = C\gamma - c\beta \tag{2.3}$$

$$\gamma C_\infty(H) = \beta c_\infty(H) \tag{2.4}$$

Where C and c are the bonded and free water concentrations respectively, c_∞ and C_∞ are the free and bonded water concentrations at saturation, β is the probability of bonding (concentration of free molecules greater than the concentration of bonded molecules) per unit time, γ is the probability of release (concentration of free molecules lower than the concentration of bonded molecules) per unit time and H is the relative humidity [40]. No parameter is specified for immersion. These parameters are specific for the fibre/resin system used and should be found for every material separately.

Langmuir's law involves more parameters and is therefore more flexible in describing diffusion properties than Fick's law. At the same time, it has been found that these parameters make a difference for temperatures higher than 40 °C; diffusion in specimens

immersed in water at 40 °C or lower have been shown to follow the much simpler Fick's law [40].

2.2.2 Parameters Affecting Moisture Uptake

2.2.2.1 Voids

One of the main features affecting the performance of composite materials are voids that can be found in various shapes and sizes. Voids occur mainly in resin rich areas and there are two main causes for their formation: air entrapment in a composite during manufacturing and volatile compounds forming gas bubbles inside a composite while curing [44]. The problem is emphasised with high viscosity resins that provide poor wetting of fibres and make it difficult for the resin to penetrate fibre bundles and displace air [44].

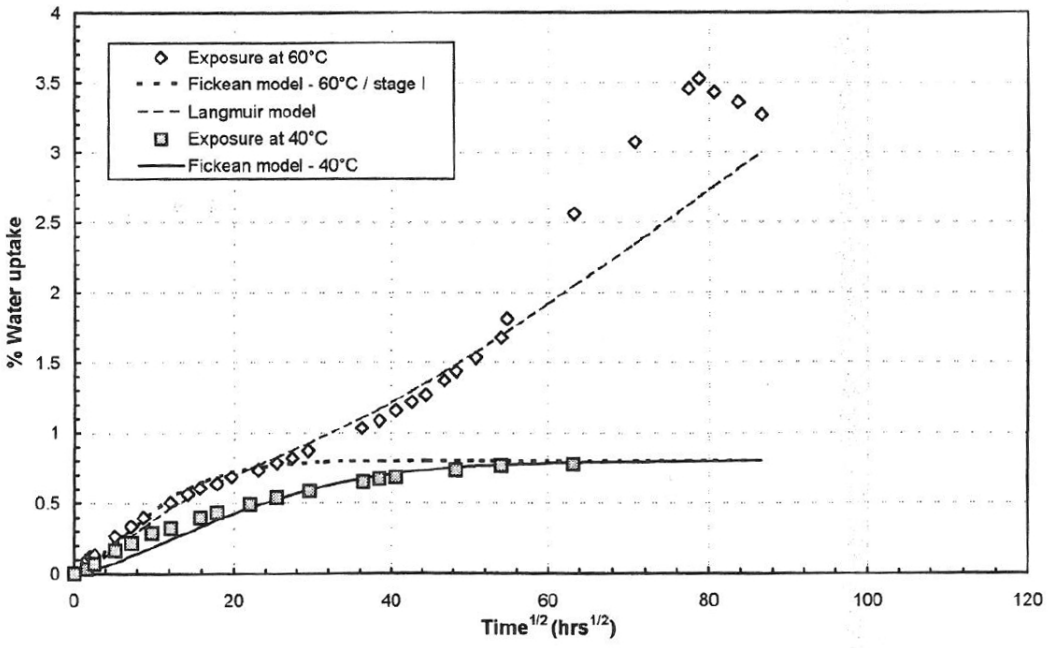

Figure 2.1: Moisture uptake curves for Fick's and Langmuir's diffusion models in glass/polyester [40]

The negative effect of voids on static strength of composites has been extensively investigated [42, 45, 46, 47, 48, 49]; there is less known about the effects of voids on moisture uptake and hygrothermal ageing. Thomason [45] looked at the effects of voids on moisture absorption in more detail and found that the rate of water uptake and the maximum level of water absorption in glass reinforced epoxy composites are highly dependent on the void content (Figure 2.2). In some composites the presence of only 1% voids in a composite was found to more than double the amount of water it absorbs. Less than 1% void content did not seem to affect the moisture uptake in the glass/epoxy

composites tested. The research carried out by Thomason clearly indicates that voids do accelerate the diffusion of water into composites. However, the role of other parameters like distribution of voids or degradation of interface have not been discussed in the work thus making the extent of the effects of voids hard to estimate. Hancox [50] also showed increase in moisture uptake with higher void content, although less extensively than Thomason.

It is hypothesised that voids also provide sites for storage of water at much higher concentrations than in the resin and are therefore raising the maximum water absorption level of composites. This is believed to be the cause of blistering in some composites [3]. Water solubles of the matrix reacting with water leads to osmotic pressure in voids and cracks, causing them to increase in size and coalesce together. In more detail, the osmotic pressure is generated in the bubble by water soluble constituents leached from the matrix and the interface, leading to bond fracture, growth of cracks into the resin from the fibre surface, and growth of discontinuous bubble-like regions at the fibre interface [51]. This theory has limited visual proof [52] and needs more research to verify how exactly does water affect the defects inside a composite.

2.2.2.2 Interface and Cracks

Composites usually absorb more water than unreinforced polymers with regard to the total volume of the polymer. The mechanisms of moisture penetration in composites are much more complex than in the case of unreinforced matrix. Water can diffuse rapidly into composites along the fibre/matrix interface if wetting of the fibres by the resin is incomplete. This together with capillary flow and moisture transport through

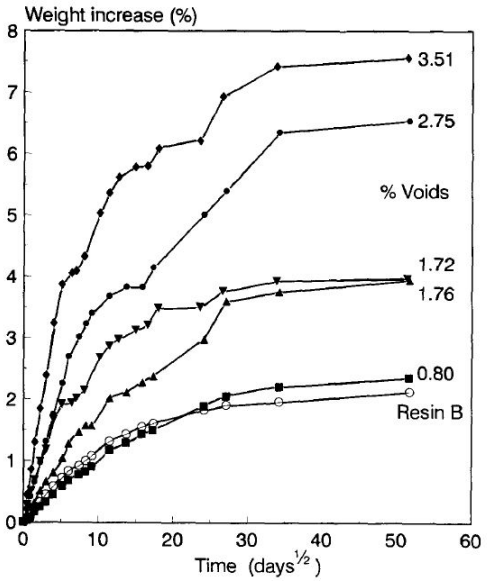

Figure 2.2: Moisture uptake curves for glass reinforced epoxy resin system with different void contents [45]

micro-cracks into the matrix present additional mechanisms of moisture penetration into composites. These mechanisms have been found to increase both the rate and the maximum capacity of moisture absorption [38].

Fibre/matrix debonding is promoted by radial stress at high moisture content and elevated temperatures. Once fibre/matrix debonding has occurred, the internal stress-state is altered and more moisture will diffuse into the debonded regions, which further accelerates the degradation process [53]. The localised water entrapment in debonded areas may lead to osmotic pressures described previously.

Capillary flow and subsequent hygrothermal degradation in composites can be suppressed by promoting good bonding between fibres and matrix. This can be achieved by good chemical bonding and increasing the wetting between the fibres and matrix, thus constricting the diffusion path of the moisture [38].

2.2.2.3 Water Chemistry and Temperature

To date, the most detailed research on the effects of water temperature and chemistry on moisture uptake of composites is from Loos et al. [39]. Loos et al. looked at different E-glass reinforced polyester composites immersed in distilled and salt water; here are discussed the two higher fibre weight fraction laminates (SMC-65 has 65% weight fraction of fibres and SMC-30EA has 28% weight fraction of fibres). The experiments were carried out at 23 °C and 50 °C. In Figures 2.3 and 2.4 the data points represent experimental data and solid line shows the theoretical moisture uptake according to Fick's law.

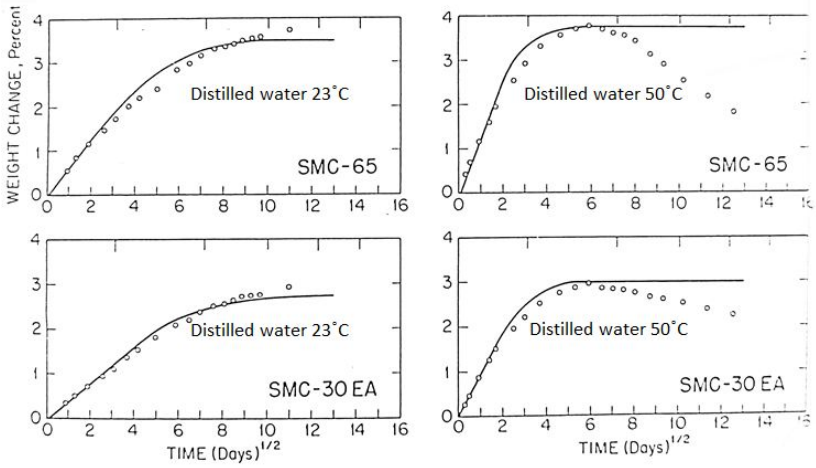

Figure 2.3: Weight change as a function of time of specimens immersed in distilled water [39]

Loos et al. [39] were mainly interested in the effects of water temperature and chemistry on the maximum moisture content and speed of moisture uptake (diffusivity). Diffusivity was found to be mainly dependent on the water temperature, less on water chemistry

and the material tested (Figures 2.3 and 2.4). The moisture equilibrium content was insensitive to temperature while being highly dependent on water chemistry and material. In salt water, the water uptake speed and quantity was less affected by temperature than in distilled water. Also, the lower fibre weight fraction specimens SMC-30EA were found to absorb much less water in salt water than in distilled water.

In glass/epoxy composites the ageing test temperature has been directly related to the rate of water diffusion and the permeability of the system has been found to increase with temperature. Also, in glass/epoxy the saturation level may depend on the temperature, though it may not be the case for all curing treatments [54].

Le Duigou et al. [55] looked at the seawater ageing of flax/PLLA (Poly(L-Lactic acid)) composites. The ageing was carried out in natural seawater at temperatures 20 °C and 40 °C. The moisture uptake of pure PLLA doubled with higher temperature being around 0.3% at 20 °C and 0.6% at 40 °C. The moisture uptake of flax/PLLA composites also doubled, being around 4–5% at 20 °C and 9–10% at 40 °C.

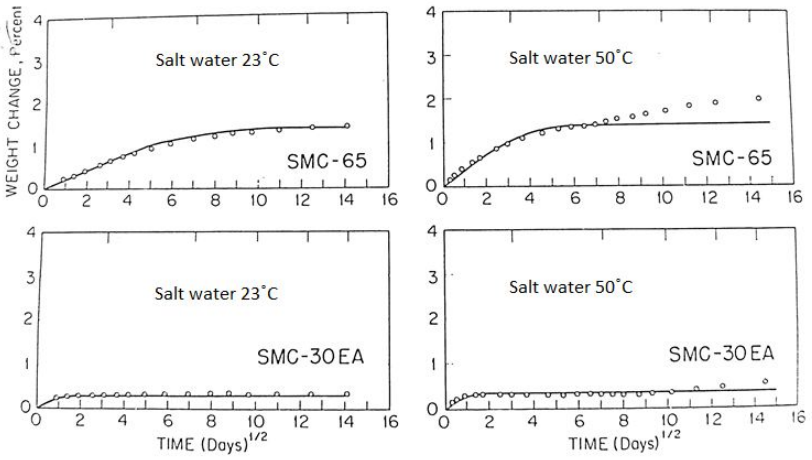

Figure 2.4: Weight change as a function of time of specimens immersed in salt water [39]

2.2.2.4 Specimen Preparation

Mouritz and Kootsookos [56] looked at the seawater durability of E-glass/polyester. They found that thicker specimens take longer time to reach moisture equilibrium content. Le Duigou et al. [55] also found the moisture uptake time and quantity to be dependent on specimen thickness of flax/PLLA samples. In their experiments the moisture equilibrium condition was reached after 15 to 37 days, thicker samples took longer to reach the equilibrium content than thinner ones. The moisture equilibrium content was 0.7–1.0% depending on the thickness. The moisture uptake started declining after reaching moisture equilibrium content, just like glass/polyester did [56]. Le Duigou et

al. [55] and Mouritz and Kootsookos [56] suggested that there may be an irreversible chemical degradation occurring.

Figure 2.5 shows moisture uptake curves for the two types of specimens tested by Le Duigou et al. [55]. The thickness of film stacked specimens was 2.1 mm and the edges were not sealed, injection moulded specimens were 4.0 mm thick and the edges were sealed. It can be seen from the figure that sealing the edges significantly reduces the moisture uptake of flax reinforced composites. Compared with glass/polyester and glass/epoxy specimens discussed in the previous sections, flax fibres increase the moisture uptake of flax/PLLA significantly (Figure 2.5) [55].

2.2.3 Detecting Moisture Uptake

2.2.3.1 Nuclear Magnetic Resonance

Water detection in composites has been successful with the nuclear magnetic resonance (NMR) imaging technique [52]. Kotsikos et al. [52] looked at salt water moisture absorption in 0 °/90 ° glass reinforced polyester immersed at 40 °C and 60 °C. It has been hypothesised that moisture does not progress with a uniform profile and that there are preferential water storage areas inside the composite. Before the research done by Kotsikos et al. [52] there was no conclusive proof to support these statements.

Kotsikos et al. [52] used nuclear magnetic resonance (NMR, also known as MRI) to investigate water ingress into composite specimens. The nuclei imaged by NMR are mobile protons (hydrogen nuclei), as in water, and also protons in rigid structures. A NMR image can therefore be thought of as a representation of the density of nuclei throughout an object. The 10 000 h aged specimens were compared to non-aged composites.

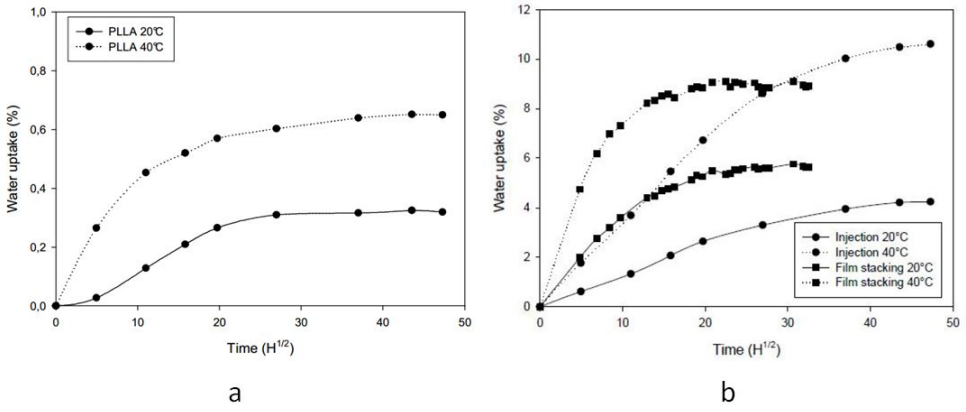

Figure 2.5: Absorption behaviour of PLLA alone (a) and flax/PLLA composite (30% fibres by weight) (b) manufactured by injection moulding and film stacking [55]

From the NMR images it was clear that the water does not diffuse uniformly in the composite but concentrates along the fibre/matrix interface. The bonding layer is extremely reactive due to its large surface area per unit volume. The degradation of the interface region seems to be more rapid than that of fibre and matrix. The NMR confirms that the concentration of water at the matrix/reinforcement interface is much higher than that of the bulk resin (Figure 2.6). The images also confirm that a wicking process is operative as it shows the water tracing the reinforcement geometry. This however may be due to the non-sealed edges of the specimens and may not be representative of through thickness diffusion.

Prolonged exposure at 60 °C resulted in microcracking of the resin and absorption of water through capillary action thus leading to the Langmuir type of diffusion model instead of Fick's model more used for composites immersed at 40 °C. The NMR images of 7000h aged specimens showed severe cracking, delamination and large voids within the samples that were not noticed before immersion, indicating growth of voids due to moisture uptake and osmosis.

2.3 Hygrothermal Ageing

Changes in the structure and the mechanical properties of composite materials due to moisture uptake are dependent on the exposure time, temperature, constituent materials and water chemistry (see section 2.2). The changes in the properties due to moisture uptake can be classified according to their effects as reversible, irreversible or a combination of both. Reversible changes include swelling and plasticisation of the polymer matrix, the mechanical properties can usually be restored by drying. Irreversible damage results usually in permanent damage to the fibres, matrix cracking, debonding of

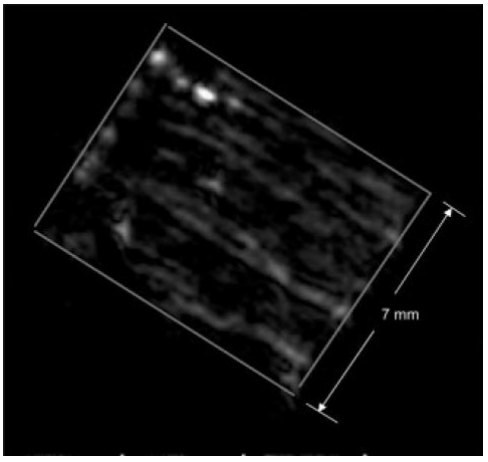

Figure 2.6: Through thickness NMR image of water in a laminate exposed at 60 °C for 7000h. Lighter areas are water in the image; the lighter the area the higher the moisture content [52]

the fibre/matrix interphase region, and delamination [57]. Because of these changes it is crucial to understand which parameters control the process of moisture absorption and degradation of mechanical properties in order to estimate the long-term performance of composite materials.

2.3.1 Matrix

As the water molecules diffuse into the polymer, there are changes in interactions between the atoms of the polymer chains, between polymer chains and diffusing water molecules, and between the penetrating molecules themselves [42]. As a result, penetration of water molecules can cause a change in the molecular structure and also swelling of the polymer. The effects of fluid ingress on the matrix are often considered secondary in comparison to the damaging effects of water on the fibres and the interface [57]. However, the performance of the matrix affects the load transfer from matrix to fibres while also protecting the latter; hence the effects of water on the performance of the matrix should not be underestimated.

The first response to diffused water is resin swelling [51]. Lin and Chen reported on increased moisture uptake after cyclic hygrothermal loading and related this behaviour to matrix swelling [42]. Their work indicates that matrix swelling and therefore the related changes in matrix properties may not be reversible as was suggested by Liao et al. [57].

The second observable change due to moisture uptake is debonding along the fibre-resin interface [3] indicating degradation of the interface region and/or hygrothermal stresses occurring inside the material. However, Plueddemann [51] stated that debonding in composite materials occurs only while being immersed in water at elevated temperatures. This suggests that temperature and thermal expansion may have a greater role than water does alone in hygrothermal stresses leading to delamination.

The molecular structure of the matrix is altered by the interactions between the hydroxyl groups of the polymer and water molecules. The results of these interactions are often observed as dimensional changes, as discussed previously, and changes in glass transition temperature (T_g) values. Generally, water ingress reduces T_g resulting in changes of the matrix structure at lower temperatures than with dry material, causing transition from a glassy polymer into a rubbery one [15]. Reduction in T_g can therefore cause a significant reduction in mechanical properties of a polymer already at room temperature. La Duigou et al. [55] found that the reduction in T_g was greater at higher water temperatures. This may affect the conversion of accelerated ageing data into non-accelerated one. The changes in T_g are often related to the plasticising effect of the water on the polymer, seen as a slight decrease in the elastic moduli [54, 58].

Permanent changes in the polymer have also been witnessed by Le Duigou et al. [55] who looked at the molecular weight of flax reinforced PLLA resin after seawater immersion. After immersion, the molar mass had reduced for all the specimens tested suggesting permanent changes in the polymer. The changes were attributed to hydrolysis and molecular chain breakage in the polymer.

2.3.2 Fibres

It has been experimentally proven that more broken fibres can be found in environmentally aged glass reinforced composites than in the unaged ones implying degraded in situ fibre strength [57].

Damage of glass fibres by fluids is initiated by chemical reactions between the two. The extent of damage depends on the fluid type, fluid concentration, as well as the composition of the fibres under attack [57]. It has been proposed that the silicate network of glass is destroyed by water molecules and as a result causing damage to the fibres.

All silicate glasses are mixtures of metal oxides dispersed in a silica network. These oxides are hygroscopic and lead to a degradation of glass fibres [51] that involves the following mechanisms:

- ingress of water molecules into the glass [15];
- ionic exchange where metal ions in the glass are replaced by the hydrogen ions of water [15, 57, 59]. In [59] this behaviour was related to the size of ions and it was proved that replacing the metal ions with larger ions resulted in fibre surface under compression instead of tension therefore eliminating the stress corrosion (corrosion that only occurs at the presence of stress) problem;
- hydroxyl ion buildup on the fibre surface and internal flaws [15, 59]. While Choqueuse and Davies [15] consider this to be reversible phenomena, Erickson and Plueddemann [59] suggest that hydroxyl ions attack the silica network of glass causing pitting on the glass fibre surface leading to irreversible damage. At the same time, Kotsikos et al. [52] state that pitting damage to fibres is negligible.

Findings about hygrothermal stresses acting in aged materials have also been presented by Liao and Tan [53]. In their research the fibre strength degradation became obvious after 500h of immersion. The results they gained strongly suggest that the accelerated rate of in situ fibre strength degradation could arise from residual tensile stress because of moisture absorption and subsequent stress corrosion of the glass fibres. From this it can be assumed that strength degradation of the composite could be attributed, at least in part, to in situ fibre strength degradation. In addition, it was shown that zero

stress (no external loads) ageing of unidirectional composite under hygrothermal loads does not imply that fibre and matrix are stress free, and the internal stresses induced by hygrothermal loads accelerate the rate of strength degradation [53].

2.3.3 Interface

Although it is recognised that moisture uptake affects the performance of fibres it is also generally assumed that majority of the moisture uptake in glass reinforced composites comes from the matrix. This results in a significant mismatch in the moisture induced volumetric expansion between the matrix and the fibres, leading to high localised stress and strain fields and to degradation of the fibre/matrix interface [60].

Numerous studies have looked at the influence of the interface region on the degradation of composite materials' properties due to moisture absorption [51, 57, 58]. As a consequence of fluid attack, the fibres may be left debonded from the matrix, making them highly vulnerable to water.

According to Liao et al. [57] the fibre/matrix interface has a controlling effect on the environmental ageing of GFRP. By using a micro-bond pull-out technique it was shown that the bond strength of E-glass/epoxy microcomposite degraded about 40% after ageing in 88 °C water for an hour. When the failed specimens were examined under SEM, fibre surfaces with adhered residue were seen in as-received specimens, Figure 2.7 (a), while smooth fibre surfaces with much less residue were seen in aged specimens, Figure 2.7 (b), indicating degraded interfacial bonding by environmental ageing [57].

Plueddemann reported [51] that the interface between clean (not silane coated) fibres and matrix is rapidly destroyed by water even at room temperature. Improved interfacial properties, especially due to chemical bonding, tend to delay degradation of the interface and reduce loss in mechanical properties of a composite [57, 58].

Surface treatment of reinforcements is a common method for improving the chemical bonding between fibres and matrix. By influencing the interface structure and properties,

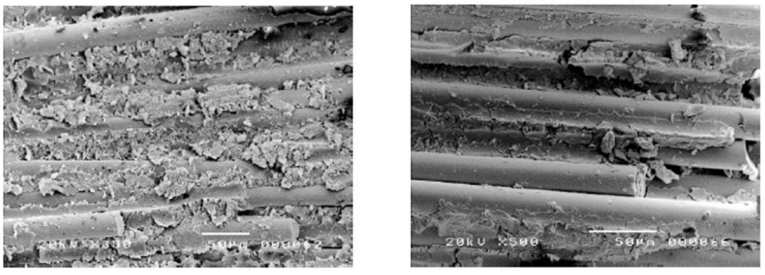

a b

Figure 2.7: Failure surface of flexural specimen before (a) and after (b) environmental ageing [57]

coupling agents have a great effect on the moisture uptake and degradation of composite materials. The most commonly used coupling agents are difunctional organosilicon compounds named silanes [51]. Nowadays, glass fibre manufacturers are still trying to improve coatings of the fibres and due to the competition very little information is available about the coupling agents used. Therefore, it is very difficult to assess the chemical bonding properties between commercial glass fibres and matrices.

2.4 Failure of Composite Materials

One of the key problems with moisture uptake in composites is the effect of water on the mechanical properties and performance of the material. Adding water to the polymer structure and free volumes inside the composite affects the material's structural performance. Composites are the strongest if the loads are successfully transferred from matrix to high load bearing fibres. Therefore, if water uptake disturbs the capability to transfer loads from the matrix to the fibres, the whole material becomes weaker.

2.4.1 Effects of Moisture on Flexural Properties

Liao et al. [57] report on the degradation of flexural properties in 0 ° (along the span) and 90 ° (across the width) fibre orientation E-glass/epoxy specimens after immersion in water at 35 °C. It is reported that the transverse modulus and strength of E-glass/epoxy were reduced to less than 50% of its dry value after 4800 h of immersion. Compared to 0 ° specimens, 90 ° specimens showed more significant drops in flexural strength and modulus, which is attributed to the degraded interface region [57].

Lassila et al. [13] looked at moisture uptake in different glass reinforced composites and its effects on the flexural properties. The authors found water absorption in unidirectional E-glass reinforced composites to be linearly dependent on the volume fraction of the fibres (V_f). The reduction in flexural strength was also found to be dependent on moisture uptake: higher moisture uptake led to a greater reduction in properties. 30 days of immersion at 37 °C resulted in 20–54% flexural strength loss and 15–43% flexural modulus loss, depending on the resin system used (45% V_f). The authors suggest that greater moisture uptake causes greater reduction in flexural strength due to matrix plasticisation. The flexural strength was also found to be dependent on the failure mode. It was concluded that if the failure includes compressive stresses, microbuckling or shear splitting, the failure stresses are lower than with tensile, fibre dominated failure.

2.4.2 Factors Affecting the Flexural Failure Modes

As stated in the paper by Lassila et al. [13], the strength of a composite depends on the flexural failure mode. If the moisture ingress causes changes from a fibre dominated failure into a matrix dominated one, it is obvious that the strength of the material will be lower. There is very little research done on the effects of moisture on failure modes; only one was found for this thesis (by Buehler and Seferis [61]). The lack of research in this field is largely due to the difficulties associated with the tests and complexity of the problem. Investigation of the failure modes forms a major part of this thesis.

Flexural failure is usually a complex problem involving fibre, matrix and interface failure. Understanding the test results may be difficult and materials parameters like fibre volume fraction, loading span-to-thickness ratio, fracture mechanisms and voids need to be considered.

Buehler and Seferis [61] looked at moisture uptake in glass/epoxy prepreg and the effects on flexural properties over a 1200h ageing period. The flexural strength reduced by 62% and flexural modulus by 30%. The authors showed that moisture and temperature exposure can lead to a change in failure modes in flexural testing from filament dominated to matrix dominated. This results in high shear rate induced in the flexural test by matrix plasticisation. The large decrease in the properties was attributed to poor interfacial adhesion and changes in the failure mode.

Davidovitz et al. [62] looked at the changes in flexural failure of Kevlar/epoxy composites with different volume fractions. The loading span-to-thickness ratio was 8, meaning that the failure was interlaminar shear (loading span-to-thickness ratio of 4) rather than flexural (ratio of 32 or 20). However, Davidovitz et al. found 2 different failure modes dependent on fibre volume fraction. Lower volume fraction (V_f=0.46) led to a failure in the longitudinal fibres on the tensile loading side of the specimens. The higher volume fraction (V_f=0.62) specimens were found to fail by shear delamination in the neutral plane. The latter failure mode was explained with increasingly high proportions of interface at the shear plane due to higher fibre volume fractions.

Falchi and Gracia [63] looked at the effects of different loading spans on the flexural failure modes of unidirectional carbon/epoxy composites. The loading span-to-thickness ratio between 25 and 50 revealed broken fibres only in the lowest plies submitted to tensile stress. Loading span-to-thickness ratios of 15 to 20 showed fibre breakage in the tensile region and transverse fault deepening towards the centre of the specimen with ratio decreasing from 20 to 15. These specimens show a mixed failure mode where compressive rupture occurs after the tensile rupture. It is suggested that flexural testing giving a compressive rupture prior to tensile rupture indicates a premature decohesion between fibre and matrix. No tensile failure was observed with loading span-to-thickness

ratios of 5 to 12.5, instead a development of compressive failure with longitudinal delamination occurred.

Cantwell and Morton [64] reported that delaminations that are more common in multidirectional long fibre composites may reduce compressive strength of a composite by 50% thus reducing the flexural strength of a composite. Delamination is often preceded by a more local mode of damage, like fibre-matrix debonding, that does not seem to have a significant effect on the load-carrying capability of a composite.

Sate et al. [65] were looking at the flexural fracture mechanisms in unidirectional 60% fibre volume fraction carbon/epoxy composites. It was noticed that the failure in the material progressed in the following order: fibre breakage, matrix cracking, partial delamination and a final catastrophic crack propagation. Such a failure progression suggests a complex compressive/tensile combined failure mode with initial failure developing on the tensile side of the specimen (as reported by Falchi and Gracia [63]). The breakage in a fibre in the early stage of failure was considered to be caused by a defect in the fibre because the breakage occurred randomly at a relatively low load [65].

2.5 Damage Detection

2.5.1 X-Ray Computed Microtomography

X-ray computed microtomography (microCT) has emerged as a method for obtaining three-dimensional images of structured materials [66]. MicroCT imaging has been proven as a useful non-destructive testing method for looking at the damage and failure areas inside composite materials [67]. MicroCT imaging method is based on the measurement of the different absorption coefficient of the materials crossed by a penetrate beam such as X- or γ-ray. A tomography system measures the attenuation of intensity from different angles to determine cross-sectional configuration with the aid of a computerized reconstruction. A series of X-ray microtomography images can then be used to characterize the object volume [66]. The term microtomography refers to results obtained with at least 50–100μm spatial resolution. Resolution lower than that is used to refer to tomography.

Schilling et al. [67] showed that commercially available microCT facilities can be successfully used to detect voids, matrix cracks and delamination, fibre breakage, and lateral delamination of glass/epoxy and glass/graphite composites. The authors managed to determine voids with sizes 0.25–0.5mm, matrix cracks and connected delaminations.

Cowley and Beaumont [68] looked at the effects the dye penetrant has on the material properties. The damaged specimens are soaked in the penetrant which impregnates any matrix microcracks or interfacial ply delaminations. One of the most commonly used dye

penetrant is zinc iodide (ZnI_2) and it has been noticed that it promotes stress corrosion cracking. The application of zinc iodide together with an applied load leads to a greatly accelerated damage evolution that is not desired in the aged composite samples.

2.5.2 Acoustic Emission Testing

Acoustic emission sensors detect elastic waves created by fibre breakage, matrix cracking and delamination and the technique has been shown to be a good indicator of damage inside composites [69, 70]. Most of the research concentrates on the parametric study as the simplest and least time consuming analysis method [70, 71, 72, 73, 74, 75, 76, 77]. However, the noise removal and separating the damage modes without inspecting the waveforms has proven to be a difficult task [75, 78]. Despite this, the parametric study still has the highest chance of being suited for structural health monitoring as it requires least data processing time; depending on the software and settings the results can be visible straight away [69].

There is parametric AE data available for conventional composites [70, 72, 73, 79] giving good basis for analysing the data from dry glass/epoxy specimens. However, the findings from different researchers rarely agree, depending on the material [70], lay-up and the specimen geometry [72, 78]. The effects of moisture uptake on the acoustic properties have been investigated less extensively, even less so with 'green' composites. Scida et al. [71], Akil et al. [74] and Le Duigou et al. [75] are some of the few researchers who have reported on AE data of aged 'green' composites.

Scida et al. [71] used AE to determine the failure mechanisms of dry and 38 days aged flax/epoxy composites. The main findings were based on amplitude and duration data, different parameter ranges were related to failure mechanisms mainly with the aid of literature. The authors concluded that with ageing the amplitudes and durations shifted towards higher values, the failure of the composites tested consisted of micro cracking of the matrix, fibre pull-out and fibre-matrix debonding. It was concluded that hygrothermal ageing does not induce any new failure mechanisms but only accelerates the degradation of the material.

Akil et al. [74] looked at the changes in AE amplitude and duration in jute reinforced polyester composites during tensile tests. Just like Scida et al. [71], the authors found that in dry specimens most of the amplitudes were in the range of 35–50 dB and that the amplitudes were increasing with ageing. The authors suggest that there is a shift from matrix related damage mechanisms to interface related ones.

Le Duigou et al. [75] report that the loss of linearity during tensile tests corresponds to the first damage detected with AE and in aged specimens the stress at first damage has dropped by 75%. The damage starts earlier in aged specimens and the development is more rapid. Just like the AE data from Scida et al. [71] and Akil et al. [74], Le Duigou et

al. also found that in unaged specimens the amplitudes of the hits concentrated around 40-45 dB and the amplitudes shifted towards higher amplitudes with ageing. None of the papers consider attenuation of the signal or any other changes in the signal due to moisture uptake; Le Duigou et al. suspect that the shift is related to the interfacial and fibre damage (they use flax/PLLA composites). As a conclusion, Le Duigou et al. consider the interfacial damage due to moisture uptake to be affecting the performance the most.

Barré and Benzeggagh [72] looked at the tensile failure of short glass fibre and polypropylene composites. With the aid of AE and SEM they found that AE hits with amplitudes of 40–55 dB correspond to matrix cracking, 60–65 dB — interface fracture, 65–85 dB — fibre pull-out phenomena, and 85–95 dB — fibre fracture.

Scida et al. [73] looked at the changes in tensile, flexural and shear properties of wet and hot aged glass/epoxy composites. The reinforcement was twill and satin weave. The authors used amplitude as the indication of changes in the damage and concluded that 40–60 dB is matrix cracking, around 65 dB interface fracture, and 90–95 dB fibre fracture. Unlike in green composites, the amplitudes shifted towards lower values with ageing and the authors relate that to the increasing matrix cracking and disappearance of interfacial cracking. The sudden failure of the aged material was explained with the weakened fibres. The analysis of the results did not consider signal attenuation, matrix plasticisation or weakened interface.

Ni and Jinen [79] tested single glass and carbon fibre epoxy composites under bending to determine the failure mechanisms. The authors acknowledged that amplitude can only be used for characterising material damage in the same test conditions due to attenuation problems. The authors also stated that amplitude cannot be used to observe differences in the interfacial strength in the material. Instead of amplitude the authors decided to use frequency and power spectra to look at the failure modes. They considered frequencies around 100 kHz to be epoxy matrix cracking, 250–320 kHz debonding of fibres/matrix and 400 kHz fibre breakage. The authors showed a clear variation of frequencies with different failure mechanisms.

Ramesh et al. [77] investigated the changes in the AE parameters of the flexural failure in dry and 5 months aged Kevlar/polyester composites. The authors related the following frequencies to failure modes: 100–180 kHz matrix cracking, 220–260 kHz debonding and 280–320 kHz delamination. The authors stated that fibre fracture was not relevant in flexural failure and did not present the AE parameters for fibre related failures.

de Groot et al. [70] carried out tests with especially designed specimens and test methods to cause specific failure modes in carbon/epoxy composites. The authors found that frequencies of 90–180 kHz are caused by matrix cracking, 180–240 kHz by fibre pull-out and fibre fracture causes frequencies above 300 kHz.

2.6 Summary of the Literature Review

In the literature review it was confirmed that currently there is no information available on the structural performance, including flexural and long term performance, of glass reinforced plant oil based composites. While there is information available on the ageing of conventional composites, it is still difficult to relate laboratory environment accelerated ageing tests to more realistic conditions for maritime applications.

There are several well established mechanisms related to the moisture uptake and resulting changes in the performance of composites. It has been hypothesised that moisture uptake causes changes in the failure modes but almost no research was found to confirm this. This is largely due to the complexity of the problem and difficulties regarding testing the hypothesis.

The damage in the composites can be visualised with multiple methods including SEM and CT. These methods are best suited for visualising the damage after it has occurred but not necessarily for determining the changes in the order of the failure events. AE has been shown to be capable of giving real time information about failure events as they are happening. Together with visual inspection techniques like SEM or microCT the AE could provide invaluable information of what is happening with the failure mechanisms in aged composites.

Chapter 3

Experimental Procedures

3.1 Overview

This research investigates the long-term performance of three materials: glass/epoxy as an industry standard, glass/linseed oil and glass/castor oil composites as new, commercially available plant oil resin based composites. The experimental work can be divided into the following main parts: ageing of the specimens in accelerated and non-accelerated conditions, testing the flexural properties of the dry and aged specimens, and determining the failure modes of glass/epoxy and glass/linseed oil specimens with the aid of microCT and acoustic emission (AE) techniques. The overview of the test programme is given in Table 3.1. Investigation of the failure modes has not been done before with glass/linseed oil specimens.

3.2 Manufacturing

E-glass/epoxy panels were manufactured with the resin infusion method as recommended for this resin system (Prime 20LV by Gurit). The infusion was followed by vacuum consolidation for at least 8 hours, cure time 24 hours and post cure for 16 hours at 50 °C as recommended by the resin supplier.

Vacuum infusion is one of the manufacturing techniques suitable for large load carrying composite and sandwich structures. The vacuum infusion process is a technique that uses vacuum pressure to drive resin into a laminate (Figure 3.1). Reinforcement is laid dry into the mould and the vacuum is applied into the laminate via carefully placed tubing. In comparison with the traditional hand lay-up, the infusion process has obvious health and safety advantages for workers (no contact with volatile organic compounds). Additionally, laminate mechanical properties are improved by higher fibre content and lower voidage [80].

Table 3.1: Test programme for the three materials tested

	Glass/epoxy	**Glass/linseed oil**	**Glass/castor oil**
Manufacturing	Resin infusion, oven post cure	Hand lay-up, UV-cure	Resin infusion, oven post cure
Accelerated ageing			
Moisture uptake	115 weeks	115 weeks	102 weeks
Flexural tests	With 2 week intervals up to week 10; at weeks 26, 68 and 115	With 0.5 week intervals up to week 2; with 2 week intervals up to week 10 at weeks 26, 68 and 115	With 2 week intervals up to week 10; at weeks 22, 55 and 102
microCT	Dry and 10 weeks aged specimens	Dry, 0.5 and 1 week aged specimens	-
AE	With 1 week intervals up to week 7; 2 years aged specimen	With 0.5 week intervals up to week 2; 4 weeks and 2 years aged specimens	-
Non-accelerated ageing			
Moisture uptake	42 weeks	88 weeks	-
Flexural tests	At weeks 3, 9, 12, 17, 37, 43	At weeks 2, 6, 8, 15, 40, 88	-

The manufacturing process of E-glass/castor oil was very similar to that of E-glass/epoxy. The resin used was two part Rescon 502 provided by Bioresin. The panels were manufactured by resin infusion and vacuum consolidation for 8 hours, cure time was 24 hours and post cure at 70 °C for 16 hours (found to be optimum in [28]).

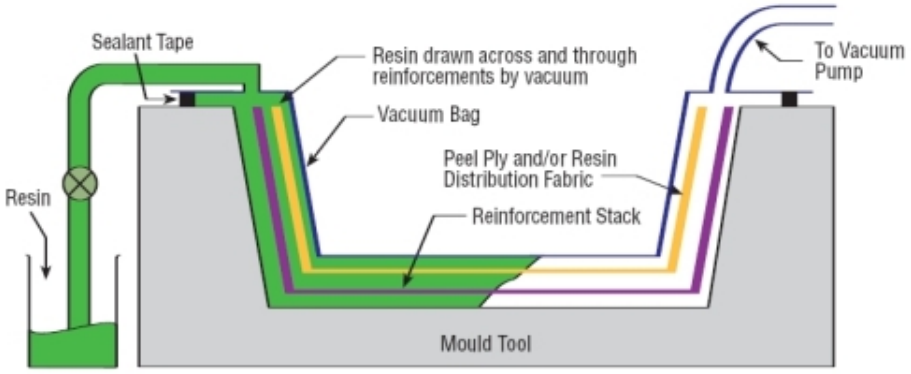

Figure 3.1: Resin infusion process [81]

E-glass/linseed oil panels were manufactured by Sustainable Composites Ltd. by using hand lay-up and UV-curing. The panels were cured 2 layers at a time: 2 layers of fabric were covered with resin, cured and then the next 2 layers were placed on top of the previous ones. The manufacturer assumes that this kind of method creates a sufficient secondary bonding between the layers.

UV-curing is not widely used yet due to the expensive equipment needed for cure activation and also the limitation of curable shapes and thicknesses. For UV-curing, all the areas of the structure have to be accessible with UV-lighting. The UV-curing initiating additive can be added to almost any resin system, the resulting resin is a one-part resin that does not need mixing, has a long pot life [82], and the curing process can be initiated even by sunlight [83]. The latter can be very useful when repairing composite structures that cannot be moved to a construction site (e.g. wind turbines). Additional benefits of using UV-curing is a reduction of styrene emissions and less voids being trapped inside a laminate due to the fast curing process [82].

All of the composites panels were manufactured using 10 layers of 0 °/90 ° unbalanced plain woven E-glass cloth with density of 210 g/m^2. The same cloth is being used by Sustainable Composites Ltd. for deck lay-up. Boat hulls are usually made with denser glass reinforcement. Due to high viscosity of castor oil resin a lighter fabric needed to be used for all of the specimens.

Laminate thickness for E-glass/epoxy specimens was around 1.7 mm, E-glass/castor oil 2.0 mm and for E-glass/linseed oil specimens approximately 2.7 mm (thickness around 2 mm was desired for a relatively short water uptake time). The fibre volume fractions were found in accordance to Method II in ASTM D3171 and void content from micrographs. The volume fractions of the different materials are given in Table 3.2.

3.3 Moisture Absorption

The moisture absorption testing was carried out in accordance to the ASTM D 5229 standard. The longest ageing test period reported here was 115 weeks for glass/epoxy and glass/linseed oil specimens and 102 weeks for glass/castor oil specimens. Standard test procedure was carried out in accelerated conditions, that is in distilled water at 40 °C. The aim of using accelerated testing was to reduce the testing time to be suitable for the time limits of this research. The accelerated ageing data is compared with the non-accelerated ageing in distilled and salt water (3.5% NaCl solution) at room temperature around 20 °C. The purpose is to check the usability of accelerated ageing data when analysing the performance of composites in their actual operating environment. Non-accelerated ageing was carried out with glass/linseed oil for 88 weeks and glass/epoxy for 43 weeks.

Moisture uptake is shown as a percentage weight change over a $\sqrt{time}$ as specified by the test standard. Fibres are assumed not to absorb water and the moisture uptake is only considered to be in the matrix and the interface. The moisture uptake of glass/linseed oil and glass/castor oil was normalised over the matrix volume fraction in respect to glass/epoxy in order to make the data more comparable; the normalising coefficients for glass/linseed oil and glass/castor oil are given as V_m/V_{me} in Table 3.2.

3.3.1 Specimen Preparation

The specimens needed for testing were cut using a rotating diamond blade saw. Moisture absorption specimens were cut into 100 x 100 mm panels according to ASTM D 5229 [43]. The preparation of flexural testing specimens was the same. The specimens were then dried in an oven at 35 °C until moisture equilibrium content was reached. The edges/sides of dried specimens were sealed with microcrystalline wax to make sure water diffused into the material only in the through thickness direction. The specimens were too thin to use stainless steel tape recommended by the test standard.

The prepared specimens were placed in distilled water (distilled water was required by the waterbaths' manufacturer due to corrosion issues) at 40 °C for accelerated ageing.

Table 3.2: Normalising coefficients (V_m/V_{me}) and fibre (V_f), void (V_v) and matrix (V_m) volume fractions of all three composites

Material	$\mathbf{V_f}$, %	$\mathbf{V_v}$, %	$\mathbf{V_m}$, %	$\mathbf{V_m/V_{me}}$
E-glass/epoxy	46.6	4.3 (SD 2.4)	49.1	—
E-glass/linseed oil	27.7	1.2 (SD 1.2)	70.7	1.44
E-glass/castor oil	39.6	2.8 (SD 1.8)	57.6	1.17

Non-accelerated ageing was carried out in distilled water and salt water at room temperature. In order to assure the specimens did not touch each other, plastic CD storage racks were used to stack the specimens. Distance between specimens was approximately 7 mm.

3.3.2 Method

The ASTM standard D 5229/D 5229M [43] was used to determine the water absorption properties of the specimens at 40 °C in the through-thickness direction. The temperature was chosen so that the ageing process would be accelerated but thermal degradation of the material could be reduced. Also, at 40 °C the material was more likely to follow simple Fickian diffusion model instead of the more complex Langmuir's diffusion model [40].

Specimens were taken out of the baths and wiped dry with absorbent lint-free cloth. Specimens were weighed with a Metler PE3600 scale with a resolution of 0.01 g. The percent moisture mass gain versus time was monitored for material specimens in a steady-state environment. From this data, the moisture equilibrium content, M_m, and the one-dimensional moisture absorption rate of the coupon can be determined and the through-thickness moisture diffusivity constant, D_z, calculated.

The calculation of the through-thickness moisture diffusivity constant assumes a single-phase Fickian material. This means that the material follows Fickian diffusion and possesses constant moisture diffusivity properties through the thickness of the specimen. The validity of Procedure A for evaluating the moisture diffusivity constant in a material of previously unknown moisture absorption behaviour will be uncertain prior to the test, as the test results themselves determine whether the material follows the single-phase Fickian diffusion model.

Fickian diffusion must satisfy the following conditions [43]:

- Absorption curve must be linear up to 60% of M_m;
- Beyond the initially linear portion, absorption curve must be concave to the abscissa until M_m is reached;
- For the same environmental exposures, absorption curves resulting from different specimen thicknesses of the same material must be essentially superimposable if each curve is plotted in the form of a normalized sorption curve in which the abscissa is $\sqrt{time/h}$ instead of $\sqrt{time}$ (where h is the thickness of the specimen).

The test method requires:

- A conditioning chamber that is capable of maintaining the required temperature to within ±1 °C;
- The specimen thickness shall not vary by more than ± 5% over the surface of the specimen;
- Specimens should have a mass of at least 5.0 g;
- The edge effects must be minimized in materials. This should be done by either:
  - Manufacturing a nominally square plate with dimensions that satisfy the relation
    $$\frac{w}{h} \geq 100 \tag{3.1}$$
    Where w is the nominal length of one side, mm; and h nominal thickness, mm;
  - Manufacturing a 100 ± 10 mm square plate with stainless steel foil bonded to the edges such that moisture absorption through the edges is essentially eliminated.

3.3.3 Calculations

All the equations are taken from ASTM D 5229 [43].

Effective moisture equilibrium (a material is in a state of effective moisture equilibrium when the average moisture content of the material changes by less than 0.01% within the span of the reference period):

$$|M_i - M_{i-1}| < 0.01\% \tag{3.2}$$

Where M is the specimen average moisture content, %; i value at current time, and $i-1$ value at previous time.

Absorption/desorption percent mass change:

$$Mass\ change, \% = |\frac{W_i - W_b}{W_b}| \times 100 \tag{3.3}$$

Where W_i is the current specimen mass, g; and W_b the baseline specimen mass, g.

Diffusivity:

$$D_z = \pi(\frac{h}{4M_m})^2(\frac{M_2 - M_1}{\sqrt{t_2} - \sqrt{t_1}})^2 \tag{3.4}$$

Where D_z is the diffusivity; h the average specimen thickness, mm; M_m is the effective moisture equilibrium content, %; $\frac{M_2-M_1}{\sqrt{t_2}-\sqrt{t_1}}$ is the slope of moisture absorption plot in the initial linear portion of the curve, $\sqrt{seconds}^{-1}$.

3.4 Flexural Properties

3.4.1 Specimen Preparation

Flexural specimens were prepared according to the ASTM standard D 7264 [84] (Figure 3.2). The nominal width of the cut specimens was 13 mm, the length was calculated according to support span-to-thickness ratio of 20:1. The thickness of the specimens were measured with a micrometer with an accuracy of ± 0.001 mm, the width and length were measured using vernier calipers with accuracy of ± 0.01 mm.

3.4.2 Method

This test method (ASTM D 7264/D 7264M [84]) determines the flexural properties of polymer matrix composite materials. Three-point loading system was used utilizing centre loading on a simply supported beam. The test method was developed for optimum use with continuous fibre-reinforced polymer matrix composites. D 7264 test method is intended to interrogate long-beam strength in contrast to the short-beam strength evaluated by test method D 2344. The standard loading span-to-thickness ratio of the specimens is 32:1 (but other ratios can be used if necessary), the standard specimen thickness is 4 mm and width 13 mm. If the standard specimen thickness cannot be obtained in a given material system, an alternate specimen thickness shall be used while maintaining the support span-to thickness ratio and specimen width.

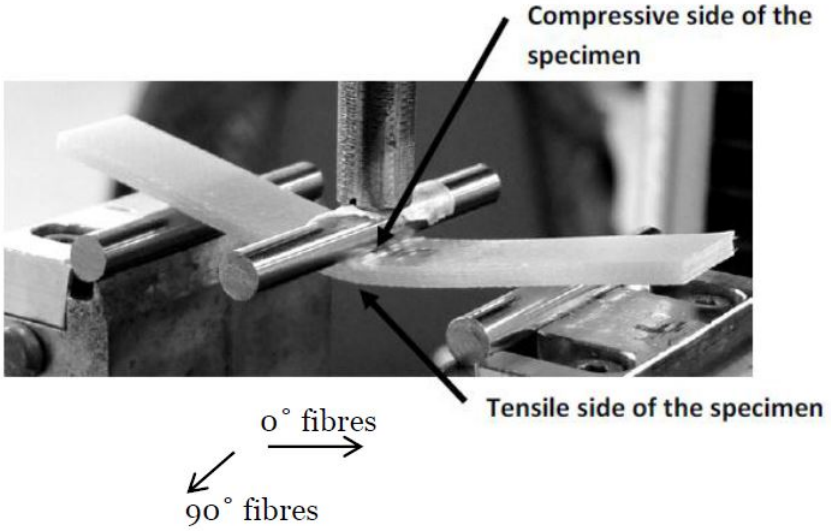

Figure 3.2: The setup of a flexural test

3.4.3 Calculations

All the equations are taken from ASTM D 7264 [84].

Maximum flexural stress:

$$\sigma = \frac{3PL}{2bh^2} \tag{3.5}$$

Where σ is the stress at the outer surface at mid-span, MPa; P is the applied force, N; L the support span, b width of beam and h the thickness of beam, all in mm.

Maximum strain:

$$\epsilon = \frac{6\delta h}{L^2} \tag{3.6}$$

Where ϵ is the maximum strain at the outer surface, mm/mm; δ the mid-span deflection, mm; L support span and h thickness, both in mm.

Flexural modulus of elasticity is the ratio of stress range and corresponding strain range:

$$E_f = \frac{\Delta\sigma}{\Delta\epsilon} \tag{3.7}$$

Where E_f is the flexural modulus of elasticity, MPa; $\Delta\sigma$ difference in flexural stress between the two selected strain points, MPa, and $\Delta\epsilon$ difference between the two selected strain points.

3.5 X-Ray Computed Tomography

X-ray Computed Tomography (microCT) imaging was performed using a benchtop Nikon/Metrix CT160 Xi scanner. Data for glass/epoxy specimens were collected at 91 kV and 105 μA with magnifications of 13.8; data for glass/linseed oil specimens were collected at 92 kV and 112 μA with magnification of 11.5. For the reconstruction of data, CT images were acquired from 1910 rotation views over 360 ° of rotation. Reconstruction was performed using CT-Pro 3D software by Nikon Metrology, Inc.

One of the benefits of microCT is that the specimens do not need any preparation as long as they can fit in the radiation chamber. The specimens were first tested under flexure, the failed specimens were attached together with tape and placed in the radiation chamber. All of the 5 specimens from the test set were scanned together and the images shown in this work are of one representative specimen from the set.

3.6 Scanning Electron Microscopy

SEM was used to look at the failure surfaces of dry and 3 weeks aged glass/epoxy specimens. The aged specimens had been immersed in distilled water at 40 °C. The

images were taken after tensile tests and were originally not part of this work but from a different unpublished project. The SEM scanned specimens were gold plated to make them conductive and placed into the vacuum chamber in SEM.

The SEM work was carried out using JSM5910 scanning electron microscope. Data for dry and aged glass/epoxy were collected at the same accelerating voltage (2.0 kV) and magnification (x350), the working distance for dry glass/epoxy was 9.8 mm and for aged material 11.8 mm.

3.7 Acoustic Emission Testing

Acoustic emission process is shown in Figure 3.3. Loads applied to a test specimen during mechanical testing cause damage inside the material. This damage releases energy as an elastic wave that travels outward from the source and through the test specimen. The wave is detected by an acoustic emission sensor that converts the energy into voltage. Analysis of the collected data means characterising the received voltage/signals [85].

For analysing the failure during flexural testing the AE sensors were attached to both ends of the test specimen. A layer of Vaseline was put as a coupling agent between the specimen and the sensors to insure the transfer of the signals from the test specimens to the sensors. The sensors were then attached to the specimen with tape to hold the sensors in place during the test. The flexural test setup with AE sensors is shown in Figure 3.4.

The signals were processed by the AEWin software by Physical Acoustics Corporation. Parametric analysis (signal parameters are extracted and analysed instead of comparing waveforms directly) was used in this study due to time limits. Most of the parameters are taken directly from the waveforms, frequencies are found through FFT and show the frequencies with the highest magnitude.

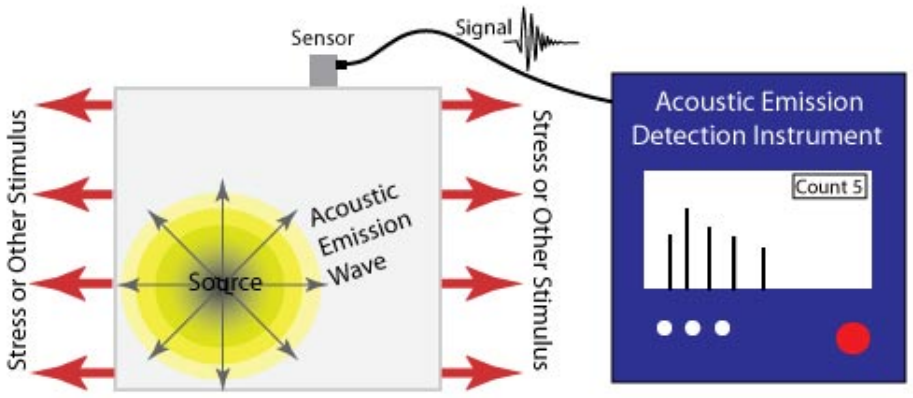

Figure 3.3: Schematic of an AE test [86]

The system used in this research was PAC AE PCI-2 based system with two PAC WD AE broadband sensors. The threshold was set to 40 dB; peak definition time was 200 μs, hit definition time 800 μs and hit lockout time 1000 μs. The maximum duration was set to 100 ms.

The AE data was collected with accelerated ageing glass/epoxy and glass/linseed oil specimens over 7 weeks of ageing. Additional tests were done with 2 years aged specimens.

3.7.1 Pencil Lead Break

Wave speed and attenuation data were collected using pencil lead break test (Figure 3.5). Pencil lead break test is done by supporting a pencil lead on the surface on the material and then breaking the lead. This has shown to be a repeatable AE source without damaging the material and suitable for wave speed and attenuation measurements [85].

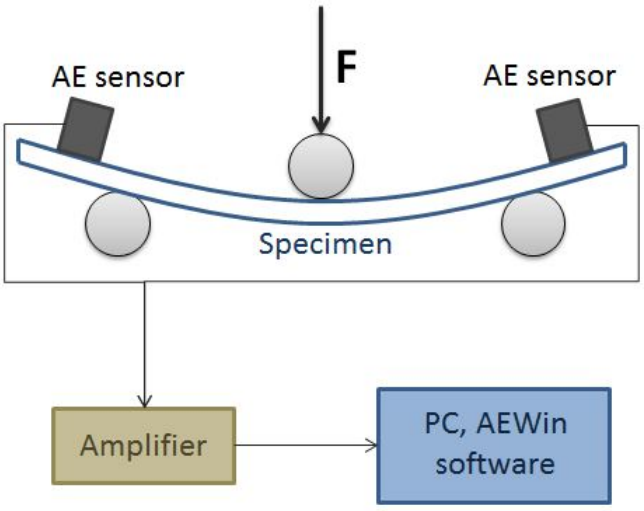

Figure 3.4: Schematic of a flexural test setup with the AE equipment

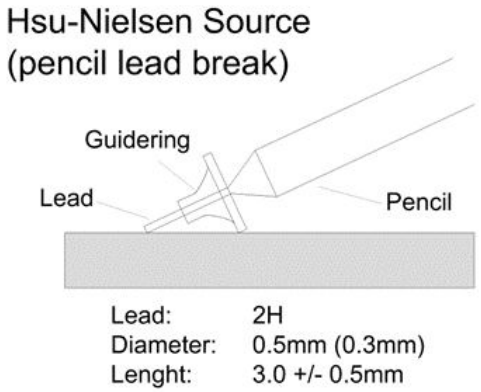

Figure 3.5: Schematic of a pencil lead break test [87]

Chapter 4

Results and Discussion: Moisture Uptake and Flexural Properties

It is known from the literature that composites do absorb water and that the moisture has a great effect on the performance of composites. In this chapter the moisture uptake and its effects on the flexural properties of glass/epoxy, glass/linseed oil and glass/castor oil composites will be discussed; there was previously no information available on the long-term performance of glass/linseed oil and glass/castor oil composites.

4.1 Glass/Epoxy Accelerated Ageing

4.1.1 Moisture Uptake

The accelerated moisture uptake curve of glass/epoxy specimens can be seen in Figure 4.1. The moisture uptake of glass/epoxy reached the equilibrium condition over the first 6 weeks of testing. After 6 weeks there was no significant loss or gain of weight and the average moisture content until the end of the test period was 2.11% (Table 4.1). From Figure 4.1 it can be seen that the variation in the accelerated moisture uptake data of glass/epoxy was quite uniform. Only after 34 weeks the scatter of moisture uptake increased, suggesting that there were further chemical or physical changes occurring in the structure of the glass/epoxy laminate.

The ASTM D 5229 standard assumes Fick's diffusion in the composite and the accelerated moisture uptake of glass/epoxy does seem to follow Fick's model (Figure 2.1, Table 4.1). The requirements for Fick's model were fulfilled (see section 3.3) and the diffusion coefficient calculated: 4.17×10^{-7} mm^2/s (Table 4.1). In literature, the diffusion coefficients of epoxy composites vary from 7.67×10^{-8} mm^2/s [88] to 2.10×10^{-7} mm^2/s [89] to 2.58×10^{-6} mm^2/s [88], depending on the type of reinforcement, water chemistry

and temperature. Based on these values the diffusion coefficient of 4.17x10^{-7} mm^2/s fits well within the expected range presented in the literature [88, 89].

4.1.2 Effects of Moisture Uptake on Flexural Properties

The flexural strength of dry glass/epoxy was 533.8 MPa (with SD of 25.4 MPa); after 115 weeks of accelerated ageing and 2.20% moisture uptake the strength had reduced down to 226.0 MPa (with SD of 11.2 MPa), that is a 57.6% reduction. The reduction of flexural strength was most significant over the initial 10 week ageing period (Figure 4.2), after 10 weeks the reduction remained between 50–60% of the original strength. While

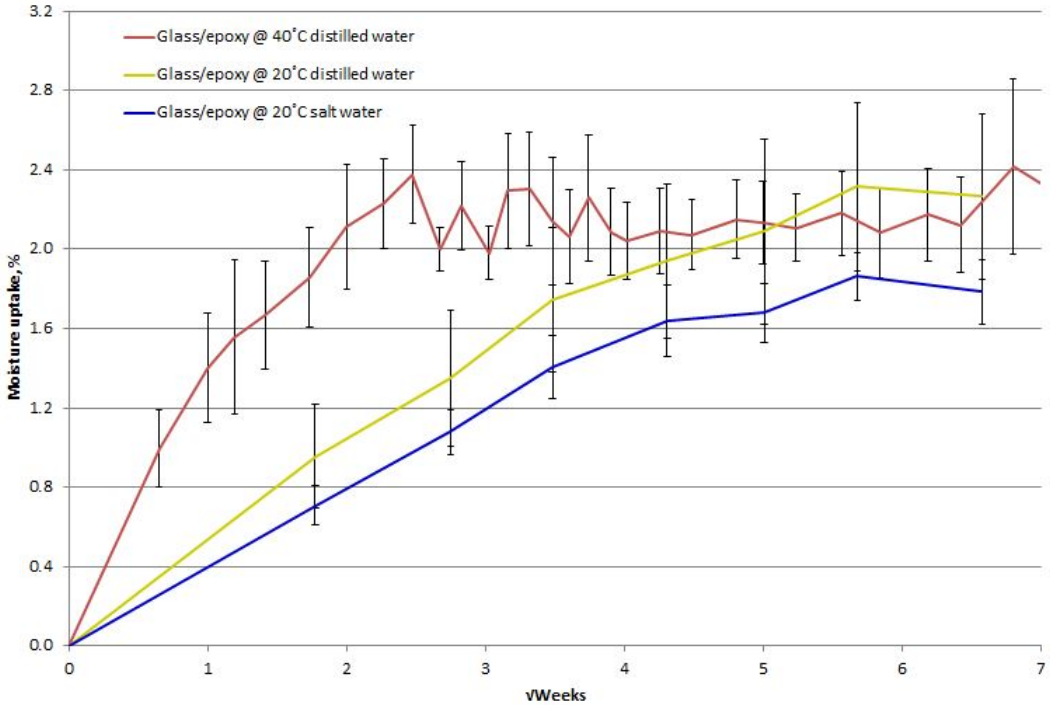

Figure 4.1: Glass/epoxy moisture uptake vs. weeks$^{\frac{1}{2}}$ in accelerated and non-accelerated conditions

Table 4.1: Moisture absorption parameters for glass/epoxy, glass/linseed oil and glass/castor oil specimens

	Moisture equilibrium %	**Last moisture content change** %	**Linear uptake** %	**Diffusion coefficient** x10^{-7} mm^2/s
E-glass/epoxy	2.11	0.01	66.4	4.17
E-glass/epoxy non-acc dist	2.29	0.04	76.0	0.46
E-glass/epoxy non-acc salt	1.82	0.07	77.5	0.48
E-glass/linseed oil	2.87	0.01	54.0	3.90
E-glass/castor oil	3.62	0.04	61.8	1.16

the reduction of strength reached the maximum in 10 weeks, the moisture equilibrium content was achieved after only 6 weeks of ageing. Degradation with a uniform moisture content suggests chemical reactions and resulting damage in glass/epoxy.

While the flexural strength reduces with moisture uptake, the flexural modulus of glass/epoxy seems to be unaffected by moisture. The modulus of dry glass/epoxy was 18.8 GPa (with SD of 0.7 GPa), after 115 weeks the modulus was 19.2 GPa (with SD of 0.6 MPa). Similar conclusions of modulus being unaffected by moisture in epoxy composites (depending mainly on the use of coupling agents) have been reported by Iglesias et al. [58].

Similar flexural modulus can result from different stress-strain curves as seen in Figure 4.3. The slope of the unaged and aged curves is similar, as is the sudden failure event, but the failure occurs at lower stresses. The stress-strain curves shown are for specific specimens that show the average behaviour among the specimens. The stress-strain curves in Figure 4.3 suggest that the aged glass/epoxy specimens are less damage tolerant and fail before any other changes to the stress-strain curves could occur.

Hygrothermal ageing damages matrix, fibres and the interface. That, however, does not entirely explain the great reduction of properties for glass/epoxy observed in this study. It was hypothesised that the failure mechanisms in the materials change due to moisture uptake. Computed tomography was used to investigate this hypothesis further.

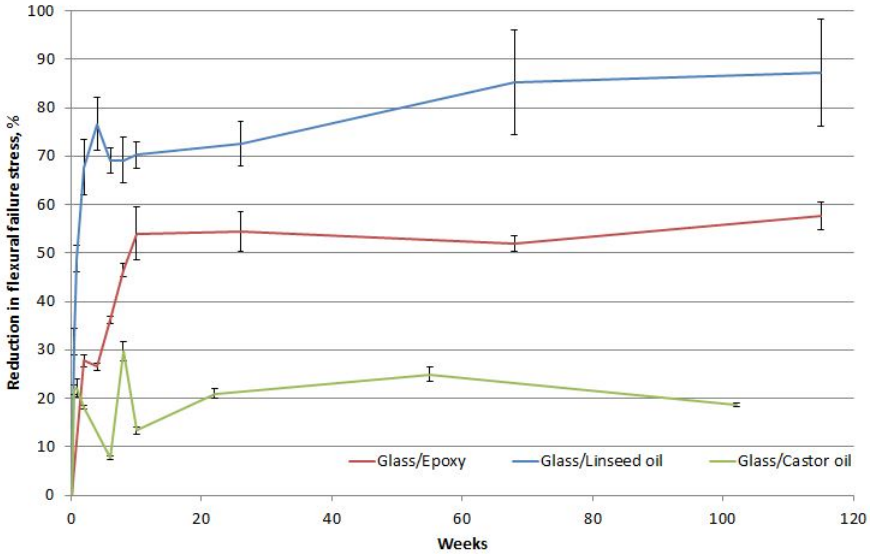

Figure 4.2: Reduction of flexural strength in glass/epoxy, glass/castor oil and glass/linseed oil during accelerated ageing in distilled water

4.1.3 Changes in Failure Modes due to Moisture Uptake

Figure 4.4 shows representative images from the microCT scans of dry and 10 weeks aged glass/epoxy specimens after flexural failure. The dry glass/epoxy specimens (on the left in Figure 4.4) failed on both tensile and compressive sides with numerous cracks developing on both sides. Cracks on the tensile side were found to propagate along the 90° interface and through the longitudinal fibre bundles. The cracks propagating through thickness were connecting numerous voids in the laminate and going through fibre bundles. An extensive delamination was found to have developed on the compressive side of the specimen.

The 10 weeks aged specimens showed failure on the tensile side only suggesting that the composite failed before compressive failure could occur. Tensile failure has been found to occur before compressive one also by Falchi and Gracia [63]. This may be explained by the damage in the interface area so that the tensile failure around 90° fibres was intense enough to fail the specimen. Instead of multiple cracks that developed in unaged specimens there was only one visible dominating crack in aged samples. However, the crack still developed through fibre bundles and joining voids. The matrix may have become less brittle leading to a single crack developing instead of several ones.

SEM images were taken of specimens from a different project where SEM was used to look at the interfacial failure in glass/epoxy specimens before ageing (Figure 4.5) and after 3 weeks of immersion in distilled water at 40 °C (Figure 4.6). The images shown here were taken after tensile tests. The images of aged and unaged specimens are shown in Figures 4.5 and 4.6 respectively. From Figure 4.5 it can be seen that the bonding between fibres and matrix is relatively good, leaving matrix well attached to the fibres even after failure. Figure 4.6 shows the failure of 3 weeks aged glass/epoxy and it can be seen that the matrix has failed with cleaner fracture surfaces. The fibres are cleaner

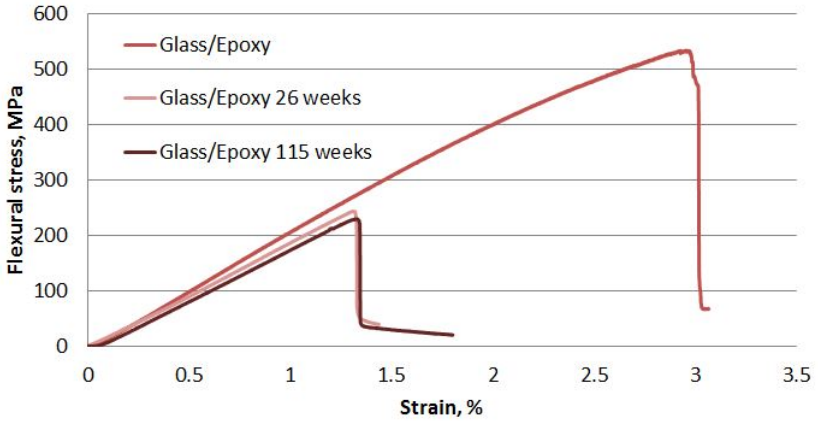

Figure 4.3: Comparison of the glass/epoxy stress-strain curves for dry and aged glass/epoxy

than in unaged specimens, also there are fibre pull-outs from the matrix indicating a damaged interface [58].

4.2 Glass/Epoxy Non-Accelerated Ageing

4.2.1 Moisture Uptake

Non-accelerated ageing tests with glass/epoxy in distilled and 3.5% salt water were carried out over a testing period of 43 weeks. Figure 4.1 shows the comparison of moisture uptake in glass/epoxy under both accelerated and non-accelerated conditions. The

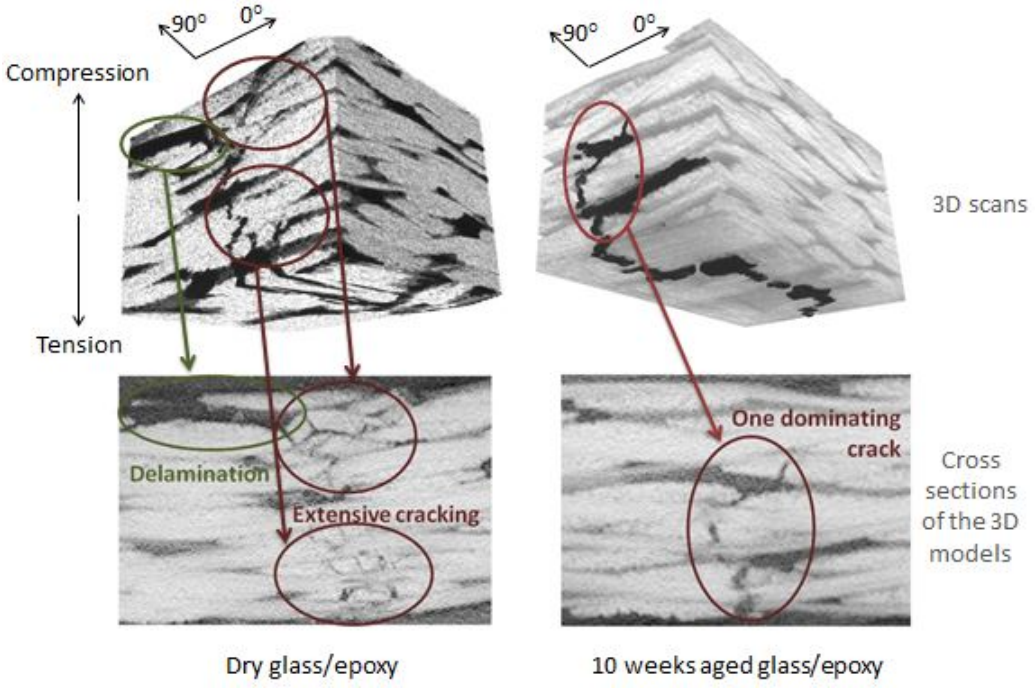

Figure 4.4: CT images (3D scan above and cross section below) showing failure mode change of unaged (left) and 10 week aged (right) glass/epoxy specimens

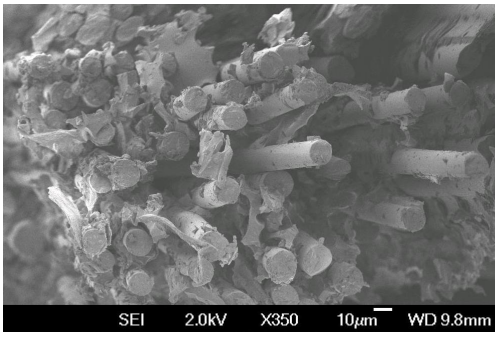

Figure 4.5: SEM image of the unaged glass/epoxy specimens after tensile failure. Pieces of matrix attaching to the fibres show a good interfacial bond.

non-accelerated moisture uptake curves show a more linear behaviour than accelerated moisture uptake (Table 4.1).

The non-accelerated samples in both distilled and salt water can be considered to have reached moisture equilibrium condition after 32 weeks of ageing, moisture uptake being significantly slower than in accelerated conditions. Generally 3 consecutive moisture uptake measurements are needed to determine the moisture equilibrium content, but here only 2 measurements are reported due to the time restrictions of the research. Reaching the moisture equilibrium condition in non-accelerated conditions took longer than in accelerated conditions. The slower moisture uptake rate is also visible from the 10 times lower diffusion coefficients of non-accelerated moisture uptake in Table 4.1.

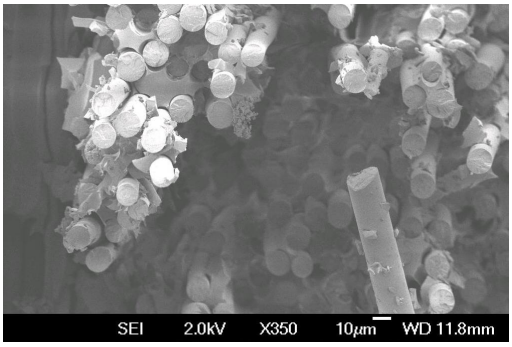

Figure 4.6: SEM image of the 3 weeks aged glass/epoxy specimens after tensile failure. Reduced number of pieces of matrix attaching to the fibres show a damaged interfacial bond.

4.2.1.1 Factors Affecting Moisture Uptake in Glass/Epoxy

There are multiple factors affecting the moisture uptake in composites, including sample preparation, residual stresses, water chemistry and voids. In this work, only the effects of water temperature, salinity and voids were investigated.

Effects of Water Temperature and Salinity

In distilled water, both elevated and room temperature ageing conditions showed similar moisture content in glass/epoxy after 43 weeks of ageing (Figure 4.1) indicating that the moisture equilibrium content is approximately the same in distilled water even at different temperatures.

The specimens aged in salt water reached the moisture equilibrium content over the same ageing period as the non-accelerated distilled water specimens, the only difference being lower moisture content in salt water specimens. It can be concluded that in glass/epoxy the ageing temperature only affects the moisture uptake speed and the water salinity affects the quantity absorbed. Elevated water temperature results in faster moisture

uptake and adding salt to the water reduces the amount of moisture absorbed. Loos et al. made similar conclusions on glass/polyester composites [39].

Effects of Voids

The specimens for non-accelerated testing were cut from different panels than accelerated ageing specimens. The panels were all manufactured with the same lay-up and in the same laboratory conditions but the specimens used for non-accelerated ageing had a varying void content, being between 1.5 and 8.0%. There were 2 specimens from a low void content panel and 3 from a high void content panel (5 specimens in total) for both distilled and salt water ageing. The moisture uptake of different void content specimens was monitored separately (Figures 4.7 and 4.8). From these figures it is clear that voids do increase the moisture uptake of composites as reported by Thomason [44, 45]. As a result there is also a greater variation in the moisture uptake of non-accelerated specimens in distilled water compared with accelerated ageing results, visible in Figure 4.1. However, the moisture uptake in salt water seems to be less sensitive to void content than moisture uptake in distilled water (Figures 4.7 and 4.8) based on a smaller difference in the moisture uptake of low and high void content specimens

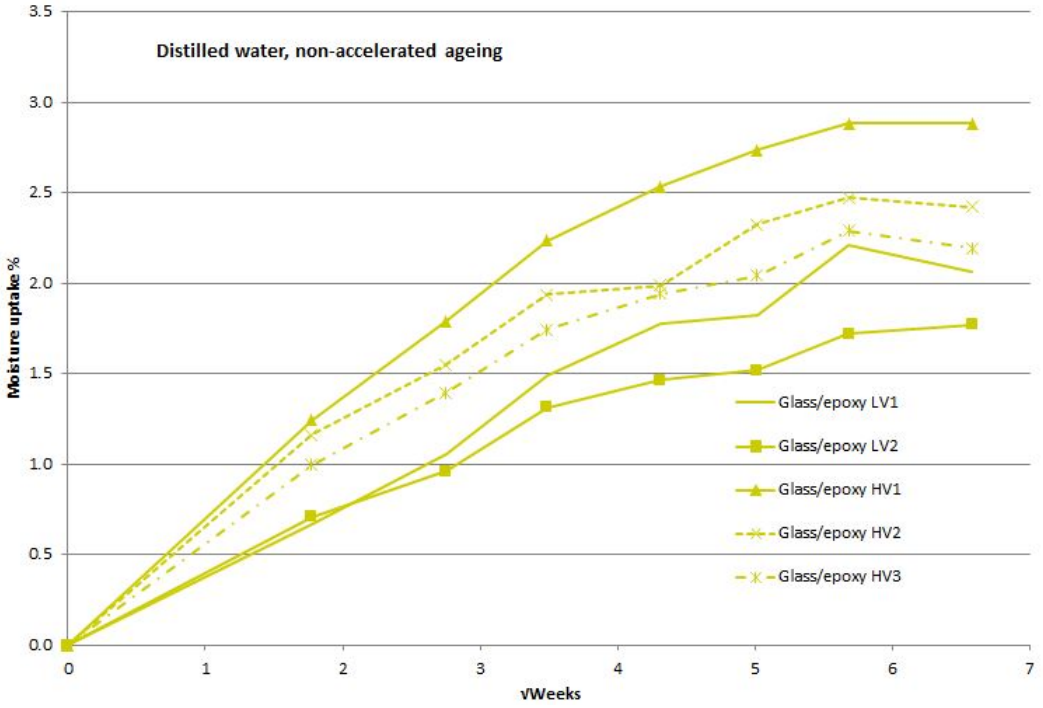

Figure 4.7: Glass/epoxy non-accelerated moisture uptake vs. weeks$^{\frac{1}{2}}$ in distilled water, comparison of moisture uptake in low void (LV) and high void (HV) content specimens

4.2.2 Effects of Moisture Uptake on Flexural Properties

Figure 4.9 shows the dependence of the reduction in flexural strength on the moisture content of the specimens. For comparison, all three ageing conditions have been presented: accelerated ageing in distilled water, non-accelerated ageing in distilled and salt water. From Figure 4.9 it is clear that moisture uptake in the specimens is greater in distilled water than in salt water but the flexural strength seems to be mainly affected by the moisture content in the material. Similar moisture content causes similar reduction of flexural strength in differently aged samples. However, there is some inconsistency in the results above 1.7% moisture content, possibly caused by the varying void content in the specimens.

The salt water aged specimens absorbed less water than distilled water specimens (both accelerated and non-accelerated) but the reduction of strength was on a similar level in all three cases. It should be considered here that the moisture uptake in non-accelerated conditions had possibly just reached the equilibrium content by the end of the test period, i.e. instead of 3 points there were only 2 moisture uptake data points available for the equilibrium condition. The flexural strength of accelerated ageing glass/epoxy kept reducing with uniform moisture equilibrium content and similar behaviour is to be expected from non-accelerated ageing specimens.

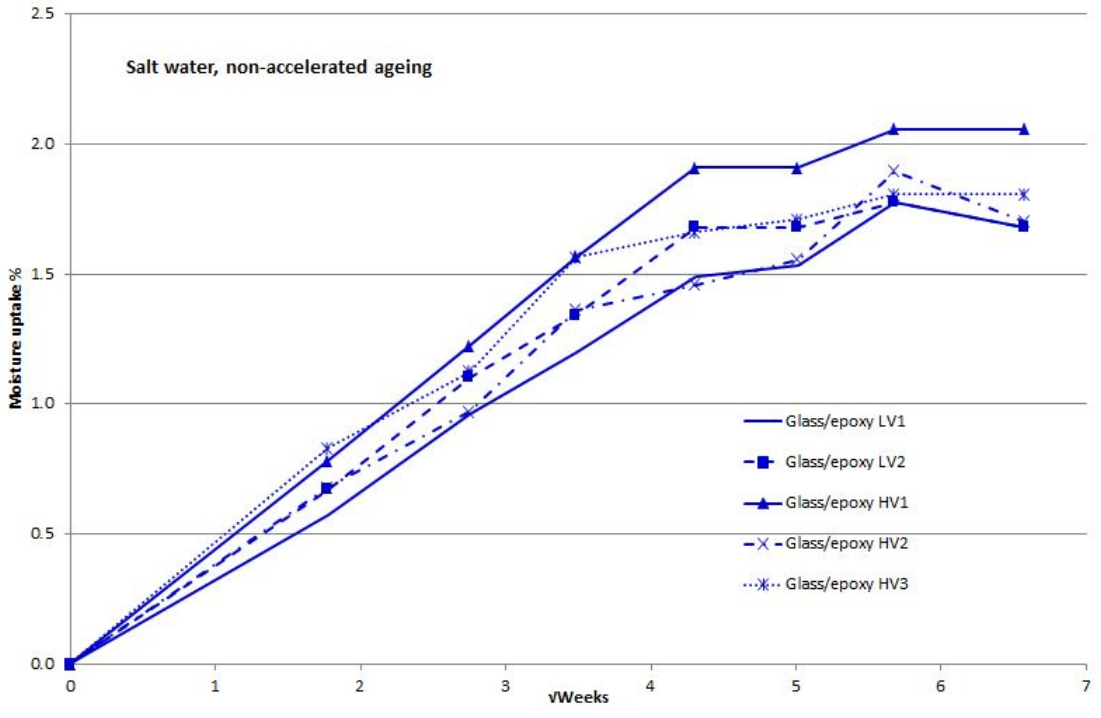

Figure 4.8: Glass/epoxy non-accelerated moisture uptake vs. $\text{weeks}^{\frac{1}{2}}$ in salt water, comparison of moisture uptake in low void (LV) and high void (HV) content specimens

The flexural modulus of glass/epoxy remained relatively unchanged in accelerated moisture uptake conditions but it was affected in non-accelerated conditions (Figure 4.10). The changes in flexural modulus under non-accelerated ageing conditions seemed to be random and with no clear trends. This behaviour is most likely due to the varying void content of the non-accelerated ageing specimens.

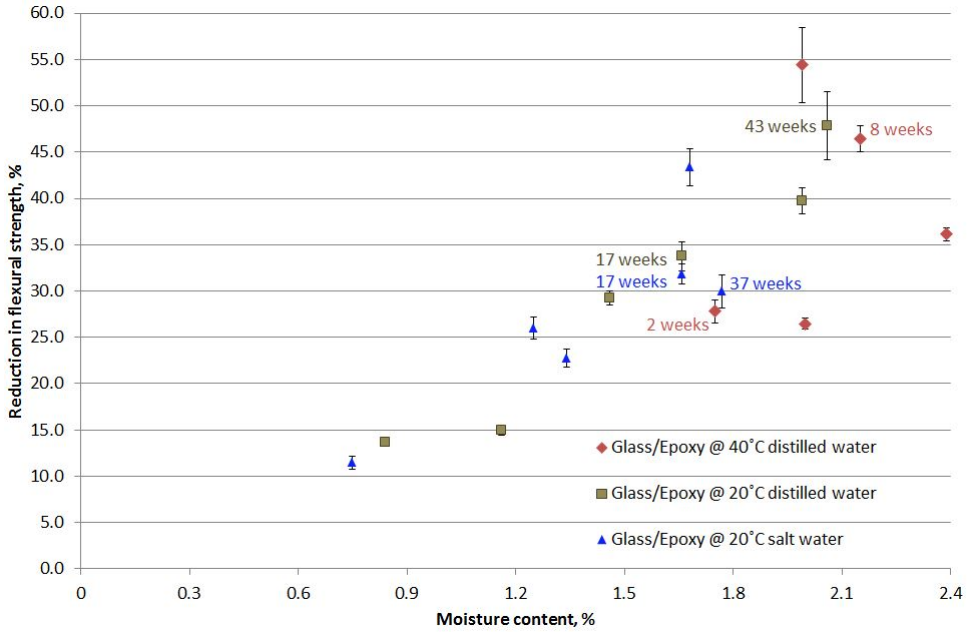

Figure 4.9: Changes in the flexural failure stresses of glass/epoxy due to moisture uptake in accelerated and non-accelerated conditions

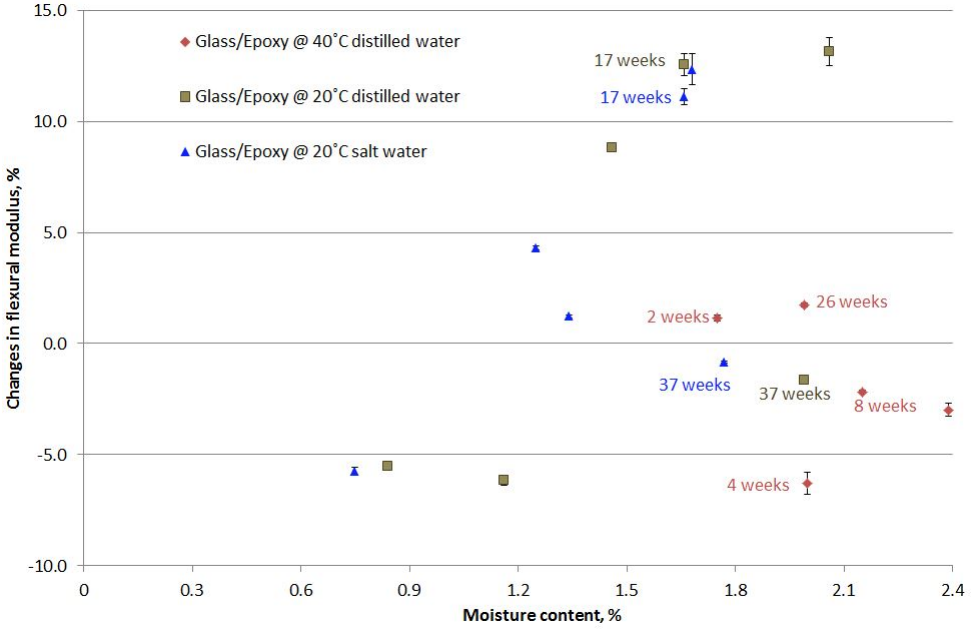

Figure 4.10: Changes in the flexural modulus of glass/epoxy due to moisture uptake in accelerated and non-accelerated conditions

4.3 Glass/Linseed Oil Accelerated Ageing

4.3.1 Moisture Uptake

The accelerated moisture uptake in glass/linseed oil was fairly linear up to week 6 (Figure 4.11). The moisture uptake stopped during weeks 6–9 and started increasing again after week 9. Up to week 6 the scatter in the moisture uptake of glass/linseed oil was very small, that can largely be attributed to the low void volume fraction (V_v=1.2%). After 6 weeks of ageing the scatter started increasing together with the moisture uptake, reaching the maximum moisture content and scatter after 49 weeks of ageing.

The moisture uptake of glass/linseed oil was more similar to Langmuir's model than Fick's (Figure 2.1). The latter requires moisture uptake to be linear for at least 60% of the equilibrium moisture content, that, however, was not the case with glass/linseed oil (Table 4.1). For comparison purposes the diffusion coefficient was still calculated for glass/linseed oil specimens. It is clear from the accelerated moisture uptake graph that Fick's model does not apply to glass/linseed oil composites and a different model may be required, although this goes beyond the scope of this work.

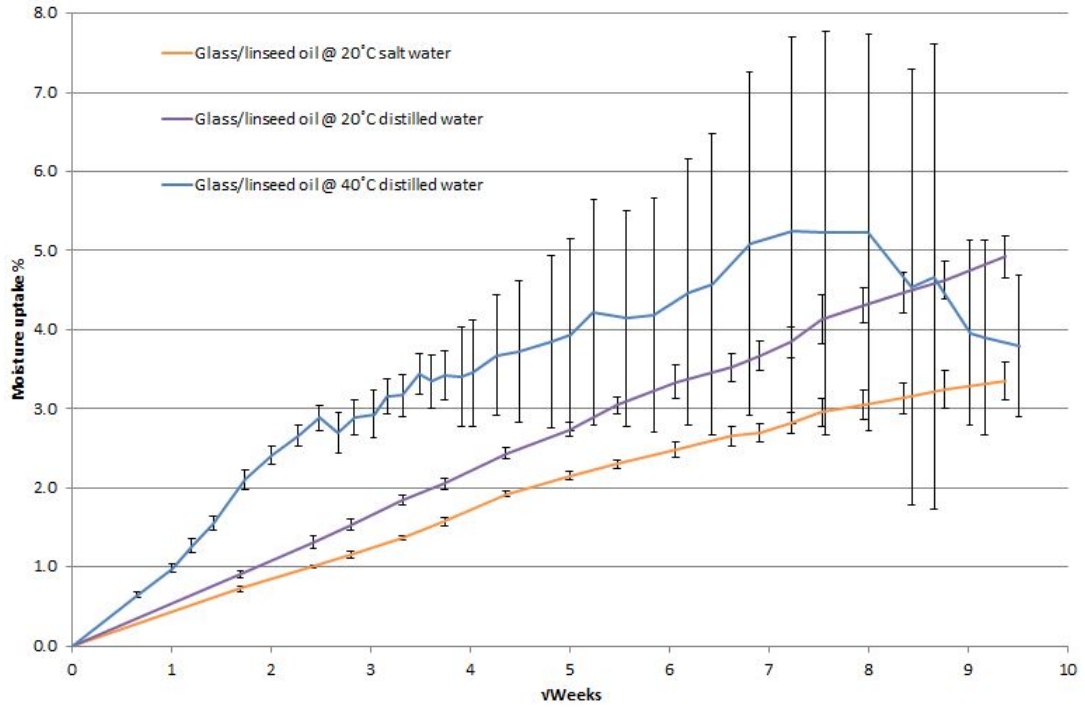

Figure 4.11: Accelerated and non-accelerated moisture uptake vs. weeks$^{\frac{1}{2}}$ in glass/linseed oil specimens

4.3.1.1 Blistering

Blisters were noticed in glass/linseed oil specimens after 5-6 weeks of accelerated ageing (Figure 4.12) being the reason behind increasing moisture uptake and scatter in the weight measurements (Figure 4.11). Not all of the glass/linseed oil specimens had blisters in them and it was possible to monitor the moisture uptake in blistered and non-blistered specimens separately (Figure 4.13). The non-blistered specimens did not absorb significantly more moisture after weeks 14–18 (depending on the specimen) and in some of the specimens the moisture content stayed around 3.0% that was achieved already after 6 weeks of ageing.

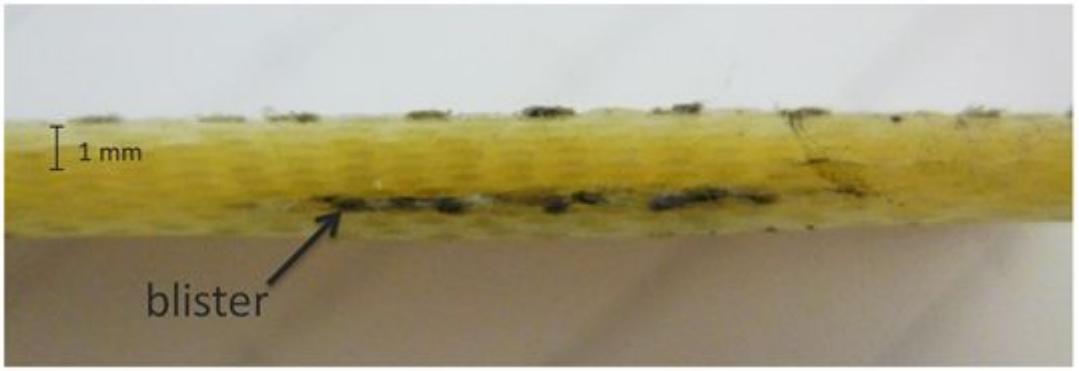

Figure 4.12: Blisters inside glass/linseed oil laminates after 10 weeks of moisture absorption

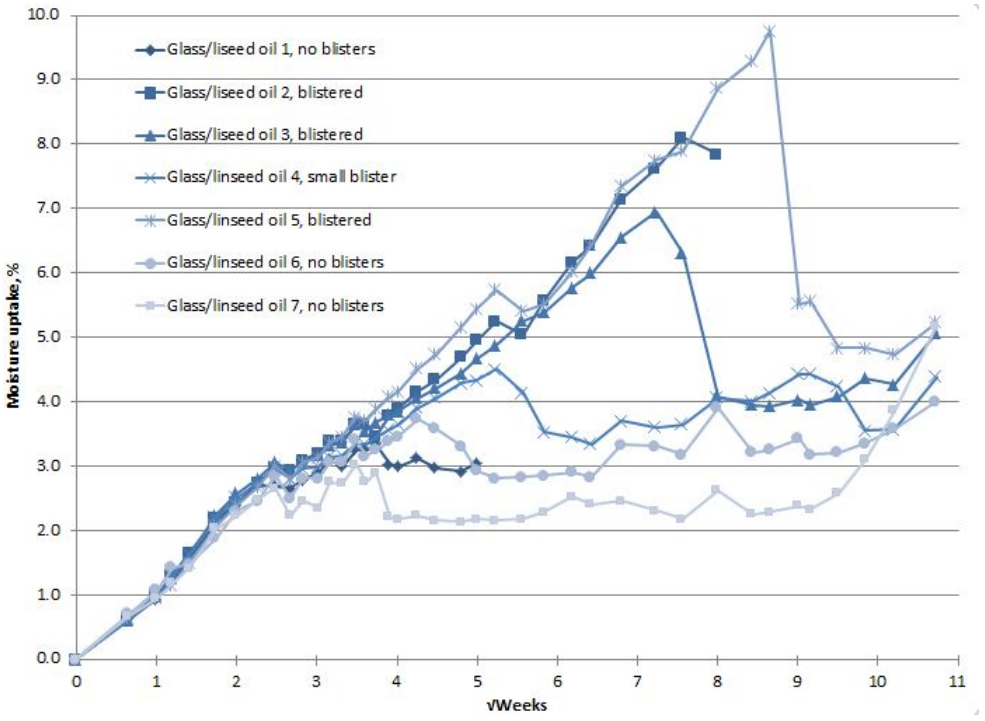

Figure 4.13: Moisture uptake comparison of blistered and non-blistered glass/linseed oil specimens

In blistered glass/linseed oil specimens the moisture content kept increasing until weeks 49–75, depending on the specimen, and then dropped suddenly. The blisters disappeared at that point, having grown so big that the laminate split into two, releasing all the moisture from the blisters. From this it is obvious that water and temperature cause severe damage to the glass/linseed oil composite in accelerated ageing conditions.

Causes of Blistering

It is obvious that the blisters affect the performance of the glass/linseed oil composite significantly. In these critical areas the water uptake has led, for some reason, to the formation of blisters that causes even greater water uptake inside the material. In the blister areas there must be some kind of a local initiator as the blister locations seem to be random and not in every specimen. In order for the blisters to form, there must be an increasing pressure in that location, probably related to osmosis: a chemical reaction between water and a constituent forcing even more water to penetrate the region to try and maintain the balance. As a result, the pressure in the area increases and if the matrix is not resistant enough it gives way for blistering to occur. However, it is not clear what initiates the blister formation in the first place.

The likely initiators for blisters can be voids, poor bonding between fibres and matrix and manufacturing defects like resin that has not fully cured. Hypothesis on osmosis causing voids to grow bigger has been reported in the literature [51]. However, the size of the blisters and small void volume fraction (V_v=1.2%) suggest that there must be another cause behind the formation of blisters. Poor bonding between the fibres and matrix should be uniform throughout the specimens and cause more blisters to occur. Also, assuming that the bonding is uniform, the blisters should occur inside all of the specimens but they did not in accelerated ageing samples.

The cause of blistering is unknown but it is hypothesised here that they are caused by manufacturing defects and non-optimised UV-curing process. The manufacturing of glass/linseed oil specimens was carried out in a non-laboratory environment that may have led to some problems often related to UV-curing. UV curing is very sensitive to UV exposure times, thickness and colour of the resin (see section 2.1.3). The darker and thicker the resin the more difficult it is to cure it. According to the literature, there are optimum time limits for UV exposure [36, 37]. The properties of the laminate suffer when the UV exposure time is either shorter or longer than necessary. If all these parameters are not carefully controlled, the curing may result in a laminate that has not fully cured or have some other manufacturing related issues.

Ultrasound (UT) scanning was carried out with dry glass/linseed oil specimens and some abnormalities were noticed in the specimens (Figure 4.14). Due to the breakdown of the UT equipment no scans were possible with the same specimens after blisters had occurred. Instead, photographs were taken of the specimens to show blister locations and it was noticed that blisters developed roughly in the same areas where the abnormalities

were noticed before moisture uptake (Figure 4.15). There is more research required in order to determine the exact reasons behind blistering in glass/linseed oil specimens.

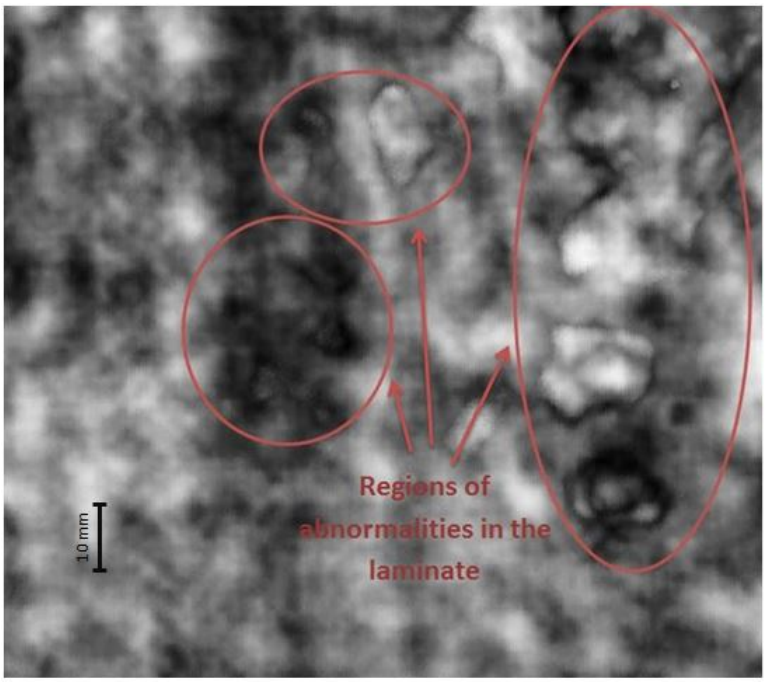

Figure 4.14: UT scan of a dry glass/linseed oil specimen showing areas that may be the cause of blistering

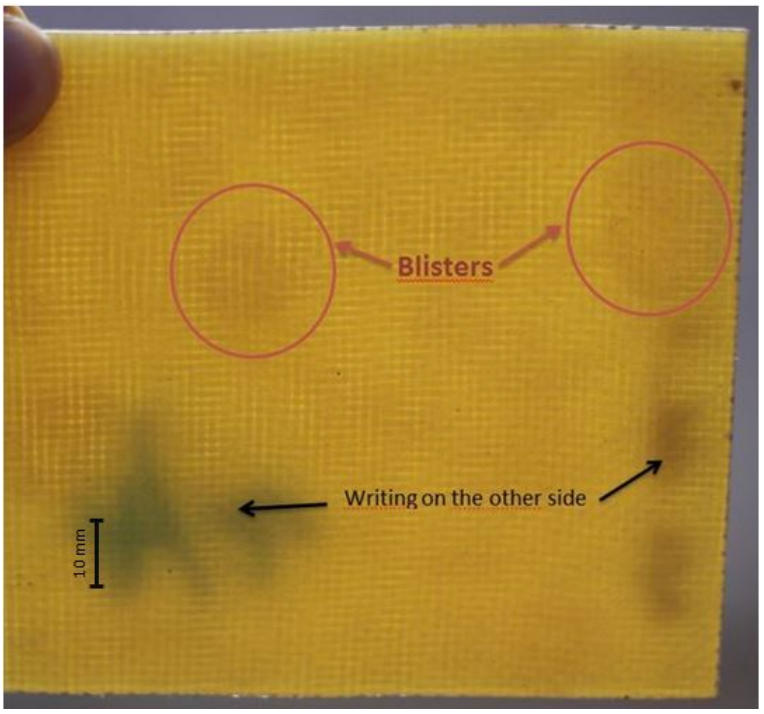

Figure 4.15: Photo showing the blisters in the same specimens that was UT scanned earlier

4.3.2 Effects of Moisture Uptake on Flexural Properties

The flexural strength of dry glass/linseed oil was 147.1 MPa (with SD of 5.3 MPa) and modulus 8.2 GPa (with SD of 0.6 GPa). After 115 weeks of accelerated ageing the flexural strength of glass/linseed oil reduced by 87.3% (Figure 4.2) and flexural modulus by 82.7%. There was a problem with blistering and after 26 weeks of ageing the blisters grew so big that flexural test specimens had split into two halves thus reducing the properties even further. Blisters can be treated as delaminations and it has been shown that small (covering less than 50% of the support span) delaminations do not affect flexural strength. However, when big enough, delaminations can cause a great reduction in properties [90]. Because of this, the comparison with the specimens beyond 26 weeks of ageing is unfavourable to the glass/linseed oil composite. 26 weeks of ageing caused a 72.6% reduction in glass/linseed oil strength and 60.1% reduction in flexural modulus.

The most significant reduction in glass/linseed oil composite flexural properties occurs over the first 4 weeks of ageing when material has not yet reached the maximum moisture content. This means that the water reaches most sensitive areas very quickly in glass/linseed oil and causes rapid damage.

For Kevlar composites it has been found that if the yield strength of the matrix is below 10 MPa then the flexural failure changes from fibre dominated to a matrix dominated failure [91]. It is possible that the yield strength of linseed oil is as low as 10 MPa, especially after ageing, thus changing the failure mode and affecting the strength of the composite as a whole.

The reduction of modulus followed a very similar trend to flexural strength except for the 115 weeks aged specimen from accelerated ageing test set (Figure 4.18). These specimens were already split into two halves explaining the further reduction of modulus. The low modulus of glass/linseed oil specimens can be explained with low fibre volume fraction, debonding issues demonstrated with blistering, and possibly low yielding strength of the matrix.

4.3.2.1 Effects of Temperature

Flexural tests were also carried out with glass/linseed oil specimens that had been in an oven at 35 °C for 2 weeks — a standard drying procedure before moisture uptake test to ensure the lowest possible moisture content in the material. No changes in the properties were expected, however, over that period the strength did reduce by 17.9% and modulus by 12.1% compared to the original specimens. This means that the accelerated ageing has drastic effects on the performance of UV-cured glass/linseed oil due to the temperature effects. All of the glass/linseed oil specimens had been dried in the oven prior to testing, meaning that the properties had reduced already before the moisture

uptake tests started. The probable cause behind this reduction of properties is the low T_g (40 °C) of this specific linseed oil resin [92].

4.3.3 Changes in Failure Modes due to Moisture Uptake

MicroCT images show that dry glass/linseed oil specimens failed on compressive and tensile side of the specimens (left image in Figure 4.16). There were several cracks developing from the tensile side; the cracks were mainly propagating along the fibre/matrix interface and through matrix rich areas with very little fibre breakage. On compressive side mainly crushing and fibre kinking was detected together with matrix and interfacial cracks. It was also observed, that there were almost no voids inside the specimens, just a few voids occurring on the mould side side of the specimens.

The aged glass/linseed oil specimens' failure scans were carried out after 3 days of ageing. After 3 days of ageing the failure occurred only on the compressive side of the specimens (Figure 4.16). The main visible damage to the material was delamination, fibre kinking and some matrix cracks developing from the delaminations. It is possible that the matrix

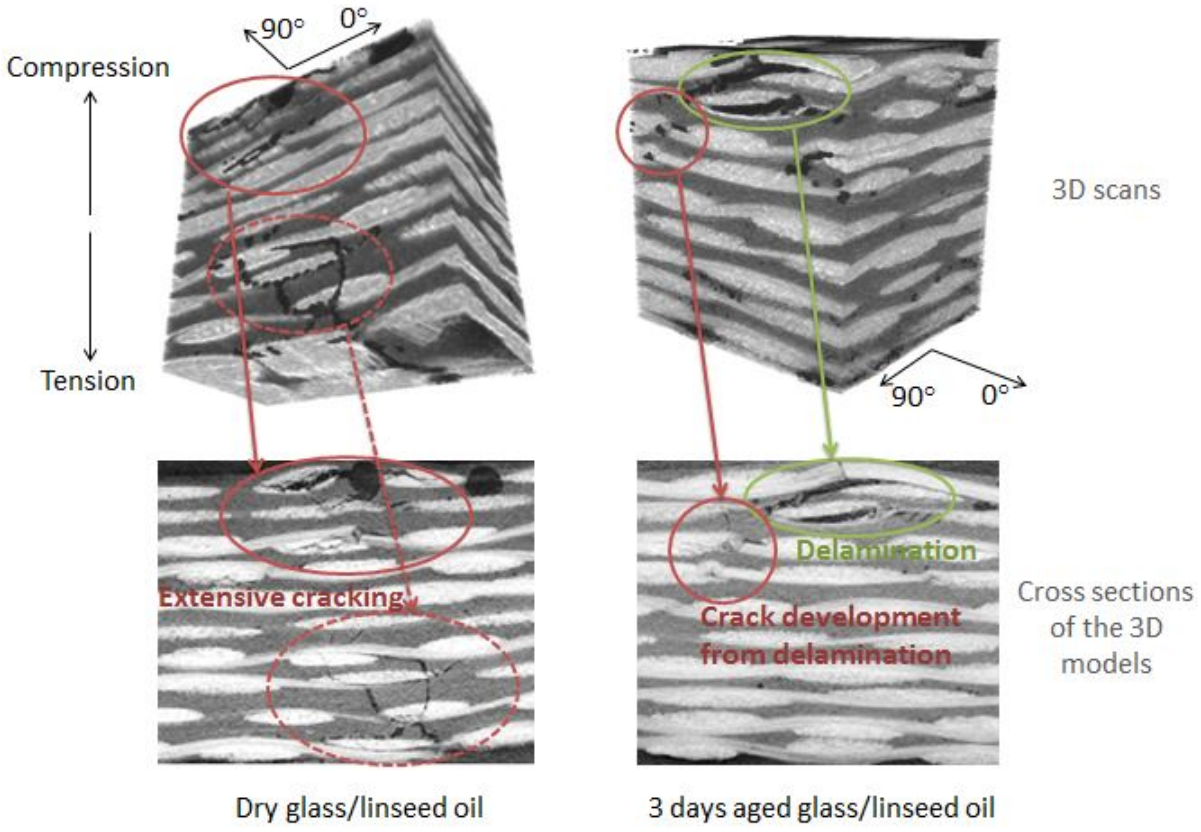

Figure 4.16: CT images (3D scan above and cross section below) of the dry glass/linseed oil (left) and 3 days aged specimen (right) showing differences in the failure

has already plasticised significantly and the yield strength of the matrix had reduced so that the compressive failure was dominating after only 3 days of ageing.

After 6 days of ageing no failure could be visually detected in the glass/linseed oil composite. There was no indication of fibre failure suggesting that after 6 days the failure was already matrix dominated and there was obvious lack of transferring loads to fibres. As there were no visible voids in glass/linseed oil specimens the main cause behind the water uptake, reduction of properties and changes in failure modes must be due to the poor performance of linseed oil matrix and the interface.

4.4 Glass/Linseed Oil Non-Accelerated Ageing

4.4.1 Moisture Uptake

Figure 4.11 shows the non-accelerated moisture uptake in glass/linseed oil composites. The moisture uptake of glass/linseed oil composites was linear in both distilled and salt water up to week 56 when the moisture uptake slowed down. By the end of the testing period the glass/linseed oil specimens had not reached the moisture equilibrium condition.

4.4.1.1 Factors Affecting Moisture Uptake in Glass/Linseed Oil

Effects of Water Temperature and Salinity

The distilled water specimens, both non-accelerated and accelerated, reached a similar moisture content of around 5%. In accelerated conditions this moisture content was achieved over 49 weeks, in non-accelerated conditions over 88 weeks. Although the moisture content in non-accelerated conditions may increase even further, it is observed that in distilled water the moisture content absorbed is of a similar scale despite the temperature. Temperature affects only the speed of moisture uptake in glass/linseed oil.

The specimens aged in salt water showed a slower moisture uptake and a lower moisture content than the specimens aged in distilled water. Reaching the same moisture content of around 3% (used for comparison purposes only) took 6 weeks with accelerated ageing, 25 weeks in distilled water (non-accelerated), and 48 weeks in salt water (non-accelerated). By the end of the 88 week testing period the salt water specimens had a moisture content of 3.35% compared to 4.92% in distilled water specimens.

In glass/linseed oil specimens the lower temperature causes slower moisture uptake but the temperature does not seem to affect the moisture content absorbed. Increasing the salinity of the water, on the other hand, reduces the uptake speed and the moisture content.

Blistering

Blisters occurred in distilled and salt water non-accelerated ageing specimens after 14 weeks of ageing. The blisters in non-accelerated ageing specimens were small but occurred in every specimen, leading to an uniform scatter in weight increase in both distilled and salt water. If there were no blisters then the specimens would have been expected to reach moisture equilibrium at around 3% of moisture uptake (like the non-blistered specimens in accelerated ageing tests). In non-accelerated distilled water the 3% moisture content was achieved after 25 weeks and in salt water after 48 weeks, long after the blisters had occurred (14 weeks). This explains why the moisture uptake in non-accelerated conditions was more linear than in accelerated conditions and did not slow down after reaching 3% moisture content like it did in accelerated ageing specimens. In glass/linseed oil the blisters increase the moisture uptake significantly even in non-accelerated conditions.

4.4.2 Effects of Moisture Uptake on Flexural Properties

From Figure 4.17 it appears that the reduction of flexural strength in non-accelerated ageing conditions follows the same trend as the accelerated ageing specimens did. In non-accelerated conditions the reduction of properties takes longer to occur but with the same moisture content the reduction of strength is very similar. The first clear comparison can be made after 2 weeks of accelerated ageing, 8 weeks of non-accelerated ageing in distilled water and 15 weeks of non-accelerated ageing in salt water. With the moisture content of 1.6–1.7% the flexural strength in all three ageing conditions had reduced by 60–68%. After that point the strength reduced slightly more and then remained around 70% with an increasing moisture content in all of the ageing conditions.

The reduction of flexural modulus shows similar trends to the reduction of strength (Figure 4.18). At the moisture content of 1.6–1.7% the flexural modulus had reduced by 33–42%. The lowest was the reduction of modulus in distilled water (non-accelerated), the reduction in salt water and accelerated conditions was more varying. In accelerated conditions the reduction stayed above 40% for the rest of the ageing period.

At room temperatures the reduction of properties occurred at a slower rate but after 8–15 weeks of ageing in distilled and salt water the reduction of flexural strength reached the same level as accelerated ageing specimens in 2 weeks (Figure 4.17). With longer ageing periods the reduction of strength maintained an uniform level. After 14 weeks of ageing the blisters occurred also in non-accelerated ageing specimens but they were smaller and there were multiple blisters in every specimen; the small blisters had no effect on the flexural properties.

Non-accelerated ageing tests show that the reduction of properties in glass/linseed oil is largely dependent on the moisture content rather than water chemistry or ageing

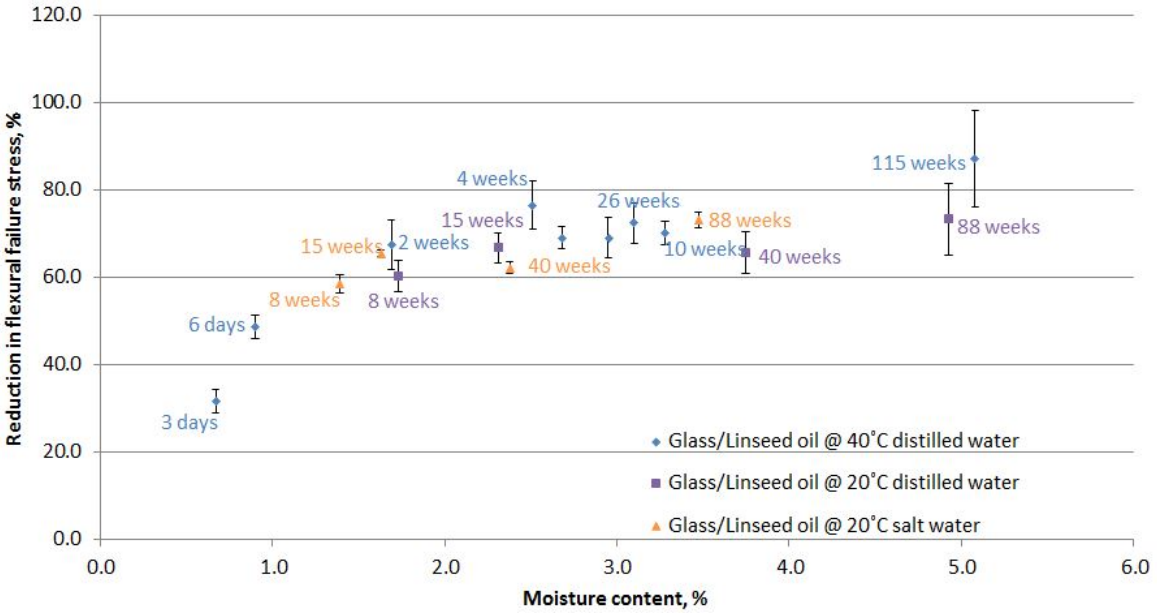

Figure 4.17: Changes in the flexural failure stresses of glass/linseed oil due to moisture uptake in accelerated and non-accelerated conditions

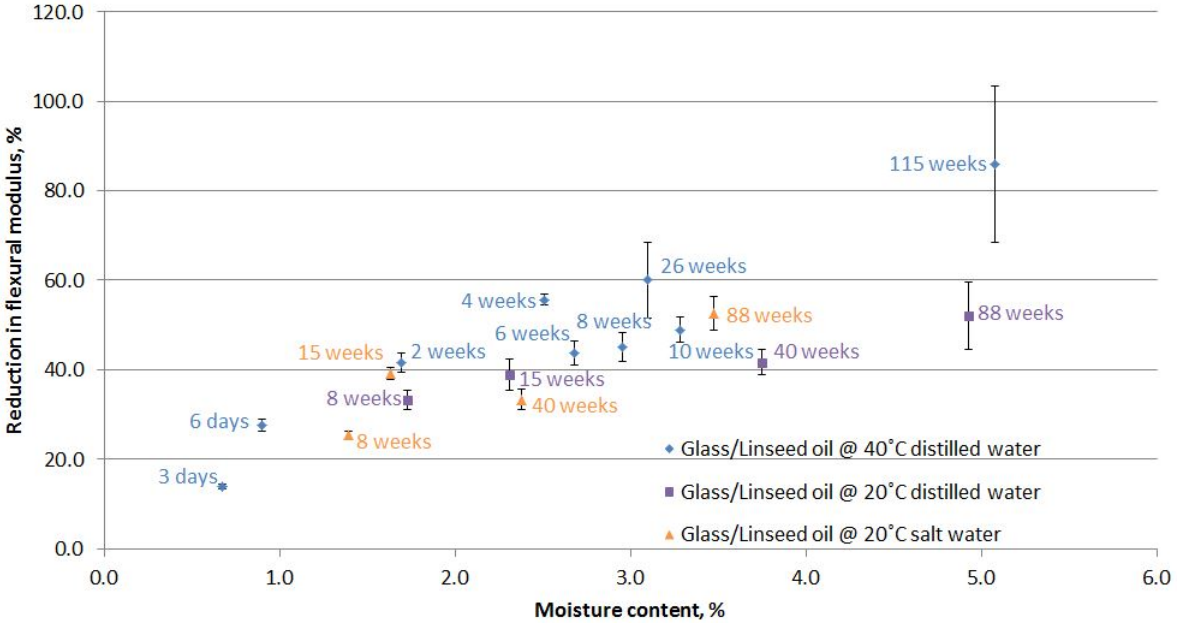

Figure 4.18: Changes in the flexural modulus of glass/linseed oil due to moisture uptake in accelerated and non-accelerated conditions

time. Beyond the 2.3-2.4% moisture content the reduction of flexural strength levels out, demonstrating that the effects of moisture are somewhat limited.

4.5 Glass/Castor Oil Accelerated Ageing

4.5.1 Moisture Uptake

The accelerated moisture uptake of glass/castor oil can be seen in Figure 4.19. The glass/castor oil specimens show a very steady moisture uptake that only slows down after 25 weeks of ageing. The scatter in the moisture uptake is low up to week 12 and starts increasing after that. The moisture uptake almost stopped after 39 weeks having reached 3.54%. By the end of the test period (102 weeks) the moisture uptake in glass/castor oil had reached 3.71%. The moisture uptake curve is not exactly linear already from the beginning of moisture uptake but the diffusion coefficient was still calculated for comparison purposes (Table 4.1). For the calculations the moisture uptake was considered to be linear up to week 5.

4.5.2 Effects of Moisture Uptake on Flexural Properties

Dry glass/castor oil had a flexural strength of 295.7 MPa (with SD of 45.8 MPa) and modulus of 16.3 GPa (with SD of 0.8 GPa). After 102 weeks of ageing glass/castor oil

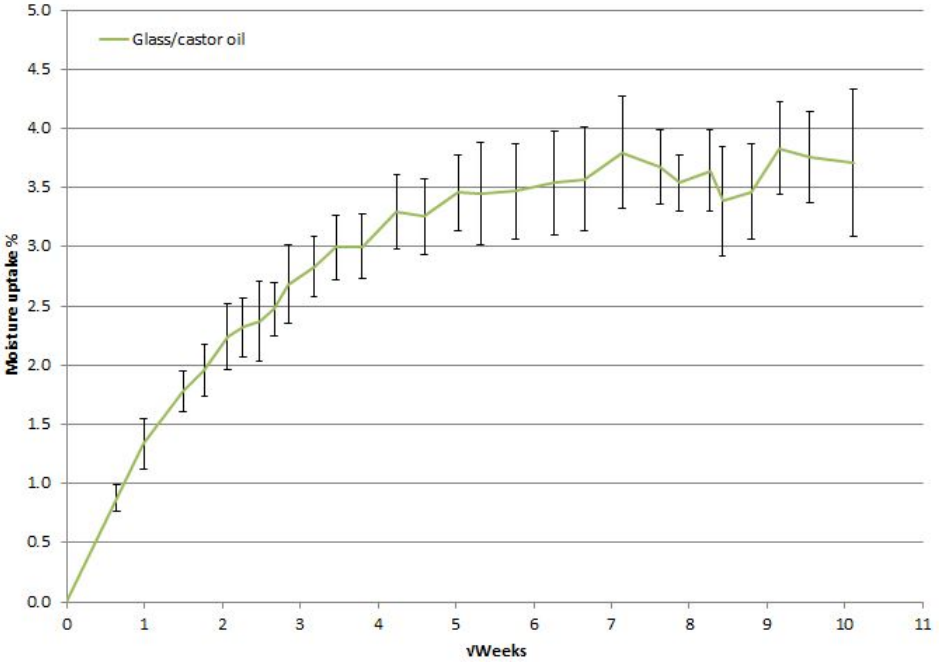

Figure 4.19: Accelerated moisture uptake vs. weeks$^{\frac{1}{2}}$ in glass/castor oil specimens

had a strength of 240.5 MPa (with SD of 5.8 MPa) and modulus of 13.8 GPa (with SD of 0.2 GPa). By the end of the test period the reduction of flexural strength in glass/castor oil was only 18.7% while the moisture content was 3.71% (Figure 4.2).

In the reduction of flexural strength the glass/castor oil showed some variation, the 3 days and 8 weeks aged specimens showed about 20% higher reduction of strength than the other specimens did. At the same time the scatter of data points in the graph was very small for all of the ageing periods. Despite the variation in the reduction of properties the general trend was a reduction of strength up to week 55. The next test was carried out with 102 weeks aged specimens and showed an improvement of flexural strength in comparison with the 55 weeks aged specimens. That could be due to the specimens being cut from different panels and having different properties or further curing of the polyurethane matrix due to the presence of water [18].

The changes in flexural modulus of glass/castor oil with moisture uptake showed similar trends to the flexural strength. There was a variation in the results after 3 days and 8 weeks of ageing, confirming the theory that these specimens were cut from a different panel and had different properties. In general the flexural modulus showed reduction with ageing but increased again after 55 weeks of moisture uptake just like flexural strength did.

Glass/castor oil shows interesting behaviour in the presence of water and its usability in maritime structures should be investigated further.

4.6 Effects of Resin Systems on Moisture Uptake and Flexural Properties

In this work three different materials were subjected to hygrothermal ageing: glass/epoxy, glass/linseed oil and glass/castor oil composites. The fibre lay-up of all three materials was the same, the differences lie in the resin systems used and manufacturing techniques. Glass/epoxy and glass/castor oil were manufactured in the same laboratory conditions and using the same technique, the post curing was carried out according to the manufacturers' recommendations. The resulting composites had a slightly different thickness leading to different fibre and matrix volume fractions (Table 3.2). The void content was lower in glass/castor oil specimens.

Glass/linseed oil specimens were manufactured with the same fibre lay-up but in a different facility using hand lay-up and UV-curing; the curing process had not been optimised. The glass/linseed oil specimens were thicker than glass/epoxy and glass/castor oil specimens, the fibre volume fraction was lower and matrix volume fraction higher than in the other two materials tested. The void content was low (1.2%) in glass/linseed oil specimens due to the benefits of UV-curing.

No information about the chemistry of the plant oil based resins was available to the author. The other relevant but currently unknown properties of the resin systems are thermal expansion coefficients, glass transition temperatures (linseed oil is known to have a low T_g [92]), and bonding between the plant oil based matrices and glass fibres. These parameters affect both the moisture uptake and the mechanical properties of the composites tested, but the effects of these parameters can only be hypothesised in the analysis of the test results.

4.6.1 Moisture Uptake in Epoxy and Plant Oil Based Composites

Comparison of the normalised moisture uptake curves shows that the accelerated moisture uptake in glass/linseed oil and glass/castor oil specimens is similar (Figure 4.20). Both of the plant oil based composites absorb more moisture than glass/epoxy does and neither glass/linseed nor glass/castor oil composites have reached the moisture equilibrium condition by the end of the testing period. In glass/linseed oil this behaviour is explained with blistering that occurred in the specimens after 5–6 weeks of ageing and were shown to significantly increase the moisture uptake in the specimens.

In glass/castor oil, the reasons behind the increasing moisture uptake remain unclear. The matrix volume fraction was higher in glass/castor oil than it was in glass/epoxy and the results have already been normalised over the matrix volume fraction. The higher moisture uptake cannot be due to the higher void content because the void content in

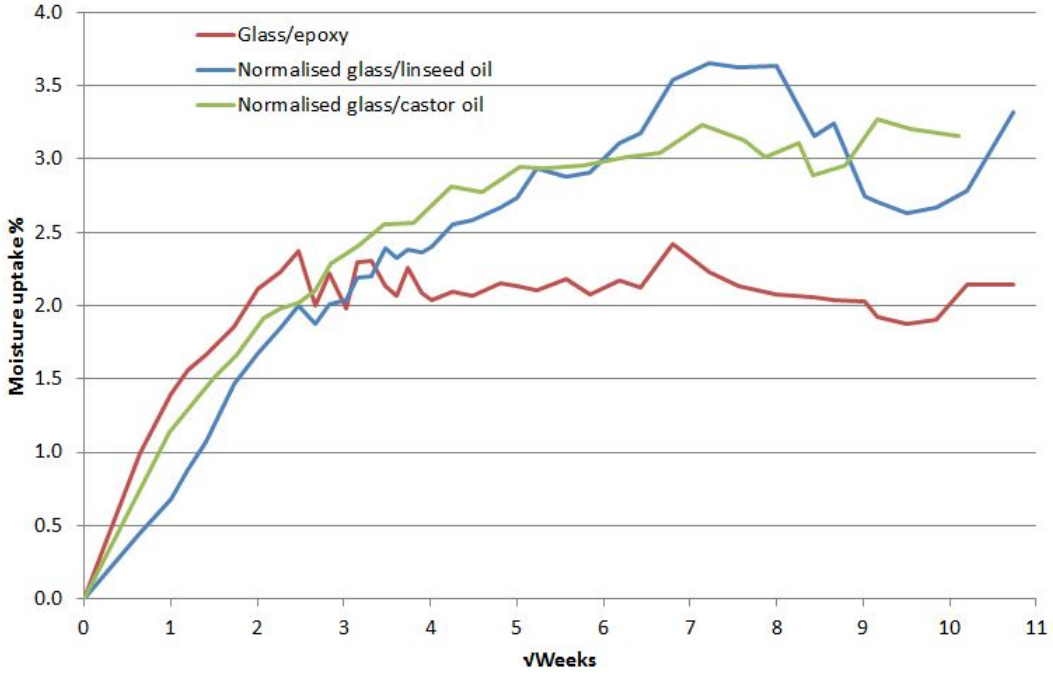

Figure 4.20: Normalised moisture uptake vs. weeks$^{\frac{1}{2}}$ in the three different composites tested

glass/castor oil specimens was 2.8% compared with 4.3% in glass/epoxy (Table 3.2). It is possible that the thermal expansion is greater in castor oil matrix than it was in epoxy. That would cause swelling of the matrix, creating additional space for the water to diffuse into. Swelling would also cause temperature induced stresses in the material due to the differences between fibres and the matrix where fibres swell less than the matrix does. This would potentially lead to cracking in the matrix and the interface, thus creating additional water storage areas inside the material. Another possibility is the curing of the polyurethane the castor oil resin is based on. It has been reported in the literature that polyurethanes cure in the presence of water [18]. This means that there could be more chemically bound water in glass/castor oil than in other two materials tested, explaining the high moisture uptake.

4.6.1.1 Effects of Temperature, Salinity and Voids

Non-accelerated moisture uptake tests were carried out with glass/epoxy and glass/linseed oil specimens in distilled and salt water. The aim was to compare the accelerated ageing with non-accelerated one and determine the usability of accelerated ageing when simulating real life operating conditions.

The non-accelerated ageing results showed similar results with both of the materials. The temperature of the water was found to affect the speed of moisture uptake but not the quantity absorbed. Both the elevated and room temperature ageing specimens absorbed similar quantities of distilled water. Increasing salinity of the water slowed down the water uptake speed further and also reduced the quantity of the moisture absorbed.

When looking at the effects of temperature only and the faster water uptake at higher temperatures, then currently it is unclear what causes the faster water ingress in both glass/epoxy and glass/linseed oil specimens at elevated temperatures. One of the options is that the water molecules are more active at higher temperatures causing the whole water ingress process to go faster. The other option (that can occur together with the first one) is that higher temperature causes the matrix to swell (thermal expansion) and through this creates more space for the water to penetrate into from the start of the moisture uptake. Also, higher temperature and thermal expansion may cause debonding within the material as the fibres do not expand as much as the matrix does. This, however, does not explain the results as in distilled water the accelerated ageing specimens should then absorb more water than non-accelerated ageing specimens but they do not; the accelerated and non-accelerated ageing specimens absorbed the same quantity of distilled water. Therefore, in this case the faster moisture uptake is most likely caused by higher molecular activity at elevated temperatures and not by swelling or damage to the material.

Adding salt in the water reduced the speed of moisture uptake compared with distilled water. The addition of salt to the water means that some of the water molecules are already chemically bound with salt and can not react with the composite material, through this reducing the amount of water entering the material. In addition, the water and salt particles combined may be too big to penetrate the matrix of the composite and to reach storage areas like voids, cracks and interface inside the material resulting in a lower water uptake.

As a conclusion, the effects of water temperature on moisture uptake speed of composites are greater than that of salt as was shown by the non-accelerated ageing tests. Salt had an effect on the quantity absorbed. The experiments need to be carried out for longer to gain the maximum water content at lower temperatures and evaluate the effects of lower temperature and salt on the moisture uptake further. The effects of thermal expansion should be investigated as part of future work.

The accelerated ageing process gave comparable results with non-accelerated ageing in both glass/epoxy and glass/linseed oil and can be used for both materials. The tests showed that the flexural properties depend mainly on the moisture content and if that is known for different water salinity then the changes in the flexural properties can be determined from the accelerated ageing tests.

4.6.2 Flexural Properties of Epoxy and Plant Oil Based Composites

Figures 4.21 and 4.22 show the differences of flexural strength and modulus of the three materials tested before and after 2 years of ageing. When dry, glass/epoxy has the highest flexural strength and modulus compared with the plant oil based composites. The lower properties of glass/castor oil and glass/linseed oil can be attributed to the lower fibre volume fractions, lower properties of castor oil and linseed oil resins, and possibly lower interfacial strength. There is no confirmation about the interfacial strength in glass/castor oil but it has been found that UV-curing matrices (like the linseed oil used in this research) create weaker bonds with fibres [35].

The lower matrix and interfacial properties in glass/linseed oil have led to differences in the failure modes of dry glass/epoxy and glass/linseed oil. While the microCT images of glass/epoxy show extensive fibre damage on the tensile side of the specimen, the glass/linseed oil specimens show mainly interfacial and matrix cracking with very little fibre breakage present on the tensile side. These differences can be attributed mainly to poor interfacial strength and lack of transferring loads to fibres in glass/linseed oil specimens. The materials tested show very different behaviour after moisture uptake and these differences will be discussed below.

4.6.2.1 Glass/Epoxy

The flexural strength of glass/epoxy reduced by 57.7% due to moisture uptake. Most of the reduction was achieved over the first 10 weeks of accelerated ageing. Similar degradation rates were achieved also in non-accelerated conditions. Majority of the reduction can be attributed to weakening of the interface as was shown in SEM images. This is affecting mainly the 90 ° fibres on the tensile side where the interface is subjected to tension. Changes in the interface strength have changed the failure mechanism as was seen in microCT images. Understanding the changes in the failure modes is one of the key factors in explaining the reduction of properties in glass/epoxy and the failure modes will be investigated further with the aid of AE in the next chapter.

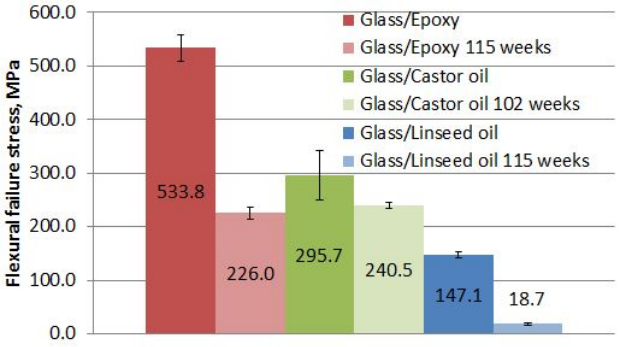

Figure 4.21: Flexural strength before and after accelerated ageing in the three materials tested

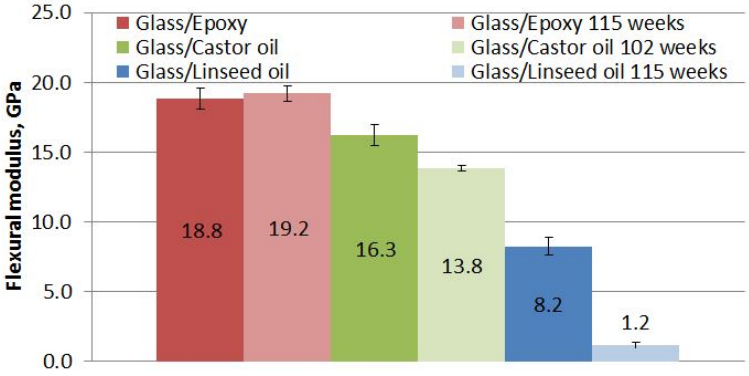

Figure 4.22: Flexural modulus before and after accelerated ageing in the three materials tested

4.6.2.2 Glass/Castor Oil

Glass/castor oil showed the lowest reduction of flexural strength after 2 years of accelerated ageing, only 18.7%. The modulus reduced by 15.3%. The resin and the interface may have been unaffected by moisture or the curing of polyurethane with moisture compensated for the damage caused to the interface. As a result it appears that, compared

to other two materials tested, glass/castor oil is relatively unaffected by moisture uptake. No further tests were possible with glass/castor oil but the material does show some potential for maritime applications.

4.6.2.3 Glass/Linseed Oil

Out of the three materials tested glass/linseed oil showed the greatest reduction of properties due to moisture uptake. Elevated temperatures were shown to reduce the properties of glass/linseed oil significantly; however, similar reduction was noticed in non-accelerated ageing specimens. It is known that the glass transition temperature of glass/linseed oil is very low and the accelerated ageing tests were possibly carried out on the edge of the glass/linseed oil performance, causing a rapid degradation of the material. Water uptake is known to reduce the glass transition temperature and that is probably the reason why non-accelerated ageing specimens showed similar reduction of properties to accelerated ageing. Blisters did not seem to affect the properties in the earlier stages of ageing, they only started reducing the properties once they had grown big enough (it has been reported that delaminations covering less than 50% of the support span do not affect flexural strength [90]). The greatest reduction of properties in accelerated ageing occurred over the first 2–4 weeks of ageing while blisters were noticed only after 5–6 weeks.

In addition to the problems with glass transition temperature in glass/linseed oil, the secondary bonding with UV-curing was not optimised and possibly the bonding between the matrix was not good as seen from the micrograph in Figure 4.23. There are clear lines where there should be bonding between the layers of composite. Having such clear lines suggests that the secondary bonding between different layers of matrix is not good and there are issues with transferring loads from one layer to the other. It is also possible that the moisture causes additional debonding between the matrix layers and reduces the properties even further.

The microCT images confirmed a rapid change in the failure modes of glass/linseed oil specimens. These failure modes are looked in more detail in the next chapter where the failure has been analysed with acoustic emission testing.

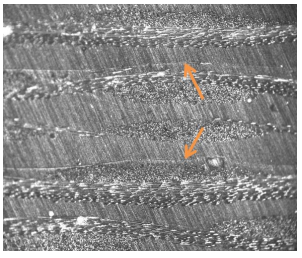

Figure 4.23: A micrograph showing the quality of secondary bonding in glass/linseed oil specimens

Chapter 5

Results and Discussion: Analysis of the Failure Modes with AE

Flexural testing and visualising the damage with microCT showed that there are differences in the failure modes of glass/epoxy and glass/linseed oil. It was also shown that these failure modes change with moisture uptake. In order to understand the reduction of properties, additional work was carried out with the acoustic emission (AE) technique to look at the failure modes. In addition to the failure modes, the changes in wave speed and different AE parameters were investigated to choose the most suitable parameters for the purposes of this research.

5.1 Effects of Moisture Uptake on the Wave Speed and AE Parameters

The effects of moisture uptake on wave speed and attenuation of an AE event in glass/linseed oil and glass/epoxy composites were determined over a 6 week period of accelerated ageing. Attenuation is measured as a change in the amplitude of a specific event at various distances from the sensors. Here the event was pencil lead break that provides a repeatable source for the AE signal [75, 85].

Figure 5.1 shows the test setup for measuring both wave speed and attenuation. The pencil lead break for wave speed tests was done at the orange crosses (Figure 5.1) and the time of arrival (TOA) in the two sensors was measured. The difference of TOA in the sensors and the known distance between the sensors was used to determine the wave speed. In direction 1 the signal first reached channel 1 (CH1, sensor 1) and then channel 3 (CH3, sensor 2). In direction 2 the signal first reached CH3 (sensor 2) and then CH1 (sensor 1). For attenuation measurements the pencil lead break was done at different distances between the two sensors. There were 6–12 measurements used for

every data point shown in the graphs. The usable measurements were chosen based on the expected wave speed and hit parameters recommended by experienced users of the AE technique.

5.1.1 Wave Speed

Wave speed information is generally used for locating the damage in structures. While it is not within the limits of this work to locate the damage in the specimens it is important to know how moisture ingress affects the wave speed in order to take the changes into account when analysing the data from structural tests.

From Figure 5.2 it was observed that in glass/epoxy the direction 1 data shows a clear trend of reducing wave speed over the ageing period. The direction 2 data matches the direction 1 data for dry, 3 and 4 weeks aged specimens. However, there are two data points in direction 2 falling out of the general trend of reducing wave speed, namely the data points of 1 and 6 weeks aged specimens. The same observation can be made in Figure 5.3 where the wave speed has been plotted against moisture uptake.

In both directions the moisture uptake causes changes in the wave speed in glass/epoxy. After 6 weeks and 2.6% moisture uptake there is a 9.4% reduction in direction 1 wave speed and 2.3% reduction in direction 2 (Figure 5.3). The latter, however, fits within the error margin of the dry specimen and may not be considered as a reduction in wave speed. After 3 and 4 weeks of ageing (2.1% moisture uptake) directions 1 and 2 show more similar reduction in wave speed, namely 2.9% and 3.8% after 3 weeks; 5.6% and 7.7% after 4 weeks. Based on this information it is unclear which direction provides more accurate wave speed prognosis, however based on the current information the trend shown by direction 1 data is clearer.

When looking at the wave speed changes in glass/linseed oil specimens then the picture is quite different (Figures 5.2 and 5.3). Data from direction 1 and direction 2 show similar trends and it seems that for the first 3 weeks of ageing the wave speed is reducing and

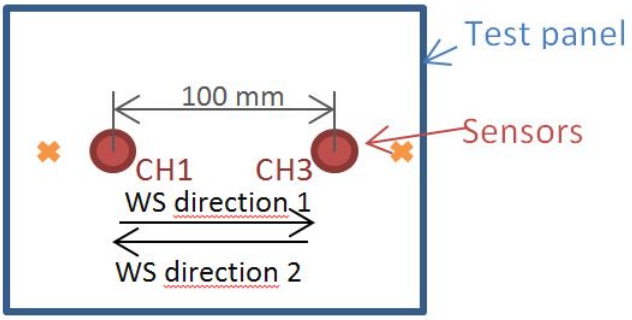

Figure 5.1: Schematic of measuring wave speed (WS) and attenuation, orange crosses show the locations of the pencil lead break for wave speed measurements

starts increasing after that. Figure 5.3 shows that the reduction of wave speed occurs until the moisture uptake reaches 2.7–2.9% and with a greater moisture uptake the wave speed increases.

Considering the longitudinal wave speed equation for solids, it appears that the wave speed is affected by Young's modulus, density and the Poisson's ratio (Equation 5.1)[93]. Moisture uptake can change the Young's modulus [58] and it is only logical that density is also changed, possibly affecting Poisson's ratio, thus altering the wave speed inside the material. It is possible that the wave speed increases after it has been initially decreasing if the changes in these parameters occur non-simultaneously at different stages of moisture uptake (Table 5.1).

When comparing the wave speed changes in glass/epoxy and glass/linseed oil then the first thing to notice is the 450–600 m/s lower wave speed in glass/linseed oil specimen. It appears that the glass/epoxy data in direction 2 is actually similar to the wave speed changes in glass/linseed oil where an initial decrease of wave speed is followed by an increase. This does not explain the differences of glass/epoxy data points in opposite directions at weeks 1 and 6 but does increase the reliability of direction 2 data in glass/epoxy. Whilst initially it looked like the direction 2 data points were showing odd behaviour it now appears that actually the direction 1 data points may be off the trend and the wave speed increases after the initial reduction in both the glass/linseed oil and glass/epoxy specimens.

It can be concluded from this data that as little as 1.0–1.5% moisture content in the specimen changes the wave speed and that needs to be counted for when using AE for structural health monitoring or other applications where composites are exposed to humidity.

$$c_l = \sqrt{\frac{E(1-\nu)}{\rho(1+\nu)(1-2\nu)}} \tag{5.1}$$

Table 5.1: The effects of changing variables on the wave speed according to equation 5.1

Variable	**Result of decreasing the variable**
Young's modulus	Decrease of wave speed
Poisson's ratio	Decrease of wave speed
Density	Increase of wave speed

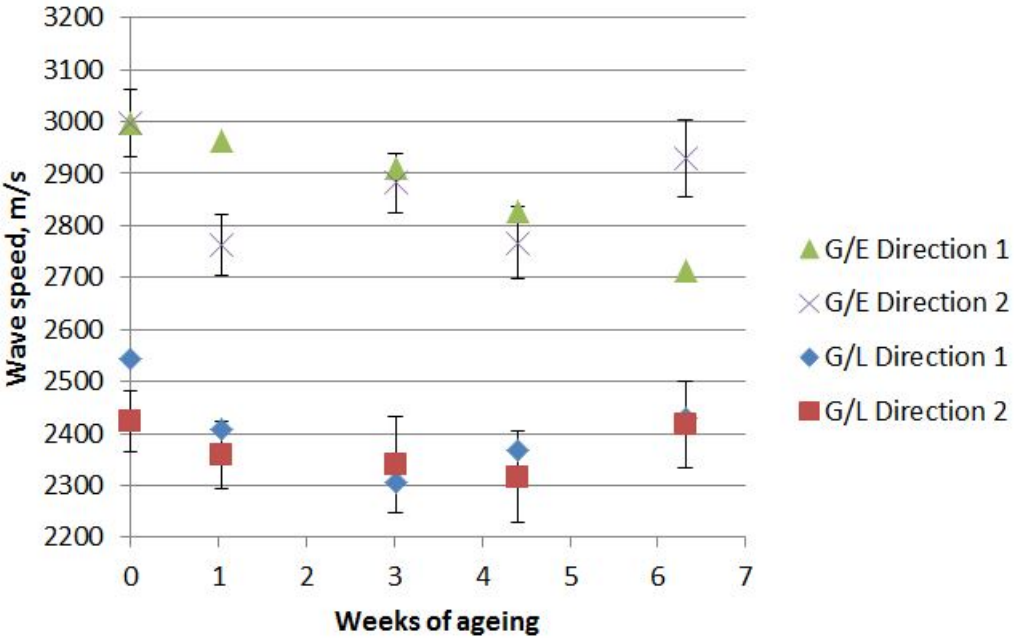

Figure 5.2: Changes in wave speed of glass/epoxy (G/E) and glass/linseed oil (G/L) specimens over the ageing period. Variation of the test results shown for direction 2 data only

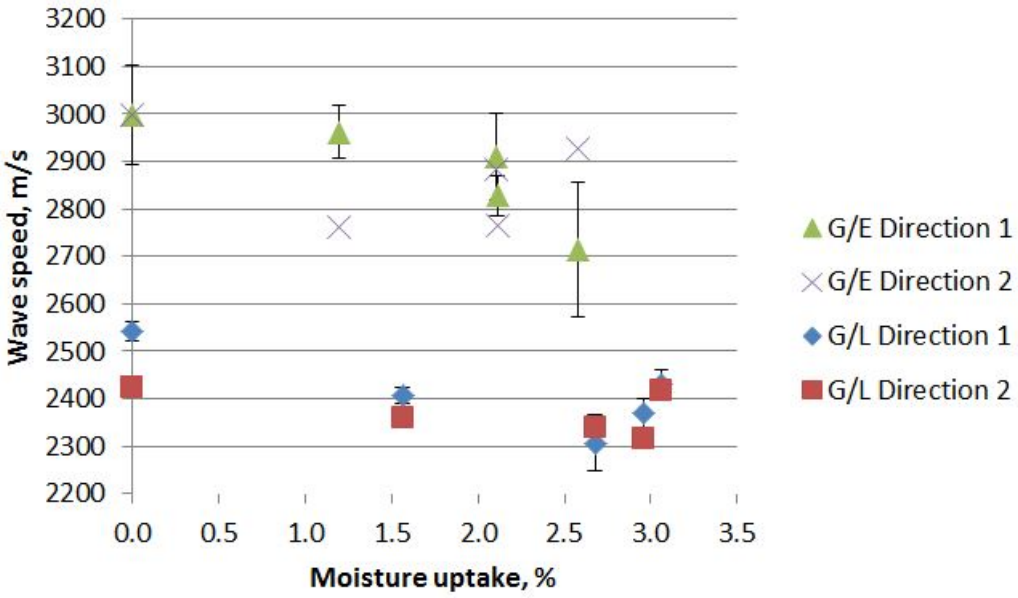

Figure 5.3: Changes in wave speed of glass/epoxy (G/E) and glass/linseed oil (G/L) specimens with moisture uptake. Variation of the test results shown for direction 1 data only

5.1.2 Attenuation and Changes in Parameters

Different parameters like amplitude, energy, duration and frequency have been used to characterise failure in composites [75, 76]. Moisture uptake can result in a modified signal in response to the same failure mechanism. In order to investigate changes in failure modes it is desirable to use parameters that remain unaffected by moisture uptake. For that reason attenuation as a change in the amplitude over distance was investigated as well as the changes of other properties (duration, energy, counts, peak frequency) over distance and ageing time. Pencil lead break was used as a repeatable event throughout these tests.

Attenuation graphs for channel 1 (CH1, Figure 5.4) and channel 3 (CH3, Figure 5.5) show differences in the trends of the two channels for both glass/epoxy and glass/linseed oil specimens. First, it is observed that CH3 shows slightly lower values for the amplitudes and the amplitudes in glass/linseed oil specimens at the same distance are 5–15 dB lower than in glass/epoxy. Channel 1 attenuation graph shows that the attenuation reduces with moisture uptake in both glass/epoxy and glass/linseed oil specimens by 1.9–9.8 dB and 2.1–10.3 dB respectively, with the difference reducing over distance in both materials. Based on the literature the attenuation should remain the same [88] or increase with moisture uptake [88, 94, 95] like shown by data from channel 3 (Figure 5.5). Figure 5.5 shows that the attenuation of glass/epoxy remains roughly the same with ageing and increases in glass/linseed oil by 3.2–7.3 dB. In this case channel 3 shows data as expected while channel 1 shows unexpected results.

Both Figures 5.4 and 5.5 show that amplitude changes with distance and moisture uptake. While amplitude is one of the most used parameters when analysing the AE results [71, 73, 74, 75], it is mostly unsuitable for the purposes of this research as the changes of amplitude over distance and ageing time may have a great effect on interpreting the results of the failure mechanisms.

From the other parameters the energy showed very similar trends to amplitude. Duration remained on the same level in glass/epoxy (both over distance and ageing time) and reduced over distance in glass/linseed oil specimens by 30%, similar trend occurred with counts. Both duration and counts showed great variation in the data points. From the parameters measured, frequency (in this work considered as the peak frequency calculated from FFT) showed least change over distance and ageing time (Figures 5.6 and 5.7), variation in the data points was also the lowest. While most of the hits in channel 1 occur around frequencies of 18–19 kHz the channel 3 frequencies are slightly lower, being around 16–17 kHz. The same case applies to amplitude where CH3 shows around 5 dB lower amplitudes. This difference is most likely caused by differences in the sensors used as two sensors never behave exactly the same way [85]. Frequency was similar in both of the materials suggesting that the same event may cause comparable

frequencies in both materials during flexural tests. For the reasons above frequency will be the main parameter used in this work for analysing the failure mechanisms.

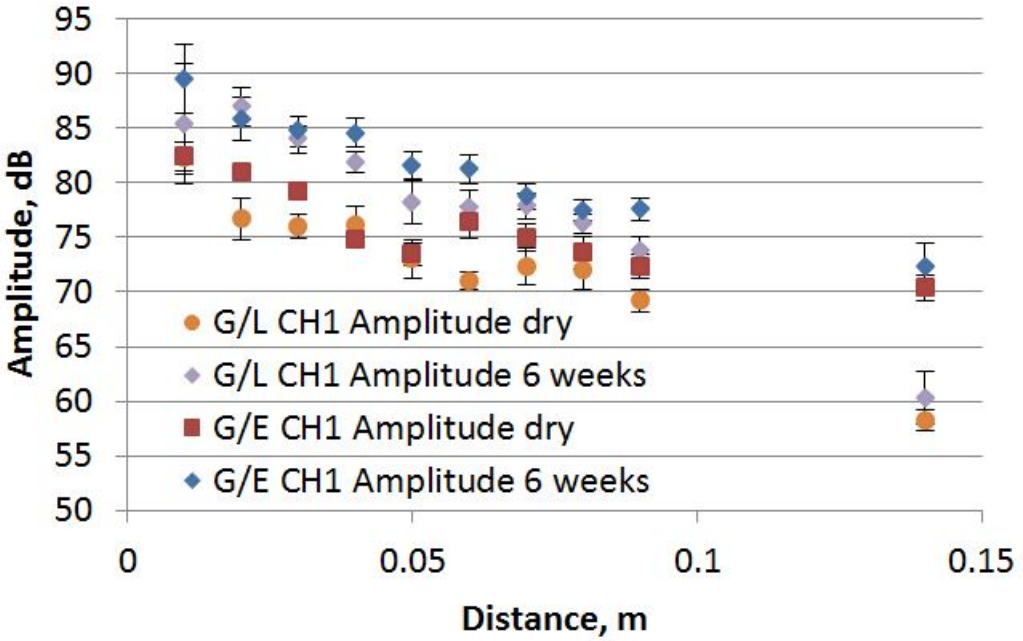

Figure 5.4: Changes in channel 1 (CH1) amplitude response in glass/epoxy (G/E) and glass/linseed oil (G/L) specimens due to moisture uptake

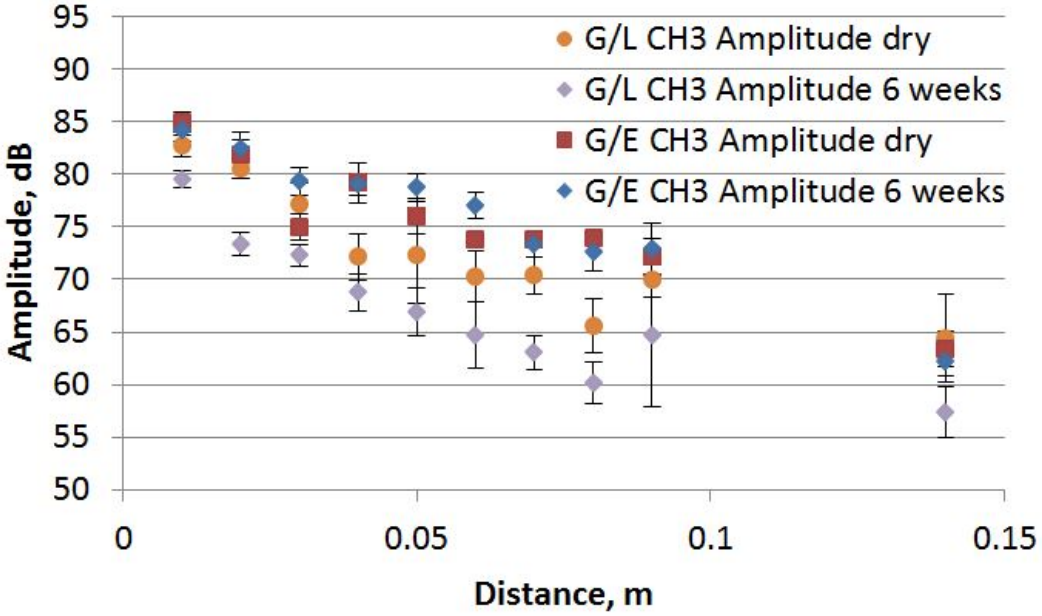

Figure 5.5: Changes in channel 3 (CH3) amplitude response in glass/epoxy (G/E) and glass/linseed oil (G/L) specimens due to moisture uptake

5.2 Effects of Moisture on the Frequency Response of the Failures

Acoustic emission testing was carried out with glass/epoxy and glass/linseed oil specimens in order to clarify the moisture induced changes in failure modes witnessed with microCT. AE tests were done with dry unreinforced matrix, dry composite, 7 weeks aged glass/epoxy specimens, and 2 years aged composite specimens. Although manufactured in the same laboratory conditions, the void content of the specimens was different. The moisture uptake, flexural tests and microCT scans were carried out with different specimens and may represent a slightly different failure.

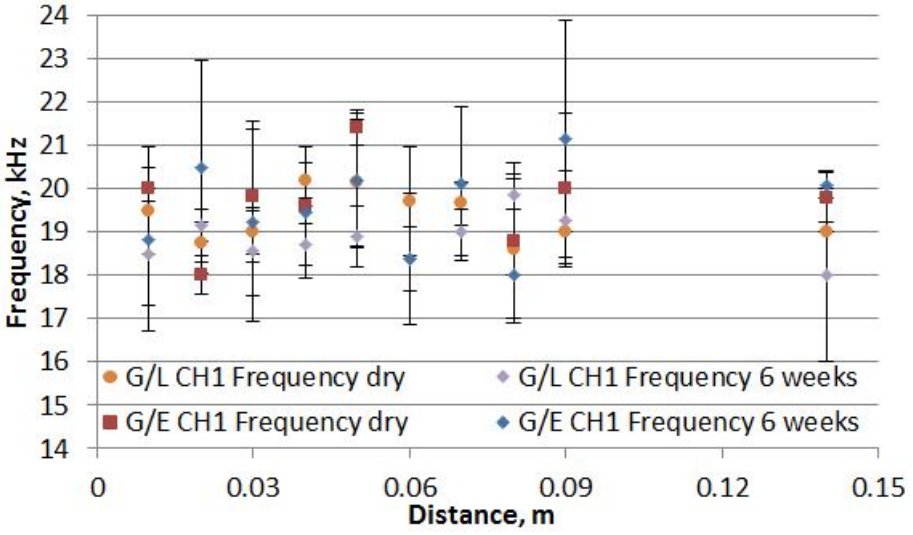

Figure 5.6: Changes in channel 1 (CH1) frequency response in glass/epoxy and glass/linseed oil specimens due to moisture uptake

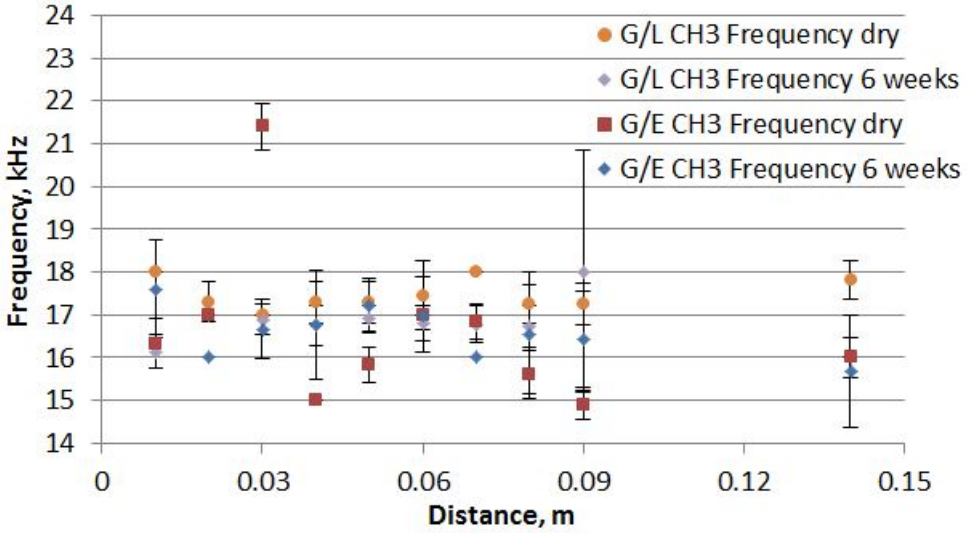

Figure 5.7: Changes in channel 3 (CH3) frequency response in glass/epoxy and glass/linseed oil specimens due to moisture uptake

The changes in glass/linseed oil performance happen significantly faster than in glass/epoxy, being a matter of 2–4 weeks. Therefore the AE tests were carried out more frequently with glass/linseed oil specimens to capture the rapid changes in the failure mechanisms. The test were done with 0.5–1 week intervals up to week 4 and then with 2 years aged glass/linseed oil specimens. It should be noted that the dry and 7 weeks aged glass/epoxy specimens were manufactured separately from the moisture uptake and flexural test.

For clarity, the frequency ranges are divided into 5 groups in the figures and discussion: *a* — 400–500 kHz, *b* — 200–300 kHz, *c* — 20–30 kHz, *d* — 100–200 kHz and *f* — around 80 kHz. In the discussion *b** refers to the higher frequencies (250–300 kHz) in range *b*. The order of the different frequency ranges occurring during testing is brought out with circled numbers in the graphs and in the discussion referred to as (1), (2) etc. The dotted lines in the graphs are used to point out the stresses of the starting AE hits.

5.2.1 Frequency Ranges Related to Failure Mechanisms

If frequency was dependent on material properties then it would have been different for glass/epoxy and glass/linseed oil during the pencil lead breaks, wave speed and attenuation tests. During the unreinforced matrix tests the fracture of matrix caused a signal with very similar frequencies in epoxy and linseed oil. For these reasons it is assumed here that information about frequency ranges in glass/epoxy can be transferred to glass/linseed oil and vice versa.

The frequency ranges were related to different failure mechanisms based on the discussion in the following sections. However, the information was found to be essential for understanding the graphs following in the rest of the chapter and therefore the explanations are presented here for clarity.

Range *c* (10–50 kHz) — in the unreinforced matrix tests all the hits (both epoxy and linseed oil) fell within this range and it was thought that this frequency range can be related to matrix cracking in a composite (see section 5.2.2). The idea was confirmed with range *c* being one of the first ranges appearing during the failure of dry glass/epoxy and glass/linseed oil specimens. The number of hits in range *c* reduced with ageing, fitting in with the theory of matrix plasticising due to moisture uptake. The disappearance of range *c* is more noticeable in glass/linseed oil where the range disappears after 1 week of ageing. At the same time the failure had become more compressive over the first 3 days of ageing and it has been reported that matrix is not acoustically very active under compression [91]. However, range *c* becomes again more dominating in the longer aged specimens. It is unlikely that in longer aged specimens this range is still related to matrix cracking, instead it could be representing a different matrix related mechanism in long-aged specimens.

Range *d* (100–200 kHz) — this range was one of the main ranges in aged glass/linseed oil specimens after 3 days of ageing. Only compressive damage could be detected with microCT in the 3 days aged specimens with some interfacial and matrix cracking. For this reason it is believed that range *d* is mainly related to compressive damage, including fibre kinking, microbuckling and delamination in the composite.

Range *a* (400–500 kHz) — in glass/epoxy the range *a* is mainly present during the final rupture of the material and in glass/linseed oil the range *a* generally appears together with a kink in the stress curve. When in tension and assuming a good fibre-matrix bonding, the final failure of a composite occurs with the fibre breakage. In case of glass/epoxy, the final failure occurs when the rest of the material has been greatly damaged and fibres in tension cannot take more load which is why range *a* (always accompanying the sudden failure in glass/epoxy) is considered to be fibre failure. To support this argument, in glass/linseed oil the final rapid rupture of the material is missing and during the failure there are only few hits in range *a*. Also, there were almost no fibre breaks detected with microCT on the tensile side of the glass/linseed oil specimen. For these reasons the range *a* is considered to be a fibre breakage under tension, supported by findings in the literature that say hits above 400 kHz are fibre breakage [79].

Range *b* (200–300 kHz) — this range is the first one to appear in most of the dry and aged glass/epoxy specimens and also in glass/linseed oil. The weakest link in the material is possibly the interface around 90 ° fibres that starts to give away under tension. Ni and Jinen [79] found that 250–320 kHz corresponds to matrix and fibre debonding; de Groot et al. [70] found that 180–240 kHz corresponds to fibre pull-out; Ramesh et al. [77] claimed frequencies of 220–260 kHz to be debonding and 280–320 kHz to be delamination. These interface related findings support the idea that hits around 200–300 kHz (range *b*) are of interfacial cracking.

Range *f* (80–100 kHz) — this range is present in most of the specimens tested. In dry specimens (both glass/linseed oil and glass/epoxy) there are not many hits in that range and these few hits occur only after all the other mechanisms. In 2 years aged glass/epoxy the range *f* is not present anymore but that is mainly because the material fails after the first hits are detected with AE and there was no time for any other mechanisms to develop. In glass/linseed oil specimens the range *f* is also present from the start but only becomes dominating after 4 weeks of ageing. In the 2 years aged specimens this is one of two remaining frequency ranges. Considering that the 2 years aged specimens were split into two halves, the main AE signals must have come from the friction between the two sides. For that reason the range *f* is considered to be friction between delaminated areas in glass/linseed oil. It may also apply to glass/epoxy as this range occurs after all the other failure mechanisms. It is possible that this range does not represent a failure mode in case of glass/epoxy but comes from the interactions and possibly friction between damaged areas.

5.2.2 AE Signals in Unreinforced Matrix

Unreinforced matrix tests were carried out with both epoxy resin and linseed oil resin to exclude any fibre and interface related damage signals from the AE data and determine the matrix cracking related signal parameters. The determined values may not be comparable directly to the signals in a composite but they should give an idea of the approximate parameter ranges. It was also hoped that by doing resin only tests it will be possible to determine rig and other noise parameters from the actual failure related data.

During the unreinforced matrix tests the only AE hits occurred during the actual failure of the specimens and the tests did not clarify the parameters that could be associated with the rig noise. The tests showed that matrix cracking can give amplitudes in the whole test range (40–100 dB). The only parameter showing a specific range that can be related to a single failure mechanism was frequency. The unreinforced matrix samples had AE signal frequencies only in the range of 10–47 kHz for both epoxy and linseed oil. Similar findings have been presented by de Groot et al. [70]. Epoxy samples had more AE hits than linseed oil did, showing that there were more matrix cracks developing in epoxy. From this it can be concluded that epoxy is more brittle as a resin than linseed oil, also shown by the linear epoxy stress curve compared to the linseed oil stress curve that shows yielding in Figure 5.8.

As no noise parameters could be distinguished from unreinforced matrix tests a different approach was taken. In the following results only the hits that reached both sensors in a specified time limit were used unless stated otherwise. The rest of the data (i.e. hits that did not reach both of the sensors) were considered as noise and were excluded from the data. The time limit within which the hits had to arrive at both sensors was calculated based on the wave speed in the material and distance between the sensors. The same

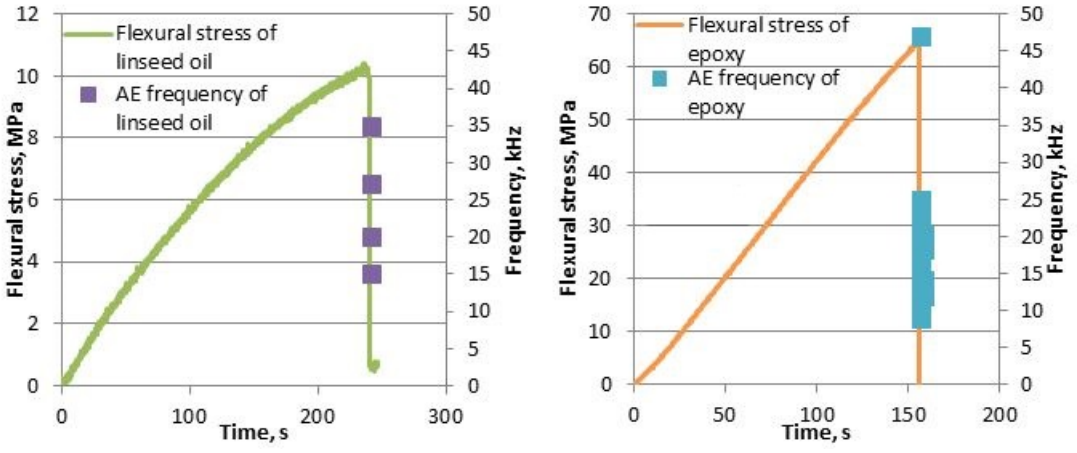

Figure 5.8: Flexural stress and the frequencies of matrix cracking in linseed oil (left) and epoxy (right) resin samples

method has been used previously by other researchers [74, 75]. One of the benefits of this method is that the 0 kHz hits are not necessarily removed as noise. The 0 kHz hits are the result of poor FFT by the AEWin software used in the acoustic emission testing PC. When the waveforms of the same hits were analysed then the DC component causing 0 kHz to occur as peak frequency was removed and the peak frequency came out to be different from 0. Due to the time limits it was not possible to process all the waveforms and parameters used in this work ended up being calculated using AEWin software. It is important to know that the hits that appear to have frequency of 0 kHz are very likely to have a different frequency in reality.

Despite the noise removal process it is not certain that all the unwanted signals have been removed; in this research the signal reflections and changes in wave propagation due to applied stresses are not considered or discussed.

5.2.3 AE Signals in Glass/Epoxy

Dry Glass/Epoxy

From the microCT images it is known that the dry glass/epoxy specimens showed extensive cracking on both tensile and compressive side together with fibre breakage on the tensile side of the material and delamination on the compressive side.

Figures 5.9, 5.10 and 5.11 show the AE data for the dry glass/epoxy specimens. Data in these figures represents an average specimen out of 5. Specimens used here had a lower flexural strength than the ones used for moisture uptake and flexural tests.

One of the first things to notice is that channel 1 (CH1, Figure 5.9) and channel 3 (CH3, Figure 5.10) show slightly different frequency response, probably caused by a difference in the sensitivity of the sensors [85]. The greatest difference between the two channels appears to be around frequencies 200–300 kHz. These differences occur in all of the data sets and need to be kept in mind when analysing the results.

In dry glass/epoxy specimens there are three most populated frequency ranges *a*, *b* and *c* as shown in Figure 5.11 and multiple well distinguishable frequency sub-ranges, especially in channel 1 data range *b*. Some of these ranges (like lower frequencies of range *b*) are populated by one channel hits only, emphasising the differences between the two channels.

In the dry glass/epoxy the AE hits start early in the failure process and give an early warning of the failure. Here failure is considered to be the sudden load drop at 200 seconds and the 10 seconds preceding that. It is noticed that a slight 'yielding' occurs in the stress curve when the first AE hits occur. The first hits (1) are in range *b* lower section (around 220 kHz). Based on CH1 data, the first hits are followed by (2) in range *c* and a few hits in range *d* (around 175 kHz) followed by simultaneous hits in ranges *b**

and *a*. Channel 3 data shows similar trend but there are also few hits in range *f* that occur after all the other frequency ranges have appeared.

7 Weeks Aged Glass/Epoxy

Figures 5.12, 5.13 and 5.14 show AE data for 7 weeks aged glass/epoxy specimens. Based on the information from moisture uptake and flexral tests, 7 weeks of ageing causes a 49.1% reduction in the flexural strength (resulting in 271.8 MPa), no significant change in the flexural modulus and moisture content of 2.1%.

In the CT images of 10 weeks aged glass/epoxy it was observed that there was one dominating crack developing on the tensile side of the aged specimen. The crack was developing through fibre bundles and the matrix and there was fibre breakage present on the tensile side. No compressive damage was visually detected but that could be due to the resolution of glass/epoxy CT images.

From the AE data of 7 weeks aged specimens it can be observed that compared to the data from dry specimens the frequency ranges have become 'wider' and more scattered, mainly in ranges *a*,*b* and *d*. As the void content of dry and 7 weeks aged specimens was similar then this scatter difference should not be caused by voids but due to the water ingress.

Figures 5.12 and 5.13 show that the AE hits now occur closer to the actual failure giving less warning time with the hits occurring at 225 MPa. The first AE hits occur in frequency range *b* just like with dry specimens, but the second event is now not in range *c* but simultaneously in ranges *a*, *b** and *c*, these hits can probably be related to the development of the dominating crack seen microCT images (although the microCT images were taken with a longer aged specimen). Due to the differences in the sensors, channel 3 shows less events in range *b* and no hits in range *c*. In channel 3 the last frequency range *f* (4) appears only after the failure of the material and is around 80 kHz. In channel 1 range *f* is also the last frequency range to appear. Same case was with dry glass/epoxy specimens (channel 3).

2 Years Aged Glass/Epoxy

After 2 years of ageing the flexural strength of glass/epoxy had reduced by 57.7% down to 226 MPa. The specimen used for this test had lower void content than dry and 7 weeks aged specimens. There was no significant change in the flexural modulus and the moisture content was 1.99% (for this specific specimen it was lower than less aged specimens, due to a lower void content).

From Figures 5.15, 5.16 and 5.17 it can be seen that in 2 years aged specimens there were far less AE hits than in dry or 7 weeks aged material. The data looks cleaner than that of dry or 7 weeks aged specimens but it is difficult to say whether this is caused by the lower void content or the effects of moisture.

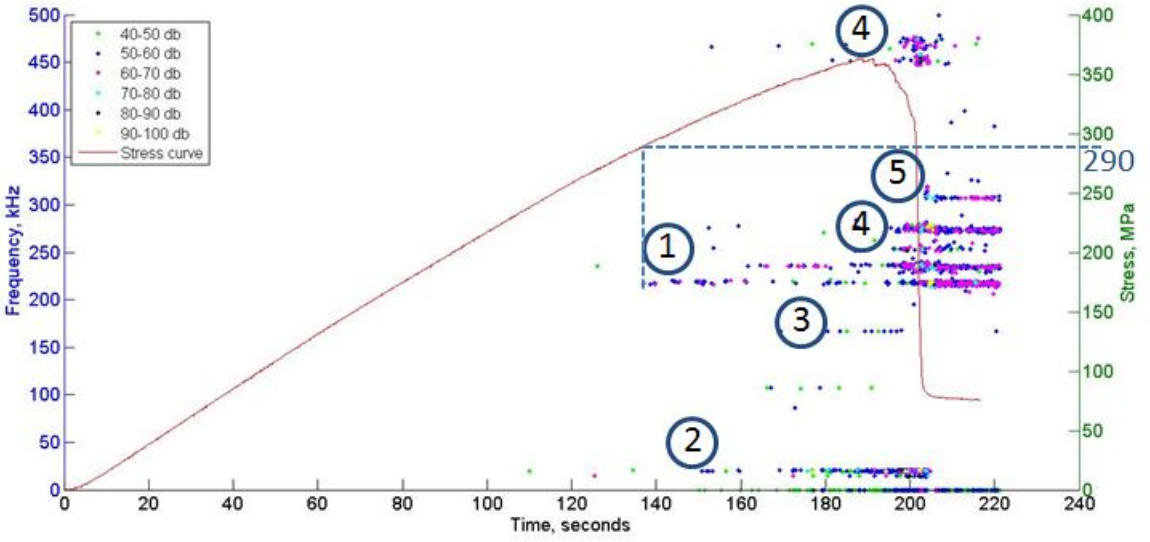

Figure 5.9: Flexural stress and frequencies of channel 1 hits in dry glass/epoxy

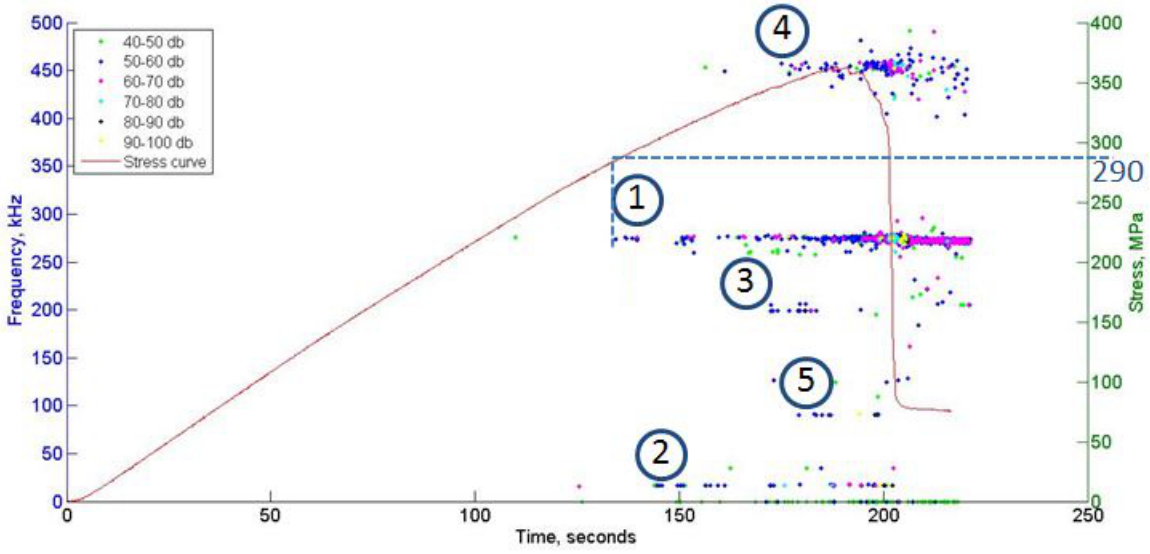

Figure 5.10: Flexural stress and frequencies of channel 3 hits in dry glass/epoxy

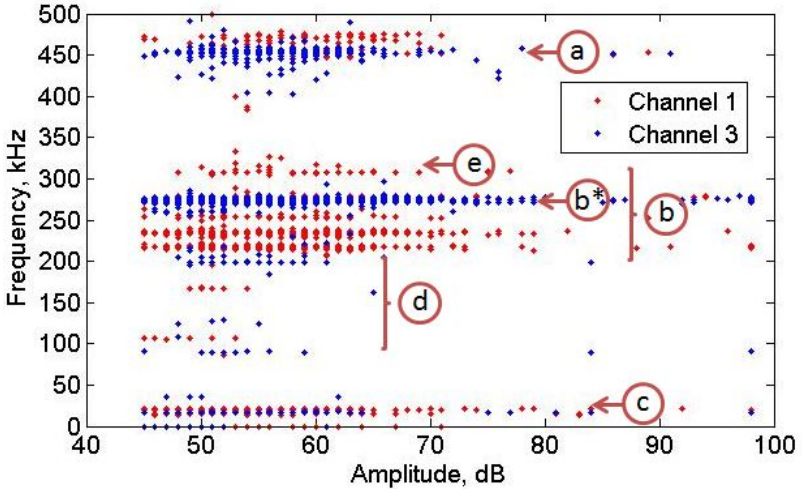

Figure 5.11: Frequency ranges and amplitudes of AE hits in dry glass/epoxy

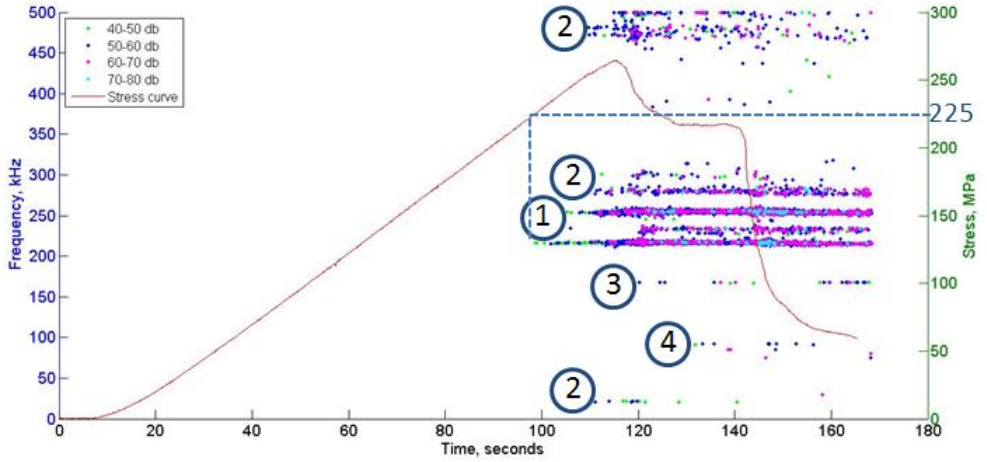

Figure 5.12: Flexural stress and frequencies of channel 1 hits in 7 weeks aged glass/epoxy

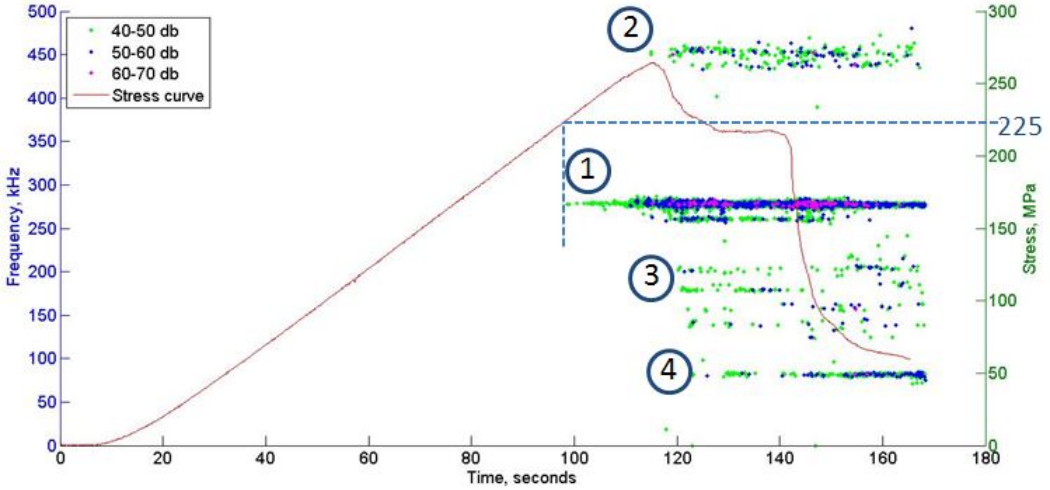

Figure 5.13: Flexural stress and frequencies of channel 3 hits in 7 weeks aged glass/epoxy

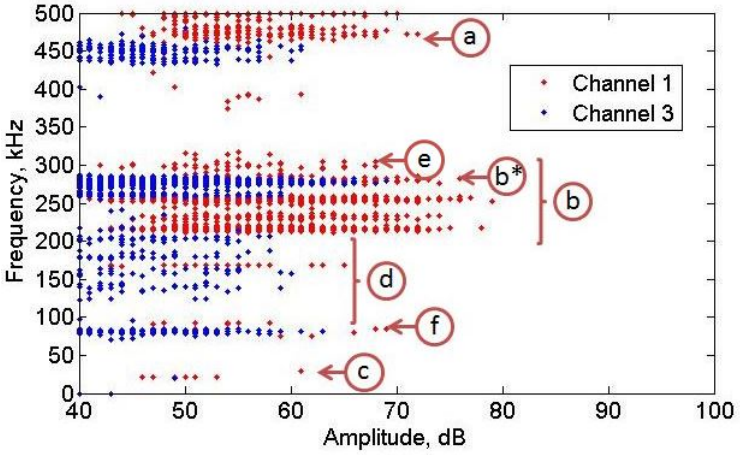

Figure 5.14: Frequency ranges and amplitudes of AE hits in 7 weeks aged glass/epoxy

It is obvious from Figures 5.15 and 5.16 that AE no longer gives any warning about the failure that is about to happen. All of the AE frequency ranges occur simultaneously during the failure of the material. The frequency ranges present in 2 years aged specimens are *a*, *b* and *c*. In 7 weeks aged specimens the range *c* had almost disappeared but it has recurred in 2 years aged specimens. There are still hits in the highest frequency range *a* but the range has thinned out significantly and ranges *b* and *c* seem to be dominating this failure, especially in channel 3.

The changes in AE data from dry to aged specimens seem striking. The most important observation is that after 2 years of ageing glass/epoxy cannot tolerate any damage and fails right after the first signs of damage.

5.2.4 AE Signals in Glass/Linseed Oil

Dry Glass/Linseed Oil

The microCT images showed that in dry glass/linseed oil specimens there was both compressive and tensile damage with mainly matrix and interfacial cracking (tensile side), fibre kinking and crushing (compressive side). There was very little fibre breakage detected on the tensile side of the specimen with microCT scanning.

The glass/linseed oil specimens used for AE testing showed lower properties than the specimens used for monitoring moisture uptake and flexural properties. All the specimens were manufactured together but the AE tests were carried out 2.5 years after the material had been manufactured. Considering the sensitivity of the glass/linseed oil composite to different environmental conditions it is possible that the properties reduced due to the storage conditions.

The AE data from dry glass/linseed oil specimens (Figures 5.18, 5.19 and 5.20) looks quite different from glass/epoxy data (Figures 5.9, 5.10 and 5.11). The first noticeable difference is in the frequency ranges present. The glass/linseed oil AE response is almost missing the highest frequency range *a*, there are only very few hits in that range present in channel 3. It seems that with glass/linseed oil specimens the frequency range *a* exists only in channel 3 and lower frequency range *c* in channel 1. Range *d* is already present in dry glass/linseed oil specimens, in glass/epoxy this range became populated only after ageing. The amplitude of the hits is also lower than in glass/epoxy, the highest amplitude being around 70 dB (Figure 5.20) compared to the near 100 dB in dry glass/epoxy (Figure 5.11).

In glass/linseed oil specimens the AE hits start about 15 seconds before the failure of the material starts, giving less warning compared to the near 50 second warning in dry glass/epoxy. However, the final failure is 70 seconds after the first AE hits. In glass/linseed oil it was very difficult to determine the actual failure from stress/strain

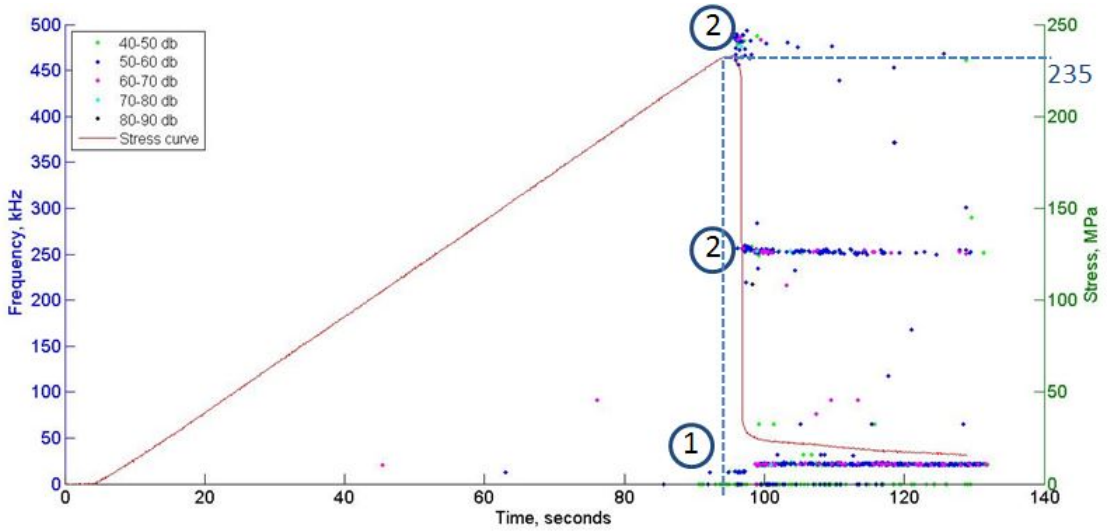

Figure 5.15: Flexural stress and frequencies of channel 1 hits in 2 years aged glass/epoxy

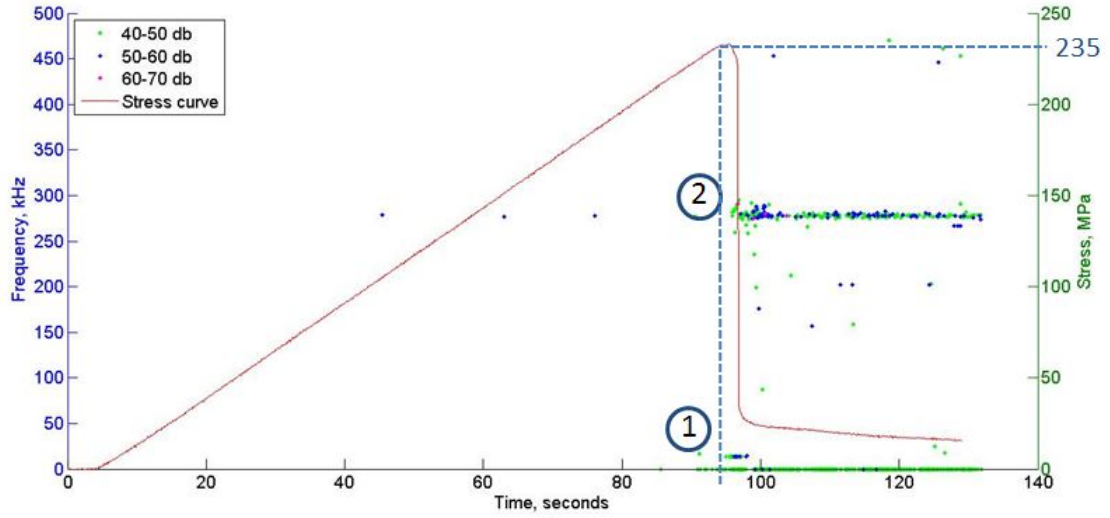

Figure 5.16: Flexural stress and frequencies of channel 3 hits in 2 years aged glass/epoxy

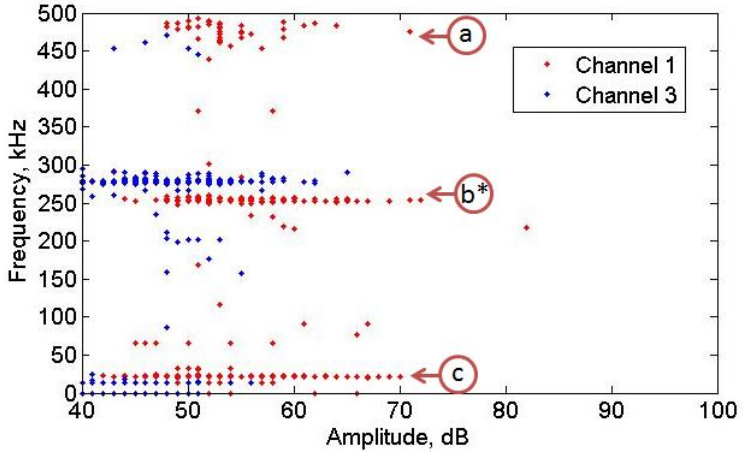

Figure 5.17: Frequency ranges and amplitudes of AE hits in 2 years aged glass/epoxy

(or time) curves. Throughout this work the failure of glass/linseed oil is considered to be the highest stress value in the stress/strain curve whenever possible. The start of the failure is considered to be the first sloping down of the curve, in this case at 150 seconds.

The first hits are from ranges *b* and *c* followed by range *d* in channel 1. Range *d* occurs only during the failure while the ranges *b* and *c* start already before the failure. In channel 3 the second range to appear was range *a*, followed by ranges *d* and *c*.

0.5 Weeks Aged Glass/Linseed Oil

In the microCT images of 3 days aged glass/linseed oil there was no visible damage on the tensile side of the specimen and the only visible damage was a compressive one with delamination and few matrix and interfacial cracks. Therefore, it is assumed here that the failure signature seen in the AE data (Figures 5.21, 5.22 and 5.23) applies to compressive failure as shown by microCT.

The frequency.amplitude data (Figure 5.23) looks fairly similar to the one of dry glass/linseed oil (Figure 5.20), just shifted towards lower amplitudes. However, after careful observation the frequency ranges *b* and *c* seem to have become slightly less populated than in dry specimens' data.

Just like in dry specimens the hits start close to the initiation of the failure, in this case giving a 15 second warning. The final failure occurs about 150 seconds after the first AE hits. The first hits were frequency ranges of *c* and *b*, although the hits from range *b* are now in the lower range (220 kHz) than in dry specimens (240 kHz). The first hits are followed by 240 kHz hits and hits from range *d*. In channel 3 the range *c* is missing but there are few hits in range *a* when failure reaches the final stage after 250 seconds.

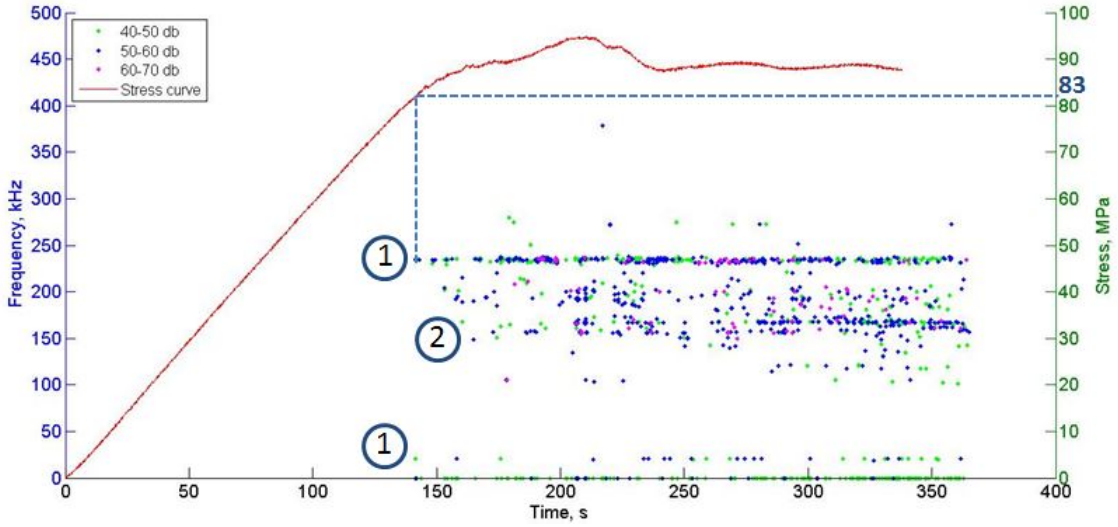

Figure 5.18: Flexural stress and frequencies of channel 1 hits in dry glass/linseed oil

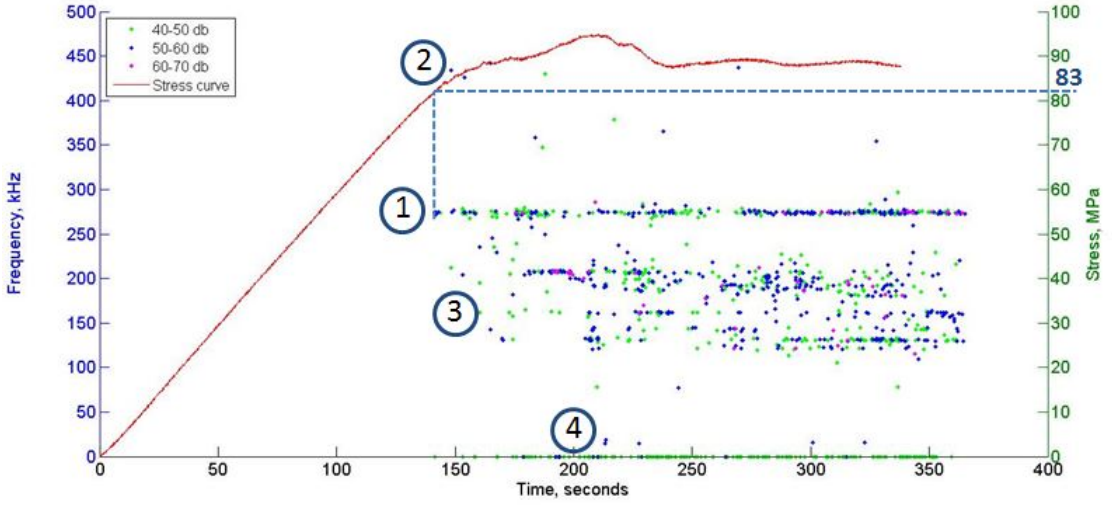

Figure 5.19: Flexural stress and frequencies of channel 3 hits in dry glass/linseed oil

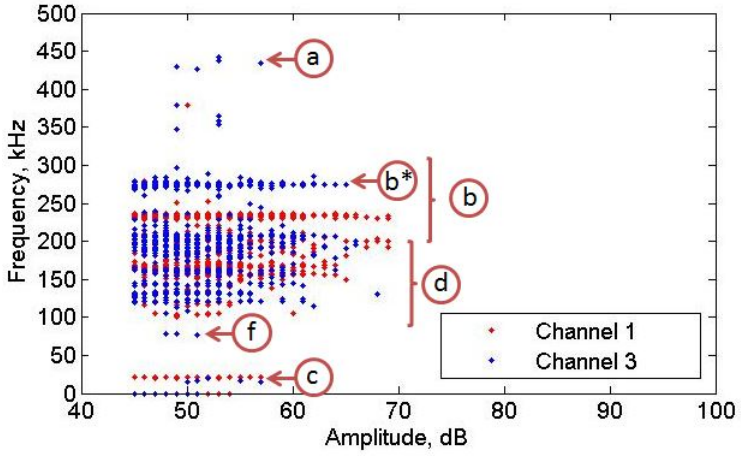

Figure 5.20: Frequency ranges and amplitudes of AE hits in dry glass/linseed oil

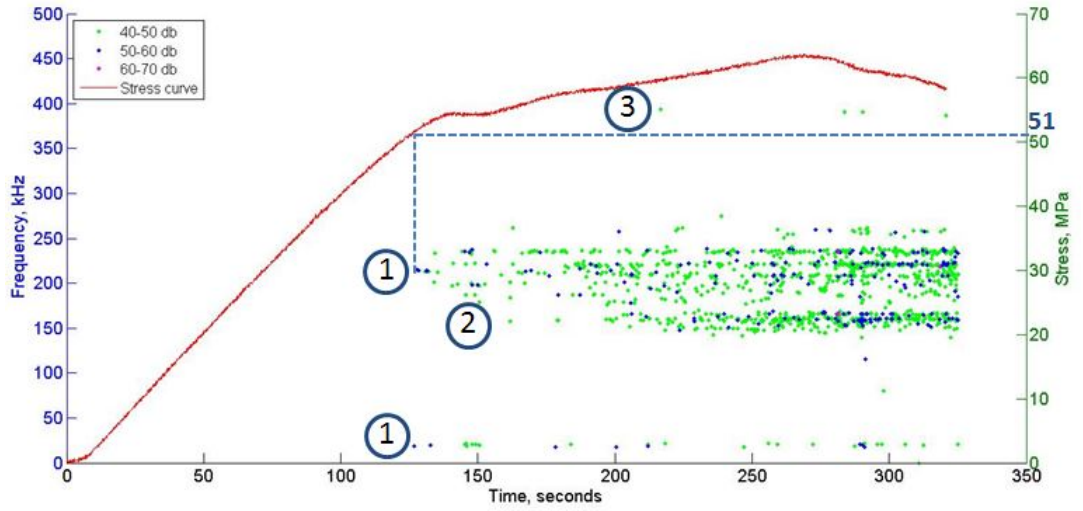

Figure 5.21: Flexural stress and frequencies of channel 1 hits in 0.5 weeks aged glass/linseed oil

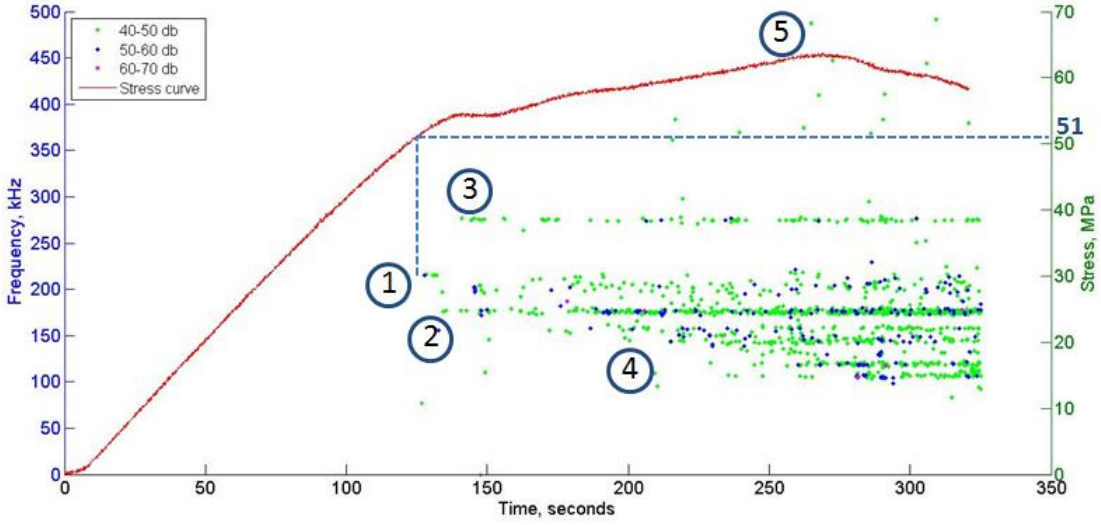

Figure 5.22: Flexural stress and frequencies of channel 3 hits in 0.5 weeks aged glass/linseed oil

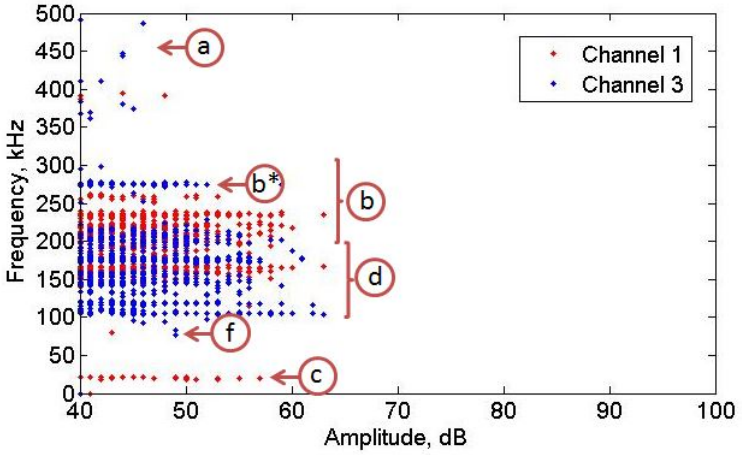

Figure 5.23: Frequency ranges and amplitudes of AE hits in 0.5 weeks aged glass/linseed oil

1 Week Aged Glass/Linseed Oil

After 1 week of ageing there was already no visual damage detected with the aid of microCT. The brittleness of the material must have reduced significantly due to moisture uptake and no visible cracks developed during the failure. During the test only crushing under the roller could be visually detected. With this in mind, one of the first observations from the AE data is that the range *c*, previously related to matrix cracking, is now missing from both CH1 (Figure 5.24) and CH3 data (Figures 5.25 and 5.26.

Like in 0.5 weeks aged specimens the first hits in range *b* (around 240 kHz) are followed by range *d* hits. The lower frequency ranges have thinned out significantly. There is a kink in the stress curve at 145 seconds. At the same time there are a few range *a* hits in channel 3. There are also few hits in range *f* (channel 1) but these appear after all the other ranges and damage.

In glass/linseed oil specimens range *f* is only present in aged specimens and appears only after the final failure has occured just like in 7 weeks aged glass/epoxy.

1.5–4 Weeks Aged Glass/Linseed Oil

After 1.5 weeks of ageing the difference in AE response is quite different from the dry specimens' data. The hits occur during the actual failure leaving no warning time before the failure initiation. Again, the specimen fails at around 250 seconds after the damage has been accumulating. The frequency ranges *a* and *c* have disappeared and the remaining ranges of *b* and *d* show far less hits than in dry or less aged glass/linseed oil. The first hits occurring are still that of range *b* soon followed by hits in range *d*. The same trends carry over to 2 weeks aged specimens (Figures 5.27 and 5.28), with the total number of hits and amplitudes reducing even further (Figure 5.29) demonstrating the effects of attenuation.

After 3 weeks of ageing there is a change in the AE data. The first hits occur now in range *d* instead of range *b* and there are two recurring ranges: ranges *f* and *c*. The same trend was noticed with glass/epoxy where ranges *f* and *c* had fewer hits in less aged material and more hits in longer aged specimens.

The AE hits from 4 weeks aged specimens look very similar to 3 weeks aged glass/linseed oil, except for the first hits to occur. The first hits in 4 weeks aged glass/linseed oil are in ranges *f* and *c* that occur simultaneously and are then followed by ranges *b* and *d* (channel 1)(Figures 5.30 and 5.32). In channel 3 the first hits occur in range *d* and are followed by range *f* (Figure 5.31).

2 Years Aged Glass/Linseed Oil

In 2 years aged glass/linseed oil samples all of the hits were filtered out as noise. Because of that the data presented here has not undergone the noise removal process. No hits were detected in channel 3.

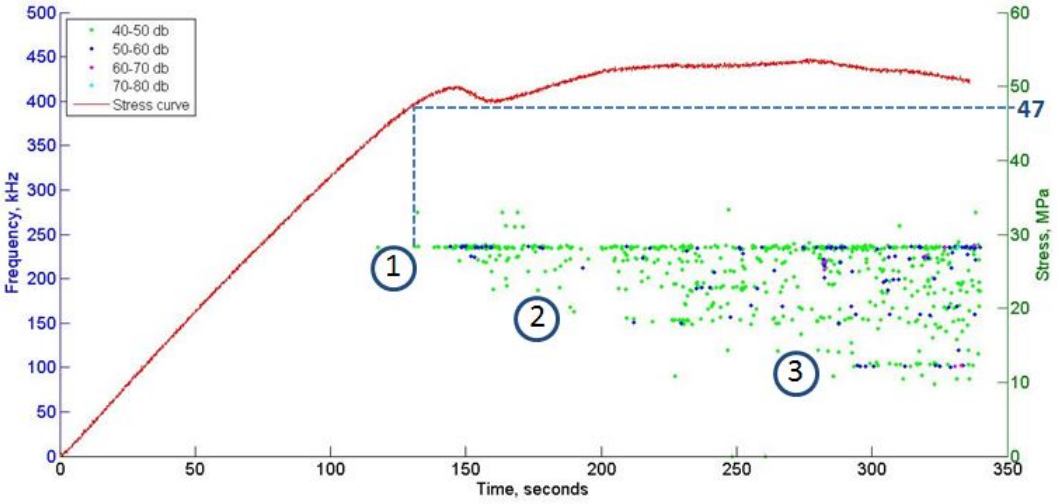

Figure 5.24: Flexural stress and frequencies of channel 1 hits in 1 week aged glass/linseed oil

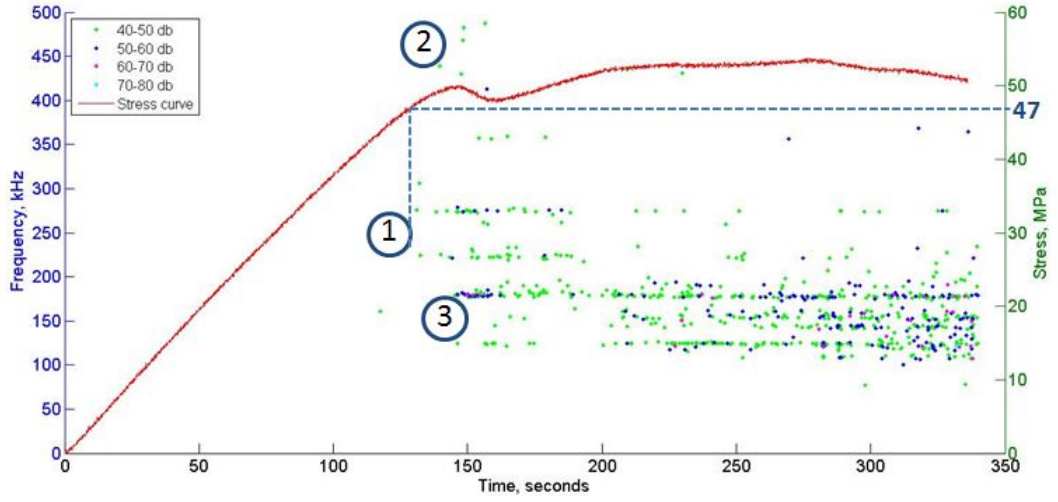

Figure 5.25: Flexural stress and frequencies of channel 3 hits in 1 week aged glass/linseed oil

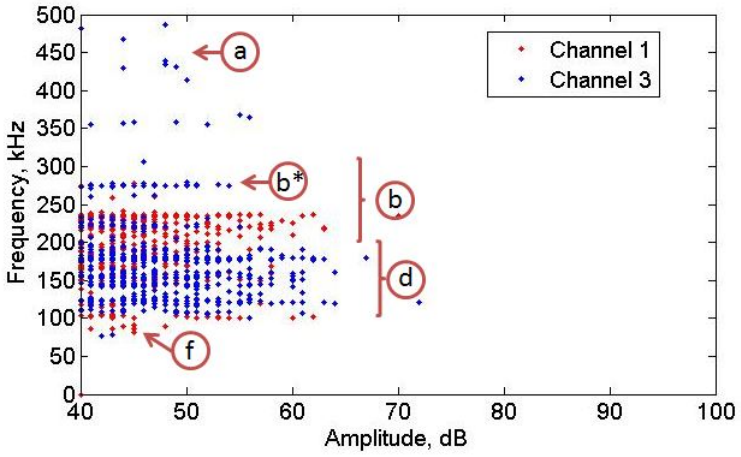

Figure 5.26: Frequency ranges and amplitudes of AE hits in 1 week aged glass/linseed oil

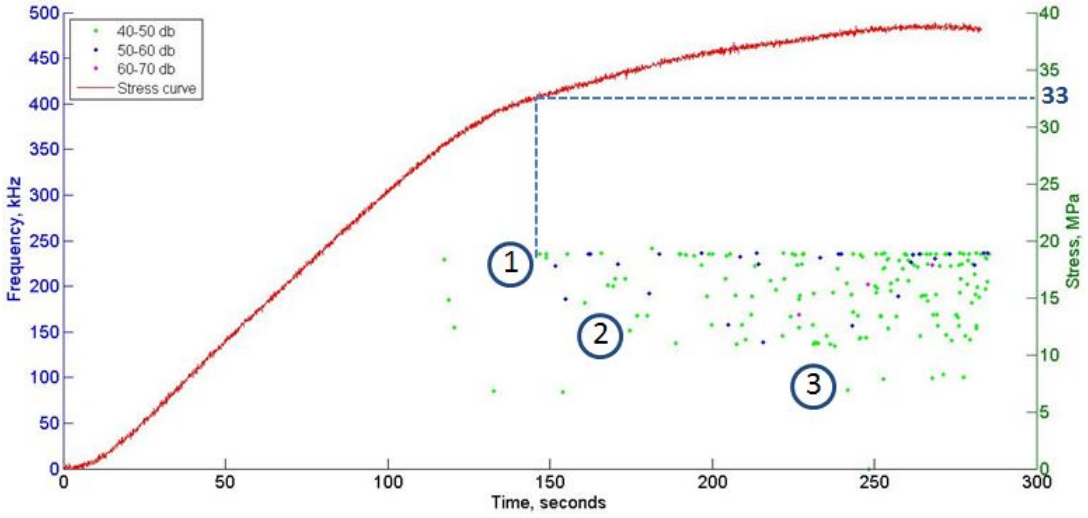

Figure 5.27: Flexural stress and frequencies of channel 1 hits in 2 weeks aged glass/linseed oil

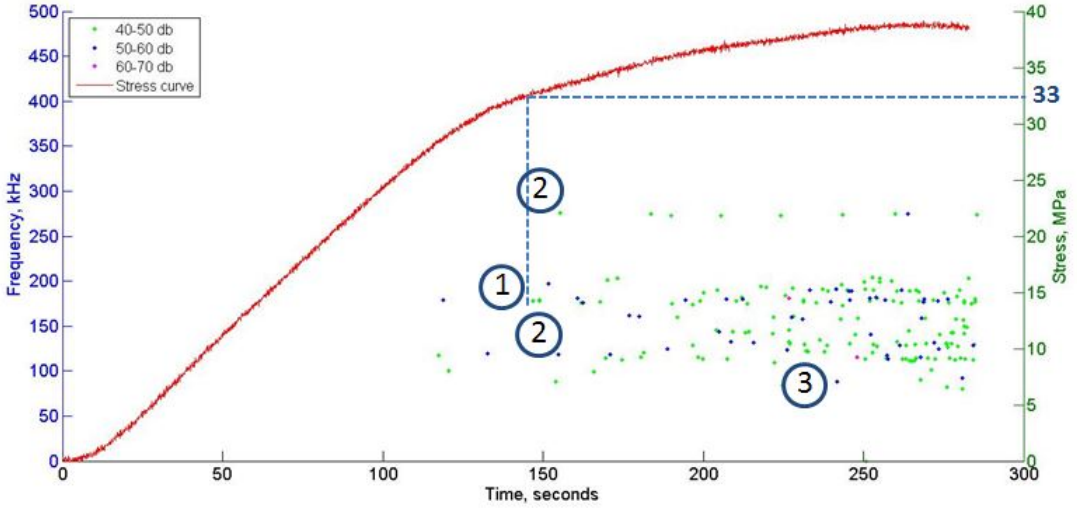

Figure 5.28: Flexural stress and frequencies of channel 3 hits in 2 weeks aged glass/linseed oil

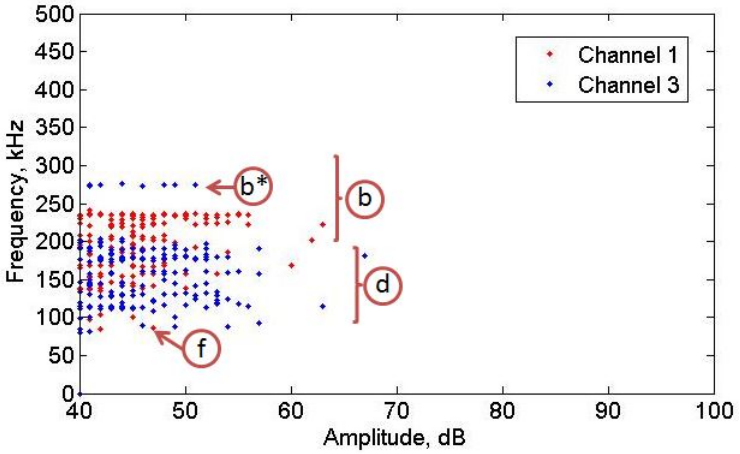

Figure 5.29: Frequency ranges and amplitudes of AE hits in 2 weeks aged glass/linseed oil

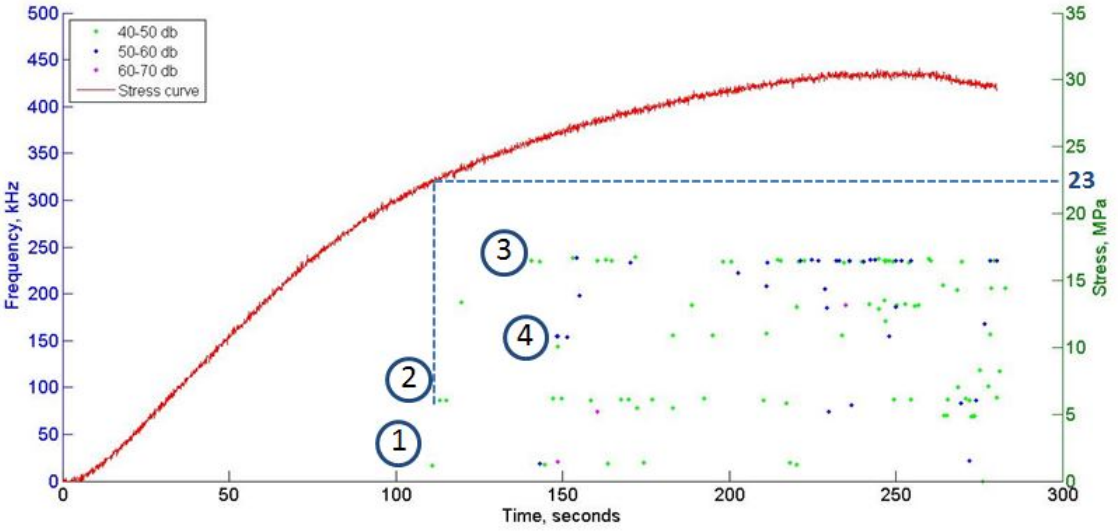

Figure 5.30: Flexural stress and frequencies of channel 1 hits in 4 weeks aged glass/linseed oil

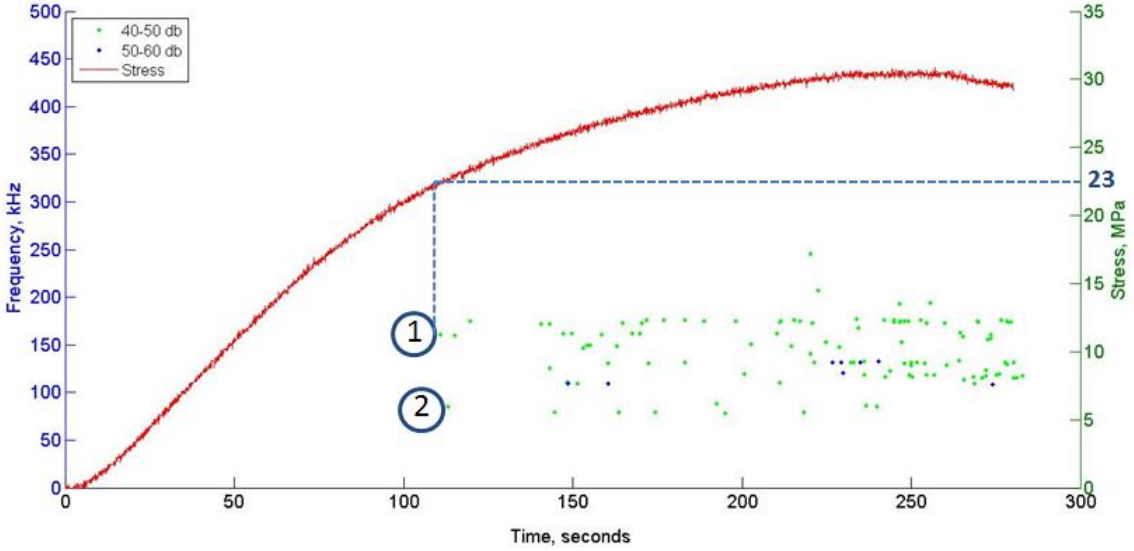

Figure 5.31: Flexural stress and frequencies of channel 3 hits in 4 weeks aged glass/linseed oil

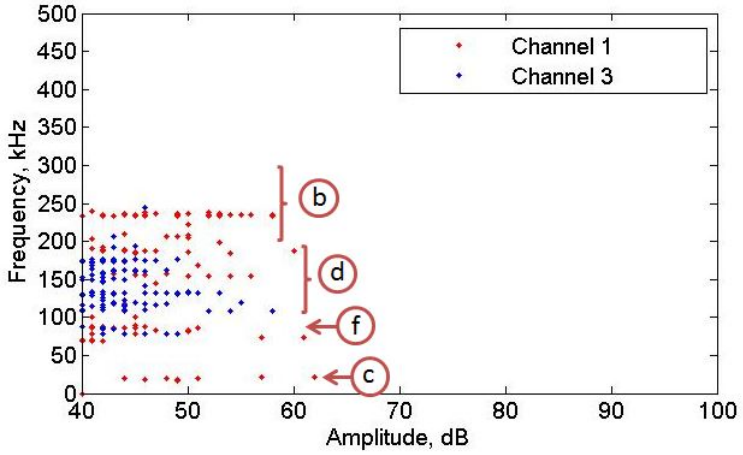

Figure 5.32: Frequency ranges and amplitudes of AE hits in 4 weeks aged glass/linseed oil

It can be seen that the number of data points in 2 years aged glass/linseed oil specimens has reduced significantly (Figure 5.33). There are also only two frequency ranges present: range *c* and *f*. By the time of testing the glass/linseed oil material had deteriorated visibly and had split through thickness into two halves held together only by friction. Because of that it is assumed here that the AE data from these tests represents sliding and rubbing of the material without any structural behaviour as a composite. From this it can be concluded that the range *c* of aged samples and range *f* show AE response of delaminated aged/plasticised material where the sides of the material are pushed together and rubbing against each other. While range *c* was present already in dry specimens' AE data, the range *f* is relevant only in aged specimens. Range *f* was also present in dry specimens but only after the other frequency ranges and most of the damage had occurred.

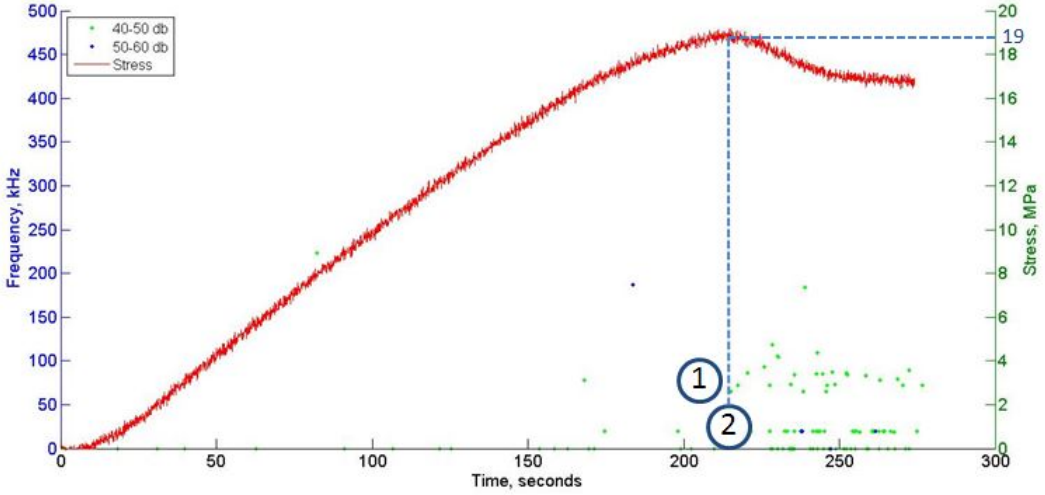

Figure 5.33: Flexural stress and frequencies of channel 1 hits in 2 years aged glass/linseed oil

Chapter 6

Summary Discussion

Hygrothermal ageing tests showed that moisture uptake affected significantly the performance of glass/epoxy, glass/linseed oil and glass/castor oil composites. The changes in flexural properties can be attributed to the changing performance of matrices, fibres and interfaces. These changes were shown to affect the failure modes in glass/epoxy and glass/linseed oil specimens. While in glass/epoxy most of the damage occurred on the tensile side even in the aged samples, in glass/linseed oil the failure changed from compressive/tensile mixed mode into a compressive one. After only 1 week of ageing no failure mechanisms could be visually detected in glass/linseed oil.

The AE technique was used to get real-time data of the failure in glass/epoxy and glass/linseed oil composites in order to demonstrate the changes in failure mechanisms in more detail. AE testing showed that with ageing the number of failure mechanisms reduced as did the number of the AE events in both materials. In glass/epoxy this can be explained with the material becoming less tolerant to the damage and general weakening of the constituents. In glass/linseed oil the capability to transfer loads to fibres reduced rapidly with ageing, leading to a matrix dominated failure. There were clear signs of the poor performance of the linseed oil matrix, shown by imperfect secondary bonding and blistering. Both of these problems are most likely caused by non-optimised curing. The performance of glass/linseed oil composite was significantly affected by the low T_g of linseed oil matrix, shown indirectly by the effects temperature has on the glass/linseed oil properties. These changes led to significant differences in the AE data of dry and aged composites. As a result of AE testing it was possible to propose the order of the failure mechanisms in dry and aged glass/epoxy and glass/linseed oil composites.

6.1 Proposed Order of Flexural Failure Mechanisms

The AE technique has provided information about flexural failure of the composites that would not have been possible with other techniques. Real-time data were collected

during flexural tests of dry and aged specimens, making is possible to map the changes in the failure modes in glass/epoxy and glass/linseed oil specimens. With the aid of AE the possible order of failure mechanisms has been proposed for glass/epoxy in Figure 6.1 and for glass/linseed oil in Figure 6.2.

The main similarities of the two materials are that the number of failure mechanisms reduced with ageing and in most of the results the first damage mechanism was interfacial cracking suggesting that the interface is the weakest part in both composites. At the same time, in glass/epoxy most of the damage mechanisms were tensile failure related while in glass/linseed oil compressive damage was dominating. In glass/epoxy the damage mechanisms occurred closer together and closer to the failure with ageing while in glass/linseed oil the damage mechanisms occurred earlier with ageing in regards to the failure. The main trends in the failure mechanisms of both of the materials are brought out in the following sections.

6.1.1 Trends in Glass/Epoxy Failure

Based on Figure 6.1 the following trends were observed:

- The number of failure events reduces with ageing;
- Compressive failure is present in dry material only (out of the ageing periods presented here);
- In dry and 7 weeks aged specimens the first damage is the interfacial cracking on the tensile side followed by matrix cracking and finally by fibre breakage and more interfacial cracking;
- In aged specimens the damage mechanisms happen closer together;
- Glass/epoxy becomes less damage tolerant due to moisture uptake.

6.1.2 Trends in Glass/Linseed Oil Failure

The trends in glass/linseed oil are less clear than in glass/epoxy. Based on Figure 6.2 the following trends were observed:

- The damage events occur earlier with ageing in regards to the failure;
- The number of damage mechanisms reduces with ageing;
- The most consistent damage mode is compressive damage;
- In dry and 0.5 weeks aged glass/linseed oil the interfacial cracking was accompanied by matrix cracking followed by compressive damage and fibre breaks;

- In dry–2 weeks aged specimens the first failure was interfacial cracking;
- In 4 weeks–2 years aged samples most of the hits were the ones associated with friction in the composite, and matrix cracking (it is thought that the same signal has a different failure mechanism in aged samples).

6.2 The Value of AE

In this work AE provided valuable real-time data on the failure mechanisms. With the aid of AE it was possible to monitor the start of the failure mechanisms. As different failure mechanisms emit different signals it was also possible to hypothesise the order of failure mechanisms. However, there are several issues with AE that were emphasised in this work.

One of the main downsides of AE is the amount of data collected. For a single specimen failure there can be around 20 000 AE hits and related waveforms. Using the raw waveforms is not mandatory as the AE software does most of the processing of the data. Using the AE software processed data is not very reliable though and it is recommended to process the raw waveforms for better accuracy. That, however, is very time consuming.

Another issue with AE is that two sensors never respond the same way to a hit. In this work it was noticed that some parameter ranges may be completely missing from one sensor response while they are present in the other. Also, even when the hits are shown in both of the sensors, the parameters associated with the hit may be different in the sensors. This makes it especially difficult to separate failure mechanisms based on hit parameters only.

In this work it was shown that AE parameters and wave speed change with moisture uptake in the composites. This changes the way parametric analysis can be used when monitoring the performance of structures or failure in aged materials.

Using AE can be beneficial in many cases where trends in failure mechanisms need to be shown. However, care needs to be taken with AE because of the differences in processing the data, sensor performance and changes in the parameters due to moisture ingress.

6.3 Potential of Castor and Linseed Oil Composites

In this work two plant oil based resin composites were subjected to hygrothermal ageing in order to look at their suitability for maritime structures. Only accelerated ageing tests were possible with glass/castor oil composite while additional non-accelerated ageing tests and failure mode analysis were done with glass/linseed oil.

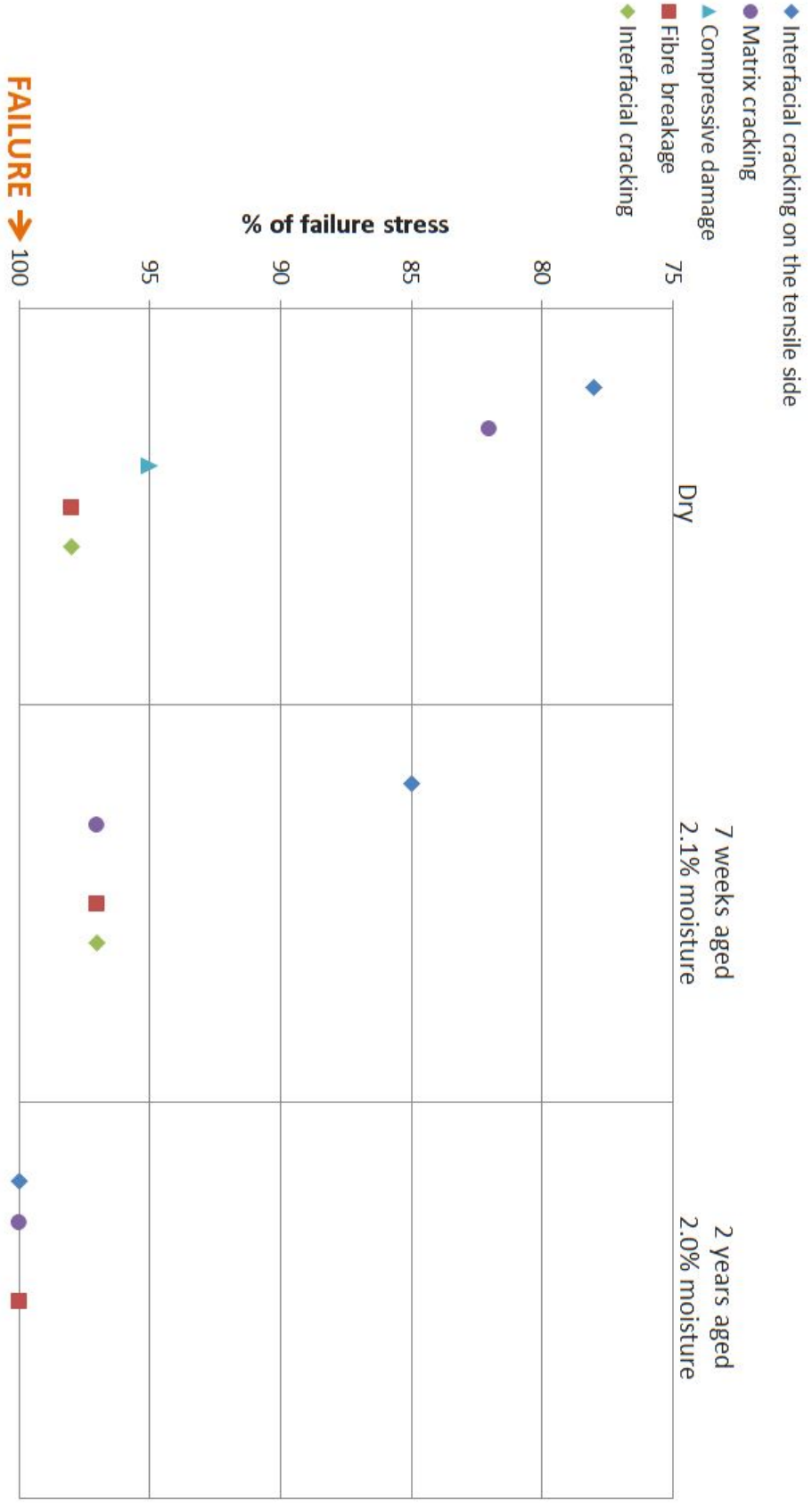

Figure 6.1: The proposed order of failure mechanisms in glass/epoxy

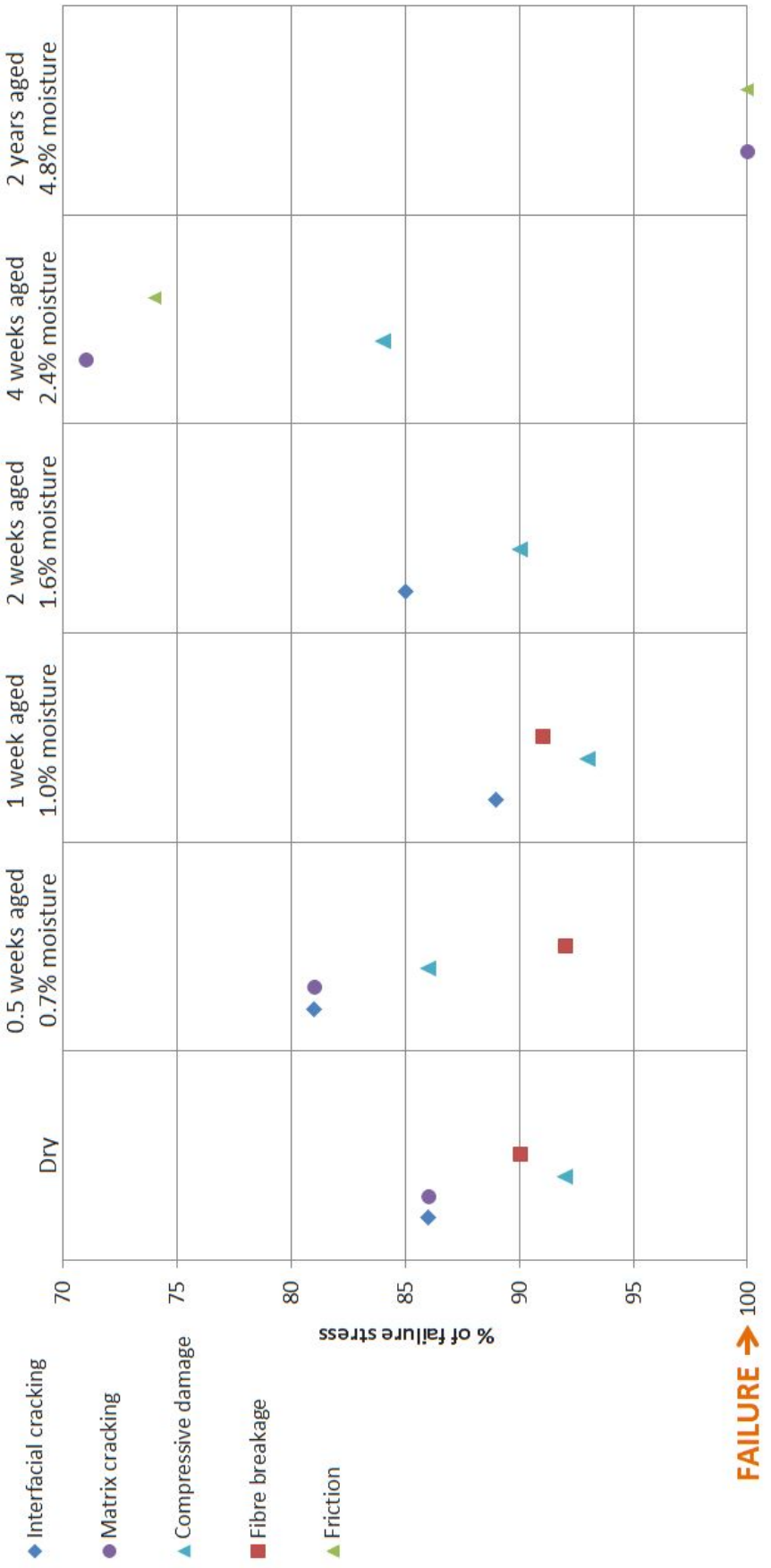

Figure 6.2: The proposed order of failure mechanisms in glass/linseed oil

Glass/castor oil showed interesting performance although not many tests were carried out with it. Before accelerated ageing the strength of glass/castor oil was about half of that of glass/epoxy. After 100+ weeks of ageing the strength of glass/castor oil was higher than in glass/epoxy. The modulus showed slight reduction but in general the properties were still acceptable for structural applications and the performance of castor oil composites should be investigated further, focussing on using the material in structural maritime applications.

From the tests carried out with glass/linseed oil, a significant and rapid reduction of properties with moisture ingress was demonstrated. In its current state glass/linseed oil is not recommended for maritime applications. Based on the performance of glass/linseed oil it is concluded that the performance is most affected by the low glass transition temperature, potentially weak secondary bonding between the layers of the composite and poor curing. While increasing the T_g requires changing the resin system, the secondary bonding and curing can be optimised more easily by changing the exposure to the UV-light. As a result it may be possible to use glass/linseed oil composites in non-structural applications.

Chapter 7

Conclusions

In this research the moisture uptake and its effects on the flexural properties on glass reinforced epoxy, linseed oil and castor oil composites were investigated. The flexural failure modes and the changes due to moisture uptake were determined with the aid of microCT and AE in glass/epoxy and glass/linseed oil specimens. The following conclusions can be drawn from the experimental results of this research:

- The moisture uptake tests showed that plant oil based composites absorb more moisture than glass/epoxy does. While glass/epoxy can be considered to follow Fick's diffusion law, the plant oil based composites were found not to follow the conventional diffusion laws. The water temperature was found to affect the moisture uptake speed, the quantity of the moisture content absorbed depends on the salinity of the water. Higher void content increases the moisture uptake in composites.

- The reduction of flexural properties was found to be mostly dependent on the moisture content rather than water temperature or salinity. As a result, accelerated ageing can be used to simulate real life conditions. In accelerated ageing the changes in flexural properties occur mainly over the first 10 weeks of ageing, meaning that moisture damages composites rapidly. The reduction of flexural strength is the greatest in glass/linseed oil and the smallest in glass/castor oil, after 2 years of ageing glass/castor oil had higher strength than glass/epoxy did. Flexural modulus of glass/epoxy remained unaffected by moisture uptake but was affected in glass/linseed oil and glass/castor oil specimens.

- Blistering in glass/linseed oil caused an increase in moisture uptake but the effect of the blisters on flexural properties depended on the size of the blisters: small blisters had no effect on the properties while big blisters caused a significant reduction in the flexural properties.

- Moisture uptake caused changes in the flexural failure mechanisms. The failure mode of glass/epoxy remained fibre dominated but with ageing the material became less tolerant of damage. The failure mode of glass/linseed oil changed rapidly from compression/tension mixed mode into a compressive failure only. The failure in both glass/epoxy and glass/linseed oil started from interfacial cracking. In dry specimens (both glass/epoxy and glass/linseed oil) there were more damage mechanisms than in aged specimens. In glass/epoxy the AE signals occur closer to the final rupture with ageing, giving less warning of the failure.

- Moisture ingress reduced the wave speed in composites, this needs to be considered when using AE for SHM in structures. Moisture ingress also caused changes in the AE signal parameters, peak frequency was the only parameter found to be unaffected by water uptake.

- The poor performance of glass/linseed oil can largely be attributed to the problems with UV-curing. In its current state the material is not suited for maritime applications but it is possible that optimising the curing process will improve the performance of glass/linseed oil composites and as a result the material becomes more suited for maritime applications.

- Glass/castor oil performed very well after hygrothermal ageing and has potential for maritime applications to replace polyester and epoxy resins; glass/linseed oil is not recommended for maritime structures in its current state, although it has potential for non-structural applications in dry environments.

As a result, this research increased the knowledge of the long-term performance of plant oil based composite materials. That kind of information has not been available before. In addition, for the first time the changes in the failure modes of a glass/linseed oil composite due to moisture uptake were demonstrated and recommendations for improving the performance were given.

Chapter 8

Future Work

The future work can be divided into five main subtopics: visualising the moisture ingress in composites, modelling hygrothermal ageing, investigating the chemistry of hygrothermal ageing, carrying out more realistic ageing tests, and investigating the long-term performance of fully 'green' composites.

- The theories of moisture storage areas inside composites currently lack proof. It should be possible to detect moisture inside composites with microCT. If possible, it would answer the questions of the preferred water ingress paths and storage areas. The technique should also be capable of showing whether the defects increase in size due to moisture uptake.
- A model of hygrothermal ageing is required in order to predict the long-term performance of composites in wet environments. Ideally this model would incorporate the different ageing mechanisms. This, however, is a very complex problem, involving moisture uptake due to diffusion, moisture storage in the cavities, swelling and the resulting stresses on the fibres and the interface, and interfacial degradation.
- Chemistry has a major role in the hygrothermal ageing. Water reacts with the matrix, fibres and the interface, causing damage to the composite. These reactions need to be understood better in order to estimate the structural performance of new plant oil based composites and also improve their performance.
- The tests carried out in this work were simplified to a great extent compared to the real-life environments. In order to get more realistic idea of how the composites perform in maritime structures, the effects of gel-coat and lower temperatures should be investigated. In structures, the materials are constantly subjected to static or dynamic loads and the effects of these on the ageing mechanisms should be investigated.

- Fully 'green' composites, using plant oil based resins as well as plant fibres, should be tested in addition to the glass reinforced composites tested in this work. Once the mechanical properties of these materials are known, more work is needed to determine the heat and chemical resistance of the materials as well as the processability and manufacturing opportunities.

References

[1] A. N. Netravali and S. Chabba. Composites get greener. *Materials Today*, pages 22–29, 2003.

[2] R. A. Shenoi, A. R. Claughton, and J. F. Wellicome, editors. *Sailing Yacht Design: Theory*, chapter Materials in Construction, pages 145–161. University of Southampton, 2006.

[3] R. A. Shenoi and J. F. Wellicome, editors. *Composite Materials in Maritime Structures*, volume Volume 1: Fundamental Aspects of *Cambridge Ocean Technology*. Cambridge University Press, 1993.

[4] R. A. Shenoi and J. F. Wellicome, editors. *Composite Materials in Maritime Structures*, volume Volume 2: Practical Considerations of *Cambridge Ocean Technology*. Cambridge University Press, 1993.

[5] G. P. Hammond and C. I. Jones. Inventory of carbon & energy (ICE). Technical report, Sustainable Energy Research Team, University of Bath, 2008.

[6] S. V. Joshi, L. T. Drzal, A. K. Mohanty, and S. Arora. Are natural fiber composites environmentally superior to glass fiber reinforced composites? *Composites: Part A*, 35:371–376, 2004.

[7] P. Wambua, J. Ivens, and I. Verpoest. Natural fibres: can they replace glass in fibre reinforced plastics? *Composites Science and Technology*, 63:1259–1264, 2003.

[8] A. O'Donnell, M. A. Dweib, and R. P. Wool. Natural fiber composites with plant oil-based resin. *Composites Science and Technology*, 64:1135–1145, 2004.

[9] S. Mishra, A. K. Mohanty, L. T. Drzal, M. Misra, S. Parija, S. K. Nayak, and S. S. Tripathy. Studies on mechanical performance of biofibre/glass reinforced polyester hybrid composites. *Composites Science and Technology*, 63:1377–1385, 2003.

[10] W. Liu, M. Misra, P. Askeland, L. T. Drzal, and A. K. Mohanty. 'green' composites from soy based plastic and pineapple leaf fiber: fabrication and properties evaluation. *Polymer*, 46:2710–2721, 2005.

[11] W. Liu, A. K. Mohanty, P. Askeland, L. T. Drzal, and M. Misra. Influence of fiber surface treatment on properties of indian grass fiber reinforced soy protein based biocomposites. *Polymer*, 45:7589–7596, 2004.

[12] Advanced materials: Key technology areas 2008–2011. Technical report, Technology Strategy Board, 2008.

[13] L. V. J. Lassila, T. Nohrström, and P. K. Vallittu. The influence of short-term water storage on the flexural properties of unidirectional glass fiber-reinforced composites. *Biomaterials*, 23:2221–2229, 2002.

[14] F. T. Wallenberger and N. E. Weston, editors. *Natural fibres, plastics and composites*, chapter Science and Technology. Kluwer Academic Publishers, 2004.

[15] D. Choqueuse and P. Davies. *Ageing of Composites*, chapter Ageing of composites in underwater applications. Woodhead Publishing Limited, 2008.

[16] F. T. Wallenberger and N. E. Weston, editors. *Natural fibres, plastics and composites*, chapter Plastics and composites from soybean oil. Kluwer Academic Publishers, 2004.

[17] J.-M. Raquez, M. Deléglise, M.-F. Lacrampe, and P. Krawczak. Thermosetting (bio)materials derived from renewable resources: A critical review. *Progress in Polymer Science*, 35:487–509, 2010.

[18] D. Ren. *Moisture-cure polyurethane wood adhesives: wood/adhesive interactions and weather durability.* PhD thesis, Virginia Polytechnic Institute and State University, 2010.

[19] Gurit, http://www.gurit.com/guide-to-composites.aspx. *Gurit Guide to Composites (v5)*, accessed March 2014.

[20] F. Seniha Güner, Yusuf Yağcı, and A. Tuncer Erciyes. Polymers from triglyceride oils. *Progress in Polymer Science*, 31:633–670, 2006.

[21] J. R. Kim and S. Sharma. The development and comparison of bio-thermoset plastics from epoxidized plant oils. *Industrial Crops and Products*, 36:485–499, 2012.

[22] R. P. Wool and X. S. Sun. *Bio-based polymers and composites*, chapter Polymers and Composite Resins from Plant Oils. Elsevier Academic Press, 2005.

[23] H. Mutlu and M. A. R. Meier. Castor oil as a renewable resource for the chemical industry. *European Journal of Lipid Science and Technology*, 112:10–30, 2010.

[24] D. S. Ogunniyi. Castor oil: A vital industrial raw material. *Bioresource Technology*, 97:1086–1091, 2006.

[25] O. Akaranta and A. C. I. Anusiem. A bioresource solvent for extraction of castor oil. *Industrial crops and products*, 5:273–277, 1996.

[26] J. M. Cangemi, A. M. dos Santos, S. C. Neto, and G. O. Chierice. Study of the biodegradation of a polymer derived from castor oil by scanning electron microscopy, thermogravimetry and infrared spectroscopy. *Polimeros: Ciencia e Technologia*, 16(2):129–135, 2006.

[27] J. M. Cangemi, A. M. dos Santos, S. C. Neto, and G. O. Chierice. Biodegradation of polyurethane derived from castor oil. *Polimeros: Ciencia e Technologia*, 18(3):201–206, 2008.

[28] S. Derobert. Performance analysis of naturally derived resin for marine sandwich structures. Master's thesis, University of Southampton, September 2008.

[29] Surabhi Distributors Private Limited. http://www.worldjute.com/flax.html. webpage, 01 2012.

[30] D. D. Andjelkovic, M. Valverde, P. Henna, F. Li, and R. C. Larock. Novel thermosets prepared by cationic copolymerization of various vegetable oils — synthesis and their structure-property relationships. *Polymer*, 46:9674–9685, 2005.

[31] Z. Zong, J. He, and M. D. Soucek. UV-curable organic-inorganic hybrid films based on epoxynorbornene linseed oils. *Progress in Organic Coatings*, 53:83–90, 2005.

[32] Gurit SP Systems. The advantages of epoxy resin versus polyester in marine composite structures. Technical report, SP, 2009.

[33] J. V. Crivello. Photoinitiated cationic polymerization. *Annual Review of Materials Science*, 13:173–190, 1983.

[34] P. Compston, J. Schiemer, and A. Cvetanovska. Mechanical properties and styrene emission levels of a UV-cured glass-fibre/vinylester composites. *Composite Structures*, 86:22–26, 2008.

[35] Joung-Man Park, Jin-Woo Kong, Dae-Sik Kim, and Jae-Rock Lee. Non-destructive damage sensing and cure monitoring of carbon fiber/epoxyacrylate composites with UV and thermal curing using electro-micromechanical techniques. *Composites Science and Technology*, 64:2565–2575, 2004.

[36] J. Ramli, A. R. Jeefferie, and M. M. Mahat. Effects of UV curing exposure time to the mechanical and physical properties of the epoxy and vinyl ester fiber glass laminates composites. *ARPN Journal of Engineering and Applied Sciences*, 6(4):104–109, 2011.

[37] J. Ramli, A. R. Jeefferie, and M. M. Mahat. The effects of photoinitiator addition to the mechanical and physical properties of the epoxy and vinyl ester fiber glass

laminated composites. *International Journal of Applied Science and Technology*, 1(3):74–79, 2011.

[38] C. T. Tsenoglou, S. Pavlidou, and C. D. Papaspyrides. Evaluation of interfacial relaxation due to water absorption in fiber–polymer composites. *Composite Science and Technology*, 66:2855–2864, 2006.

[39] A. C. Loos, G. S. Springer, B. A. Sanders, and R. W. Tung. Moisture absorption of polyester E-glass composites. *Journal of Composite Materials*, 14:142–154, 1980.

[40] G. Kotsikos, K. Morris, and J. Mawella. Durability assessment of marine composites. In J. R. Matthews and D. E. Veinot, editors, *10th CF/DRDC meeting on naval applications of materials technology*, pages 742–758. Defence R & D Canada, September 2003.

[41] J. Crank. *The Mathematics of Diffusion.* Oxford University Press, 1957.

[42] Y. C. Lin and X. Chen. Moisture sorption–desorption–resorption characteristics and its effect on the mechanical behavior of the epoxy system. *Polymer*, 46:11994–12003, 2005.

[43] *ASTM D 5229/D 5229M – 92: Standard Test Method for Moisture Absorption Properties and Equilibrium Conditioning of Polymer Matrix Composite Materials.*

[44] J. L. Thomason. The interface region in glass fibre–reinforced epoxy resin composites: 1. sample preparation, void content and interfacial strength. *Composites*, 26:467–475, 1995.

[45] J. L. Thomason. The interface region in glass fibre–reinforced epoxy resin composites: 2. water absorption, voids and the interface. *Composites*, 26:477–485, 1995.

[46] M. R. Wisnom, T. Reynolds, and N. Gwilliam. Reduction in interlaminar shear strength by discrete and distributed voids. *Composites Science and Technology*, 56:93–101, 1996.

[47] M. L. Costa, S. F. M. de Almeida, and M. C. Rezende. The influence of porosity on the interlaminar shear strength of carbon/epoxy and carbon/bismaleimide fabric laminates. *Composites Science and Technology*, 61:2101–2108, 2001.

[48] P. Olivier, J. P. Cottu, and B. Ferret. Effects of cure cycle pressure and voids on some mechanical properties of carbon/epoxy laminates. *Composites*, 26:509–515, 1995.

[49] S. F. M. de Almeida and Z. dos Santos Nogueira Neto. Effect of void content on the strength of composite laminates. *Composite Structures*, 28:139–148, 1994.

[50] N. L. Hancox. The influence of voids on the hydrothermal response of carbon fibre reinforced plastics. *Journal of Materials Science*, 16:627–632, 1981.

[51] E. P. Plueddemann, editor. *Interfaces in Polymer Matrix Composites*, volume 6 of *Composite Materials*. Academic Press, Inc., 1974.

[52] G. Kotsikos, A. G. Gibson, and J. Mawella. Assessment of moisture absorption in marine GRP laminates with aid of nuclear magnetic resonance imaging. *Plastics, Rubber and Composites*, 36(9):413–418, 2007.

[53] K. Liao and Y.-M. Tan. Influence of moisture–induced stress on in situ fiber strength degradation of unidirectional polymer composite. *Composites: Part B*, 32:365–370, 2001.

[54] P. Nogueira, C. Ramirez, A. Torres, M. J. Abad, J. Cano, J. Lopez-Bueno, and L. Barral. Effect of water sorption on the structure and mechanical properties of an epoxy resin system. *Journal of Applied Polymer Science*, 80:71–80, 2001.

[55] A. Le Duigou, C. Baley, and P. Davies. Seawater aging of flax/PLLA biocomposite. In *International Conference on Innovation in High Performance Sailing Yachts*. The Royal Institution of Naval Architects, 2008.

[56] A. Kootsookos and A. P. Mouritz. Seawater durability of glass- and carbon-polymer composites. *Composite Science and Technology*, 64:1503–1511, 2004.

[57] K. Liao, C. R. Schultheisz, and D. L. Hunston. Effects of environmental aging on the properties of pultruded GFRP. *Composites: Part B*, 30:485–493, 1999.

[58] J. G. Iglesias, J. Gonzalez-Benito, A. J. Aznar, J. Bravo, and J. Baselga. Effect of glass fiber surface treatments on mechanical strength of epoxy based composite materials. *Journal of Colloid and Interface Science*, 250:251–260, 2002.

[59] P. W. Erickson and E. P. Plueddemann. *Composite Materials*, volume 6: Interfaces in polymer matrix composites, chapter Historical background of the interface-studies and theories. Academic Press, Inc, 1974.

[60] D. Karalekas, J. Cugnoni, and J. Botsis. Monitoring of hygrothermal ageing effects in an epoxy resin using FBG sensor: A methodological study. *Composite Science and Technology*, 69:507–514, 2009.

[61] F. U. Buehler and J. C. Seferis. Effect of reinforcement and solvent content on moisture absorption in epoxy composite materials. *Composites: Part A*, 31:741–748, 2000.

[62] M. Davidovitz, A. Mittelman, I. Roman, and G. Marom. Failure modes and fracture mechanisms in flexure of Kevlar-epoxy composites. *Journal of Materials Science*, 19:377–384, 1984.

[63] A. Falchi and J. Gracia. Effects of three-point bending test controlled by acoustic emission on carbon epoxy laminates. In *ICCM-VI and ECCM-II*, volume 1, pages 1.375–1.384, 1987.

[64] W. J. Cantwell and J. Morton. The significance of damage and defects and their detection in composite materials: A review. *Journal of Strain Analysis*, 27(1):29–42, 1992.

[65] N. Sate, T. Kurauchi, and O. Kamigaito. Fracture mechanism of unidirectional carbon-fibre reinforced epoxy resin composite. *Journal of Materials Science*, 21:1005–1010, 1986.

[66] E. Bayraktar, S. D. Antolovich, and C. Bathias. New developments in non–destructive controls of the composite materials and applications in manufacturing engineering. *Journal of Materials Processing Technology*, 206:30–44, 2008.

[67] P. J. Schilling, B. P. R. Karedla, A. K. Tatiparthi, M. A. Verges, and P. D. Herrington. X-ray computed microtomography of internal damage in fiber reinforced polymer matrix composites. *Composites Science and Technology*, 65:2071–2078, 2005.

[68] K. D. Cowley and P. W. R. Beaumont. Damage accumulation at notches and the fracture stress of carbon-fibre/polymer composites: combined effects of stress and temperature. *Composite Science and Technology*, 57:1211–1219, 1997.

[69] A.A. Pollock. *Metals Handbook*, chapter Acoustic emission inspection, pages 278–294. ASM International, 1989.

[70] P. J. de Groot, P. A. M. Wijnen, and R. B. F. Janssen. Real-time frequency determination of acoustic emission for different fracture mechanisms in carbon/epoxy composites. *Composite Science and Technology*, 55:405–412, 1995.

[71] D. Scida, M. Assarar, and C. Poilâne. Influence of hygrothermal ageing on the damage mechanisms of flax-fibre reinforced epoxy composite. *Composites: Part B*, 48:51–58, 2013.

[72] S. Barré and M. L. Benzeggagh. On the use of acoustic emission to investigatedamage mechanisms in glass-fibre-reinforced polypropylene. *Composites Science and Technology*, 52:369–376, 1994.

[73] D. Scida, Z. Aboura, and M. L. Benzeggagh. The effect of ageing on the damage events in woven-fibre composite materials under different loading conditions. *Composites Science and Technology*, 62:551–557, 2002.

[74] H. M. Akil, C. Santulli, F. Sarasini, and J. Tirilló. Environmental effects on the mechanical behaviour of pultruded jute/glass fibre-reinforced polyester hybrid composites. Accepted manuscript in Composites Science and Technology, 2014.

[75] A. Le Duigou, C. Baley, and P. Davies. Seawater ageing of flax/poly(lactic acid) biocomposites. *Polymer Degradation and Stability*, 94:1151–1162, 2009.

[76] K. Ono. Acoustic emission behavior of flawed unidirectional carbon fiber-epoxy composites. *Journal of Reinforced Plastics and Composites*, 7, 1988.

[77] C. Ramesh, Hrishi Ragesh, V. Arumugam, and A. Joseph Stanley. Effect of hydrolytic ageing on Kevlar/polyester using acoustic emission monitoring. *Journal of Nondestructive Evaluation*, 31:140–147, 2012.

[78] J. J. Scholey, P. D. Wilcox, M. R. Wisnom, and M. I. Friswell. Quantitative experimental measurements of matrix cracking and delamination using acoustic emission. *Composites: Part A*, 41:612–623, 2010.

[79] Q. Q. Ni and E. Jinen. Fracture behavior and acoustic emission in bending tests on single-fiber composites. *Engineering Fracture Mechanics*, 56(6):779–796, 1997.

[80] *Composites Engineering: Lecture Notes*. A. Chambers, 2009.

[81] http://www.gurit.com/. *Gurit webpage*, accessed March 2011.

[82] S. Black. Techonologies for UV curing of composite laminates demonstrated. *Composites Technology*, 2004.

[83] *Emerging Low Cost Manufacturing Processes for* UV *Cure Resins*, 1997.

[84] *ASTM D 7264/D 7264M–07: Standard Test Method for Flexural Properties of Polymer Matrix Composite Materials*.

[85] C. Hellier and C. Hellier. *Handbook of Nondestructive Evaluation*, chapter 10: Acoustic emission testing. McGraw Hill Professional, 2003.

[86] http://www.ndt-ed.org. *NDT Resource Center webpage*, accessed March 2014.

[87] http://http://www.ndt.net/. *NDT webpage*, accessed March 2014.

[88] D.H. Kaelble. Methods for detecting moisture degradation in graphite-epoxy composites. Technical report, Iowa State University, 1977.

[89] H. N. N. Murthy, M. Sreejith, M. Krishna, S. C. Sharma, and T. S. Sheshadri. Seawater durability of epoxy/vinyl ester reinforced with glass/carbon composites. *Journal of Reinforced Plastics and Composites*, 00:1–9, 2009.

[90] J. J.Tracy and G. C. Pardoen. Effect of delamination on the flexural stiffness of composite laminates. *Thin-Walled Structures*, 6:371–383, 1988.

[91] H. T. Hahn, M. Sohi, and S. Moon. Compression failure mechanisms of composite structures. Technical report, NASA, 1986.

[92] A. S. Dzielendziak, J. I. R. Blake, and A. R. Chambers. Durability of sustainable composites in ship design for enhanced environmental performance: a multiscale approach. Presented at ICCS17 in June 2013, Portugal.

[93] K. S. Kim, K. I. Lee, H. Y. Kim, S. W. Yoon, and S. H. Hong. Dependence of particle volume fraction on sound velocity and attenuation of EPDM composites. *Ultrasonics*, 46:177–183, 2007.

[94] S. A. Nielsen and H. Toftegaard. Ultrasonic measurement of elastic constants in fiber-reinforced polymer composites under influence of absorbed moisture. *Ultrasonics*, 38:242–246, 2000.

[95] A. Garg and O. Ishai. Characterization of damage initiation and propagation in graphite/epoxy laminates by acoutic emission. *Engineering Fracture Mechanics*, 22:595–608, 1985.